

Smart Beehive System for Measuring Honey Level and Controlling Temperature

By

Sajad Mirzaei

A Thesis submitted to the Faculty of Graduate Studies of

The University of Manitoba

in partial fulfillment of the requirements of the degree of

MASTER OF SCIENCE

Department of Electrical and Computer Engineering

University of Manitoba

Winnipeg, MB

Copyright © 2024 by Sajad Mirzaei

Abstract

The designs for a remote managed honey level and temperature control system for a beehive are presented in this thesis. These designs can be useful in beekeeping, as apiarists can have better understanding of environmental factors and stresses affecting the honeybee population. For monitoring honey level in the hive boxes, interdigitated capacitor sensors fabricated up on the frames in the hive box are presented. Simulations and experimental testing of prototypes are presented for measuring the level of honey on top of the frames. For the temperature control in the hive, various heater designs with performance simulations are presented to heat the brood in the hive to 35 °C regularly, and further increase temperature to kill Varro mites. This system will measure the temperature in each region of the frame board. If any mite is detected, the temperature will be increased on that region to kill the mite, and this can protect other honey regions from destroying and save energy. The prototype interdigitated capacitor sensors were built and experimentally tested in the lab to measure the level of water on the frames. They showed that the capacitance would increase with the level of water on top of the sensor from 1 mm to 10 mm. Electronics were constructed to record the data from the interdigitated capacitor sensors and record the data on an SD card.

Acknowledgements

I would first like to thank my advisor Dr. Cyrus Shafai for taking me as a graduate student and sharing his technical knowledge and insights into the many problems addressed in this thesis.

My deep and sincere gratitude to my family for their continuous and unparalleled love, help and support. I am forever indebted to my parents for giving me the opportunities and experiences that have made me who I am.

I also say thank you to my friend and especially to my brother-in-law, Mohammad, who supports me all the time.

Last but not least; I should thank my lovely sister. I remember every single time that you have come to my aid, and I will be grateful forever. For all the time you made me smile, I bless you, I love you sister, hope you do not forget that. You are the most adorable sister in this world, thanks for always loving me at my worst.

Table of Contents

Abstract.....	i
Acknowledgements.....	ii
Chapter 1: Introduction.....	1
1.1 Motivation.....	1
1.2 Problem Definition.....	3
1.3 Proposed Solution.....	4
1.3.1 Cell Content and Bee Activity Detection.....	5
1.3.2 Monitoring temperature.....	7
1.4 Thesis Formulation and Objectives.....	8
1.5 Thesis Organization.....	9
Chapter 2: Background on Bees, Beekeeping, and Existing Remote Hive Monitoring.....	10
2.1 General Background of the Honey Industry.....	10
2.2 The Importance of Bees in Nature.....	10
2.3 Honeybee Population and Usage in Industry.....	11
2.4 Temperature Changes on Bees and Bees Products.....	12
2.5 Colony Population and Brood Rearing.....	13
2.6 Commercial Hive Structure.....	15
2.6.1 Hive Boxes.....	16
2.6.2 Hive Frames and Foundation.....	18
2.7 Existing Remote Hive Monitoring Systems.....	22
2.8 Varroa Mite Background.....	27
2.9 Existing Methods for Treating Colonies Against Varroa Mites.....	28
Chapter 3: Cell Contents Monitoring within the Hive Supers and Brood Nest.....	34
3.1 Background.....	36
3.1.1 Honey Production Process.....	36
3.1.2 Physical and Electrical Properties of Honey.....	38
3.1.3 Capacitance of Brood Cells.....	39
3.1.4 Existing Capacitance Sensor Systems.....	40
3.1.5 Interdigitated Capacitor Sensor.....	42
3.2 Initial Simulations and Prototype Board Design.....	45

3.2.1	Simulations	45
3.2.2	2D simulations Results of IDC Sensors.....	46
3.2.3	Comparison of sensor designs:	52
3.2.4	3D simulations Results of IDC Sensors.....	54
3.2.5	Design and Test of a Small Prototype Board.....	55
3.2.6	Results and Discussion	62
3.3	Chapter Summery	64
Chapter 4:	Cell Contents Monitoring within the Hive Supers and Brood Nest.....	65
4.1	Background.....	65
4.1.1	Factors that Can Have Effect on Temperature on Honeybees	65
4.1.2	Existing Hive Temperature Monitoring Systems	66
4.2	Simulations of heat flow within the honeycomb	68
4.2.1	Finding the best way to simulate a resistor as a heater	71
4.2.2	Modeling the heat conductor region	73
4.2.3	Modeling the copper tape.....	77
4.2.4	Simulation of four heaters.....	81
4.2.5	Simulation of nine heaters for a region of 100x100 mm	89
4.2.6	Simulation of nine heaters for a region of the board	94
4.2.7	Comparison of Simulations Results.....	107
4.2.8	Further Models and Simulations for Determining Board Requirements	108
4.3	Chapter Summary	109
Chapter 5:	Conclusions and Future Work	110
5.1	Conclusions.....	110
5.2	Future Work	112
	References:	113
	Appendix A	125

List of Figures

Figure 1.1 A hive structure.	2
Figure 1.2 Cell content monitoring. (a) Capacitor layout. (b) Placement within a honeycomb.	6
Figure 2.1 Example of hive setup with one brood box and two honey supers.	17
Figure 2.2 Sample hive box (a) front view and (b) top view with half of the frames and dimensions.	19
Figure 2.3 Sample of hive frame (a) front view and (b) hexagonal-shaped tubes.	21
Figure 3.1 (a) Side view relative to the honeycomb. (b) Top view of prototype IDC boards.	35
Figure 3.2 Electric field due to stored charge between the electrode terminals.	42
Figure 3.3 Parallel Plate Capacitor	43
Figure 3.4 (a) 2D simulations of the first IDC sensor with water block on top of the IDC sensor. (b) Heat map of first IDC sensor, showing electric field values in V/m. (c) Capacitance changes when water level goes up from 1 mm to 10 mm.....	47
Figure 3.5 (a) 2D simulations of the second IDC sensor with water block on top of the IDC sensor. (b) Capacitance changes when water level goes up from 1 mm to 10 mm.	48
Figure 3.6 (a) 2D simulations of the second IDC sensor with water block on top of the IDC sensor. (b) Capacitance changes when water level goes up from 1 mm to 10 mm.	49
Figure 3.7 (a) 2D simulations of the second IDC sensor with water block on top of the IDC sensor. (b) Capacitance changes when water level goes up from 1 mm to 10 mm.	50
Figure 3.8 Existence of bees on top of come.	51
Figure 3.9 All four IDC designs compared.....	53
Figure 3.10 Comparison of all designs with normalized data.....	53
Figure 3.11 (a) A small board of IDC sensor for all four sensor designs (b) The IDC sensor with an Arduino UNO.....	56
Figure 3.12 A plot of the capacitor voltage over time for the charging circuit.	58
Figure 3.13 Test results for lab trials with small prototype boards.....	61
Figure 3.14 Normalization of data from all experimentally tested designs.	61
Figure 3.15 Comparison of simulation and experiment results.	63
Figure 3.16 Normalized data for simulations and lab test results.	63
Figure 4.1 General board design indicating the placement of the heaters, heat conductor, honey cells and copper tape to distribute the heat.	68
Figure 4.2 (a) Simulation of block heater (b) Simulation of line heater (c) Simulation of point heater.....	72
Figure 4.3 The results of the three different heaters between 1 and 600 seconds.	73

Figure 4.4 Pre-simulation of heat conductor region and copper tape.	74
Figure 4.5 Temperature simulation results with the 1x1x1.6 mm heat conductor and different thickness of the copper tape.	75
Figure 4.6 Temperature simulation results with the 3x3x1.6 mm heat conductor and different thickness of the copper tape.	75
Figure 4.7 Temperature simulation results with the 5x5x1.6 mm heat conductor and different thickness of the copper tape.	76
Figure 4.8 Simulation of one heater with 50x50 mm copper tape.	77
Figure 4.9 Temperature simulation with the 1x1x1.6 mm heat conductor and copper tape with thickness of 0.03 mm.	78
Figure 4.10 Temperature simulation with the 1x1x1.6 mm heat conductor and copper tape with thickness of 0.07 mm.	78
Figure 4.11 Temperature simulation with the 1x1x1.6 mm heat conductor and copper tape with thickness of 0.1 mm.	79
Figure 4.12 Temperature simulation with the 1x1x1.6 mm heat conductor and copper tape with thickness of 0.3 mm.	79
Figure 4.13 Temperature simulation with the 1x1x1.6 mm heat conductor and copper tape with thickness of 0.7 mm.	80
Figure 4.14 Simulation of four heaters with water and air block.	81
Figure 4.15 Simulation study for 0.03 mm copper tape. (a) Temperature distribution on top of the copper tape. (b) Temperature distribution at 5 mm in water block. (c) Temperature distribution on top of the 10 mm water block.	82
Figure 4.16 Simulation study for 0.07 mm copper tape. (a) Temperature distribution on top of the copper tape. (b) Temperature distribution at 5 mm in water block. (c) Temperature distribution on top of the 10 mm water block.	83
Figure 4.17 Simulation study for 0.1 mm copper tape. (a) Temperature distribution on top of the copper tape. (b) Temperature distribution at 5 mm in water block. (c) Temperature distribution on top of the 10 mm water.	84
Figure 4.18 Simulation study for 0.3 mm copper tape. (a) Temperature distribution on top of the copper tape. (b) Temperature distribution at 5 mm in water block. (c) Temperature distribution on top of the 10 mm water block.	85
Figure 4.19 Simulation study for 0.7 mm copper tape. (a) Temperature distribution on top of the copper tape. (b) Temperature distribution at 5 mm in water block. (c) Temperature distribution on top of the 10 mm water block.	86
Figure 4.20 Comparing temperature distribution on top of the heaters.	87
Figure 4.21 Heat distribution around the heaters.	88
Figure 4.22 Comparing temperature distribution at 10 mm from the heater on top of the copper.	89

Figure 4.23 Simulation of nine heaters on 100 mm x 100 mm of FR4.	90
Figure 4.24 Simulation study for 0.03 mm copper tape. (a) Temperature distribution on top of the copper tape. (b) Temperature distribution at 5 mm in water block. (c) Temperature distribution on top of the 10 mm water block.	91
Figure 4.25 Simulation study for 0.7 mm copper tape. (a) Temperature distribution on top of the copper tape. (b) Temperature distribution at 5 mm in water block. (c) Temperature distribution on top of the 10 mm water block.	93
Figure 4.26 Simulation of nine heaters in one region of the board.	94
Figure 4.27 Simulation study for 0.03 mm copper tape side of the board. (a) Temperature distribution on top of the copper tape. (b) Temperature distribution at 5 mm in water block. (c) Temperature distribution on top of the 10 mm water block.	96
Figure 4.28 Simulation study for 0.03 mm copper tape middle of the board. (a) Temperature distribution on top of the copper tape. (b) Temperature distribution at 5 mm in water block. (c) Temperature distribution on top of the 10 mm water block.	98
Figure 4.29 Simulation study for 0.7 mm copper tape. (a) Temperature distribution on top of the copper tape. (b) Temperature distribution at 5 mm in water block. (c) Temperature distribution on top of the 10 mm water block.	100
Figure 4.30 Simulation study for 0.7 mm copper tape. (a) Temperature distribution on top of the copper tape. (b) Temperature distribution on top of 5 mm water block. (c) Temperature distribution on top of the 10 mm water block.	102
Figure 4.31 Simulation study for 0.1 mm copper tape. (a) Temperature distribution on top of the copper tape (b) Temperature distribution at 5 mm in water block. (c) Temperature distribution on top of the 10 mm water block.	104
Figure 4.32 Simulation study for 0.1 mm copper tape. (a) Temperature distribution on top of the copper tape. (b) Temperature distribution on top of 5 mm water block. (c) Temperature distribution on top of the 10 mm water block.	106

List of Tables

Table 3.1 Results of capacitor simulations for water levels from 1 mm to 1 cm.....	52
Table 3.2 Results of capacitor simulations for water levels from 1 mm to 1 cm.....	54
Table 3.3 Results of capacitors when water level rose from 1 mm to 1 cm in lab test.....	60
Table 4.1 Specific heat capacity for different materials.....	70
Table 4.2 Thermal conductivity for different materials.	71
Table 4.3 The results of different heaters with increasing time.	73
Table 4.4 The results of different heat conductor with increasing time.....	76
Table 4.5 Heat distribution with different copper tape thicknesses.	87
Table 4.6 Heat distribution when four heaters are applied.	89
Table 4.7 Heat distribution when nine heaters are applied with 0.03 and 0.7 copper tape thicknesses.	94
Table 4.8 Heat distribution with 0.03 mm copper tap when the heaters are inside and middle of the board.....	99
Table 4.9 Heat distribution with 0.7 mm copper tap when the heaters are inside and middle of the board.....	103
Table 4.10 Heat distribution with 0.1 mm copper tap when the heaters are inside and middle of the board.....	107

Chapter 1: Introduction

1.1 Motivation

Honeybees are one of the important insects around the world, and they support both natural and managed ecosystems through their pollination services to flowering plants [1]. In Canada, between 250 and 500 beekeepers produced queens both for their own use and for selling to other beekeepers. [1]. Honey production is lucrative, as beekeepers have around 803,352 colonies over the 2018-2019 [1]. In Canada, eighty percent of honey is produced in provinces of Alberta, Saskatchewan, and Manitoba by 475,000 colonies [2]. Although the number of colonies has increased from 2017 by around 16,000 colonies, beekeepers have a serious concern about colony mortality, as the US beekeepers reported 38 percent colony mortality over the 2018-2019 [1]. This is a serious issue, and the Canadian honeybee colony winter mortality has also been significant throughout the past decade [1]. Colony protection is one the most important things to control bee population and to ensure good honey production.

As can be seen in Figure 1.1, a beehive typically consists of different floors or sections that serve specific functions within the colony:

- 1- Bottom Board: The bottom board is the base of the hive, providing stability and support. It usually has an entrance for bees to come and go. It also helps regulate the hive's temperature and provides ventilation.
- 2- Brood Box or Deep Hive Body: The brood box, also known as a deep hive body, is the main section of the hive where the queen bee can lay her eggs and where the brood

(developing bees) is raised. It contains frames with wax foundation or comb, and worker bees build honeycomb cells on these frames for the queen to lay eggs in.

- 3- Queen Excluder: Positioned above the brood box, the queen excluder is a mesh or grid-like barrier that allows worker bees to pass through but restricts the movement of the queen bee. Its purpose is to confine the queen to the brood box, preventing her from laying eggs in the honey supers (upper sections) of the hive.
- 4- Honey Supers: Honey supers are additional sections added above the brood box. These supers contain frames where bees store surplus honey. Beekeepers typically harvest honey from these supers while leaving enough honey for the bees' winter food supply. Honey supers can be added or removed as needed, depending on honey production.

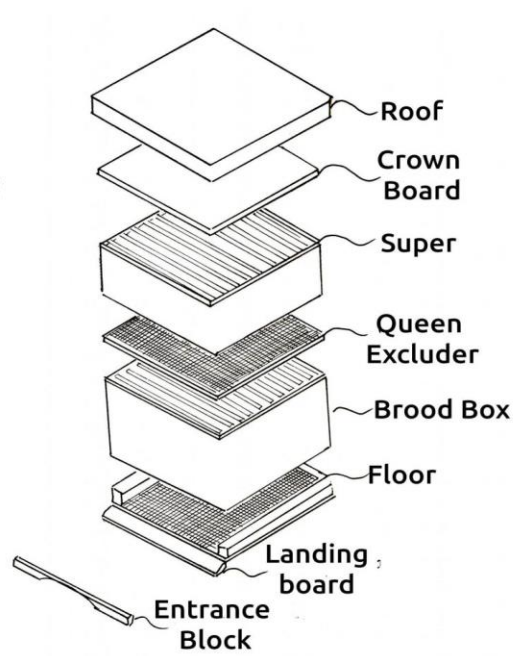


Figure 1.1 A hive structure.

Many large beekeeper operations usually have more than thousand colonies and they should protect the colonies from various types of causes of colony losses. For instance, queen issues, starvation, Varroa mite, weather, wild animals, pesticides and colony collapse disorder that happens when the majority of worker bees in a bee colony disappear [1]. Therefore, beekeepers need to protect their colonies, but this can be difficult and a remote monitoring system can be helpful. Because of the time required to check many colonies one by one, automated hive management solutions that can monitor data such as level of honey, movement of bees, and even mites, would be very valuable. Bees can also suffer stress from actions such as beekeepers inspecting hives. Remote hive monitoring would allow beekeepers to react in a timely manner to harvest full hives or solve any problems that may arise, reduce costs, and reduce stress on the bee colony from the need for routine inspections.

There are other factors which can affect bee colonies as well, such as environmental conditions. Therefore, a hive management system that can offer environmental control can give further benefit, and can help to improve the health of bees and honey production.

Beehive monitoring of variables such as level of honey, colony humidity, colony temperature, bee traffic can provide valuable information for apiarists and scientists [5]. Having data and information of the situation inside of colonies can help beekeepers to think about how to protect colonies better from outside factors that can affect colonies, and scientists can also study about nature factors to increase honey production and improve colony health [4].

1.2 Problem Definition

Many factors can have a significant effect on the honey production and bee health. Temperature and humidity are two factors that can affect the colonies, and the antennae of bees

are highly sensitive to fluctuations in both temperature and humidity [11, 12]. Factors such as environmental pesticides, noise, light, carbon dioxide, or Varroa mite infestation are also important. A remote-control system and monitoring of hive colonies are very useful for beekeepers to have knowledge of the conditions inside of colonies, and researchers also can take advantage of data provided by the system. A remote management system allows researchers and beekeepers to investigate factors that can affect products and bee population as they can predict some solutions to solve these factors. Smart hives technologies have been investigated by many group, and will be presented in more detail in Chapter 2. For instance, controlling humidity, temperature, detecting or managing Varroa mite infestation, and so on. This could enable improved honey production, because beekeepers can detect problems and solve them. The purpose of the technologies investigated in this thesis are:

- 1- Employ capacitive sensors to monitor honey produced and bee activities.
- 2- Employ a heater array on the frames in the hive to enable control of overall hive temperature and enable local increase of the temperature in particular locations on a frame.

1.3 Proposed Solution

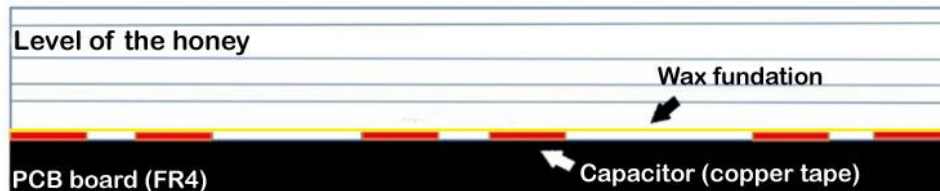
Two systems are proposed in this thesis. The first provides cell monitoring to recognize the level of honey, and population and movement of bees in the hive. The second provides temperature control inside of colonies, as it can change the local temperature on a hive frame at any specified point individually.

1.3.1 Cell Content and Bee Activity Detection

This part of the system includes an interdigitated electrode array fabricated on the frames inside the beehive. The sensor frames are fabricated from a printed circuit board (PCB), which has been divided to 12 regions, and each region has an interdigitated capacitor (IDC) to monitor the honey content and bee activity over each region. This method can also be used to monitor the larvae in the brood box of the hive. Measurement of liquid level has been done employing various methods, such as permittivity, permeability, conductivity, etc. [6]. Capacitive measurement of permittivity using an IDC electrode has been used for water level, milk level, fat and even bacterial monitoring [8-10]. The IDC sensor of this thesis is made from two conductive wire electrodes patterned of a hive frame as is shown in Figure 1.2. Both electrodes can store electrical charges and allow for the estimation of capacitance between them [6, 7]. The functional details of the IDC design of this thesis can be found in Chapter 3. Overall, the sensors monitor any changes in measured capacitance when the nectar and honey content change, or the location of larvae around the capacitor would change. Chapter 3 will present four different IDC designs and discuss the best IDC sensor design to enable the detection of changes in the level of the honey.



(a)



(b)

Figure 1.2 Cell content monitoring. (a) Capacitor layout. (b) Placement within a honeycomb.

Bees can produce more honey if they can find more free space around themselves, and beekeepers can influence the continuous production of honey if apiarist removes honey on time. Currently, beekeepers need to physically go and check the honeycombs to determine the level of honey. If honey needs to be harvested, beekeepers can remove the honey loaded frames from the hive colonies and add an empty frame, to give space for the bees to produce the honey again. It should be noted that, depending on the type of the hive, the number of bees and the location of the hive, this process could take considerable time and energy from farmers, since they need to check the hive boxes to find which one of frames is full and need to be replaced. Therefore, a remote honey level monitoring system that can tell farmers when the hive or a frame is full would be useful to save energy and time by limiting unnecessary trips to hives.

Another feature that would be useful for a remote monitoring system for a beehive is to monitor the bee population. The presented IDC system of this thesis can provide data about bee activity, as well as information about the larvae and potentially their numbers or developmental stage. The monitoring system can also be useful for checking colony health and bee behavior.

1.3.2 Monitoring temperature

One of the most important factors in beekeeping is the temperature in the hive, with the ideal temperature for the colonies to be around 33-35 °C [13, 14]. If the temperature drops, honey production will stop and honeybees crowd tightly together in the center of comb at the low temperatures [15]. Bees gather to warm each other when cold or in the winter, and it is a negative point for beekeepers because bees stop producing honey. Therefore, controlling temperature remotely to around 35 °C can be useful. In addition, elevated temperature control can be used to destroy Varroa mites. By using small heaters, which can be installed on the frame boards, the system will turn the heater on at that specific place to kill the mites remotely.

This thesis also explored the use of small heaters integrated on the hive frame, and heat can be transferred from heaters over the frame by using heat conductors. Temperature sensors are employed to measure temperature in different areas of the frame. As will be discussed in Chapter 4, the temperature sensors can be useful to find what factors from inside and outside of the hive box may affect different parts of the hive.

Many methods have been used to destroy Varroa mites that can infest beehives. Some of these methods are physical like Drone brood removal and breaks in the brood cycle, and the others are chemical (for instance Apivar or Oxalic Acid can be used but they can have detrimental effect on bees and the product) [16, 17]. The proposed usage of heated frames can destroy Varroa mites

and in so doing, it can offer a lower impact on the hive than chemical treatments. The presented system can control the temperature locally over a small number of cells, and so reduce the loss of larvae and eliminate Varroa mites.

1.4 Thesis Formulation and Objectives

The main objectives of this thesis are:

- 1- Study the use of interdigitated capacitor electrodes for monitoring cell content and bee activity.
 - a. Investigate by simulation to determine appropriate design of IDC board to enable measurement of increasing honey.
 - b. Design prototype IDC boards.
 - c. Test the prototype boards in the lab.
- 2- Study the monitoring of temperature locally over a hive frame.
 - a. Simulate the heat flow between cells to determine temperature range across heated frames, based on placement and power level of heaters.
 - b. Simulate the heat flow over the frame and honeycomb cells to determine best location for measuring temperature within a honeycomb.
- 3- Study the use of small heaters to heat brood frames to enable the use of temperature for killing mites.
 - a. Simulation of heaters on a PCB board to determine how much energy is needed to warm the board and based on their location and distribution.
 - b. Simulation of the use of heat conductor to investigate the ability of heaters to control frame temperature, and with consideration of time.

- c. Explore heated frame design to enable heating to 47 °C in a reasonable amount of time.

1.5 Thesis Organization

Chapter 2 gives general information about the beehive design, review of Canadian beekeeping, the impact of various types of factors on the beehive and honey production, population of bees and larvae and a review of some existing remote beehive monitoring technologies.

Chapter 3 will discuss measuring the level of honey remotely and monitoring the cell contents within the honeycomb. Some background information about honey properties and the honey production process are provided. This chapter also provides details of the interdigitated capacitor sensor, IDC sensor simulation, design and testing of four different small prototype boards. The concluding section of Chapter 3 is dedicated to creating a printed circuit board (PCB) with 12 regions, which will be used to replace the honeycomb structure inside the beehive.

Chapter 4 provides a background information about some factors that can affect the temperature in the beehive, as well as background on Varroa mites and existing methods to kill the mites and protect the beehive. Then some simulations are provided to show the rate of heat dissipation in the comb. Afterwards, a prototype PCB is designed to test and measure the temperature using temperature sensors. The results will be compared to the simulation of the heater.

Chapter 5 prepares a summary of the conclusions, which can be drawn from the work done in this thesis and summarizes the future work that could be performed.

Chapter 2: Background on Bees, Beekeeping, and Existing Remote Hive Monitoring

2.1 General Background of the Honey Industry

Honey is a widely produced and consumed food around the world. The largest volume of honey is produced from the nectar of flowers by *Apis mellifera* (the western honeybee). Honey consists of sugars, small amounts of proteins and amino acids, minerals, enzymes, trace elements, vitamins, aroma compounds, and polyphenols. [18]. Honey has been used as food and medicine throughout history by all traditions and civilizations, and it is also used in Asian countries to treat a lot of internal and external problems of the body.

Bees use their proboscis to extract nectar from flowers, which they store in their honey sacs and transport it back to the beehive. At the beehive, the bees transform the nectar into honey. Bees start to build honeycomb in their hive to store the nectar, which has been converted into the honey.

2.2 The Importance of Bees in Nature

Pollination is a crucial role in ecological systems, and the absence of pollination can lead to significant problems in agricultural production [22]. Pollination refers to the transfer of pollen from the male reproductive organ, known as the anther to the female reproductive organ, called the stigma. There are two types of pollination: self-pollination and cross-pollination. Self-pollination occurs through the transfer of pollen from the anther to the stigma within the same flower or plant. Conversely, cross-pollination needs external assistance for the transfer of pollen between different plants or flowers. Bees are one of the important agents in facilitating the process of cross-pollination [23]. Honeybees are responsible for more than 80 percent of pollination of

various types of plants worldwide, with the exception of fruits, flowers, and vegetables. They play a critical role in pollinating more than 100 crops, such as nuts, forage, herbs, spices, oilseed crops, medicinal plants, and countless other plants [25]. In comparison to other insects, bees are uniquely adapted for collecting and transporting pollen. They have a large and dense covering of hair on their bodies, enabling them to carry a significant quantity of pollen. Furthermore, bees have a relatively large population size, enhancing the probability of visiting numerous flowers within a specific area. As bees feed on nectar from flowers, pollen naturally adheres to their hairy bodies, facilitating cross-pollination between plants. As bees visit numerous flowers, pollen is easily transferred between flowers. A study conducted in [24] revealed that pollination by bees increased the commercial value of strawberry fruit. Specifically, compared to wind pollination, bee pollination resulted in a remarkable 38.6% increase in commercial value per fruit, while compared to self-pollination the increase was even higher at 54.3%. In addition, honey serves as a remarkable food source. Bees make honey to feed their colonies during the cold weather. Additionally, other animals, such as birds, opossums, insects, and raccoons can also benefit this product [26]. In order to produce one pound of honey, bees undergo extensive flights in search of nectar, gathering about a twelfth of a teaspoon of honey during each foraging trip. A honeybee visits an impressive range of 50 to 100 flowers during each trip [27].

2.3 Honeybee Population and Usage in Industry

Apiculture is important in the United States and Canada, with the number of honeybee colonies steadily increasing every year [19]. In 2019, Canadian beekeepers managed to produce a substantial 37 million kilograms of honey, valued at 173 million Canadian dollars although, the number of colonies in Canada declined 2.1% from a year earlier to 773,182 in 2019 due to

unfavorable weather condition. This production was attributed to the efforts of 10,344 beekeepers across the country. Notably, the provinces of Alberta, Saskatchewan, and Manitoba contributed the largest share to the overall honey production [20]. The sale of honey presents a remarkable opportunity to earn money, and Canada was able to reach around 12,000 metric tons of honey and generate an estimated \$54 million Canadian dollars in revenue. Liquid honey and beeswax are used in industry. They serve as an edible food product, act as ingredients for other goods, and are even employed in medicinal applications [21].

As previously mentioned, honeybee pollination plays a crucial role in various industries, including the impact it has on Canada's agricultural sector. In 2016, the total harvest value of apple production was \$223 million, of which honeybees were responsible for 90%, amounting to \$200 million. Honeybees also can play an important role in other crops, with an estimated economic contribution of \$720 million attributed to honeybee pollination in the production of vegetables and fruits. Overall, the annual economic contribution of honeybees was estimated to be \$2.57 billion in 2016 [28].

2.4 Temperature Changes on Bees and Bees Products

Honeybees show different distinct behavioral throughout different seasons. Summer is a favorable season for honeybees, since they can collect nectar and produce honey especially in temperature-zone. Honeybees encounter challenges during the cold winter. It is crucial for apiarists to be ready for winter and protect honeybees from the harsh cold weather.

The summer is considered the best time for honeybees to engage in flight and collect nectar from a wide variety of flowers to make noticeable production. In areas where honeybees reside, their ability to manage honey production is influenced by the prevailing temperature conditions.

Temperature zones, which provide a comfortable environment for honeybees, are those with temperatures that are neither excessively hot nor extremely cold, allowing honeybees to continue to produce honey for longer. Optimal colony temperature for honeybees is around 35°C and bees maintain this temperature by bringing water to the nest and spreading it within the interior of the nest, promoting evaporation when exposed to air circulation. Bees also regulate the temperature by flying inside the colonies and utilizing their wings to create airflow [29]. On the other hand, in cold weather, particularly in regions like Canada, bees must protect themselves. This can have a significant impact on their survival and well-being. When the temperature drops to around 14°C, honeybees form a tight cluster to maintain warmth, reaching a temperature of around 35°C within the cluster. This cluster not only includes adult bees but also encompasses eggs, larvae and pupae, and protecting them is crucial [29, 30]. During the colder months, honeybees stop their honey production activities, and they use the stored honey as a source of sustenance to survive. It becomes crucial for beekeepers to ensure optimal conditions and protect the colonies from cold weather, in order to allow honeybees to maximize their honey production. Making a remote hive monitoring system can help apiarists protect the colonies, and monitor bees' activities.

2.5 Colony Population and Brood Rearing

The population of a beehive experiences fluctuations throughout the year, in response to seasonal changes and food availability. There is a reduction of nectar and pollen during the winter, and the queen stops laying eggs. Therefore, the number of broods reduce, and bees cluster together to warm up the colonies and protect the remaining eggs within the group [29]. In early spring, the number of bees in a colony range between 10,000 and 15,000, while in the summer this number rises significantly to reach approximately 50,000 to 60,000 bees [31]. As spring progresses, new

sources of pollen and nectar become available, which stimulates the queen to lay more eggs, and the population of bees increases dramatically. Worker bees are also included in this growth, they gather nectar and pollen. Worker bees store extra nectar and pollen as honey in new comb to feed larvae in the winter months. Moreover, to store honey, older combs are utilized for pollen storage and brood rearing purposes. The brood population is one of essential things that beekeepers should monitor, to ensure the health of their hives and enabling more honey production.

Each beehive is home to a single queen bee, who can lay around 2000 eggs per day, equivalent to around one egg every 10 seconds. Spawning varies in different seasons, as she will lay around 100-1500 eggs per day to maintain hives numbers during the honey production season. She lays between 175,000-200,000 eggs each year in total [32, 33]. Beekeepers usually replace the queen after one or two years, while the queen can lay eggs for around 4-5 years, because after two years, the queen cannot control and maintain the number of bees inside the hive.

Honeybee larvae lifecycle has some stages from egg to adult bee [34-37]. The first stage, which takes around three days, is depositing of an egg by the queen in cells. If the queen makes a mistake and lays unfertilized eggs, the worker bees have the ability to identify, remove and destroy them from the colony. Worker bees also do the most important work in the beehive, and they are responsible to take care of young brood and feed them. The second stage is the change of an egg to larvae, which is similar to a small maggot. In order to facilitate rapid growth, worker bees feed larvae with royal jelly, which is a dense nutritional secretion. After three days if the larvae are not destined to become a queen, the food transitions to honey. However, if the larvae are identified as a potential queen, the nurse bees continue to feed it with royal jelly. After five days of nonstop eating and growing, the size of larva reaches approximately 1500 times bigger than when they first hatched. At this point, worker bees seal the cell with wax to create a protective enclosure. The

duration of the larval stage varies based on the type of bee, with approximately six days being the average timeframe. This period is shorter for the queen and longer for worker bees. Following the larval stage, the next phase in the bee's life cycle is the pupa stage. The small white larvae starts to develop in the cell. Depending on the type of bee in the cocoon, this stage lasts approximately between seven and eighteen days. During this time, the pupa's legs, wings, eyes, and other body parts begin to form within the protective cocoon. After the completion of the pupa stage, which lasts around 18 days, adult bees chew their way out of the cells, and they will be a productive member of the hive.

2.6 Commercial Hive Structure

A beehive is an enclosed structure that includes several combs. There is a distinction between the nest and hive, as bees construct the nest naturally, whereas a hive is created by humans artificially. Presently, the majority of beekeepers utilize hives in their colonies and there are many combs in each hive that are made with beeswax. The hive can be used as storage for honey, pollen, nectar, and larvae [38].

Hives can be categorized into two types, one is traditional hives, and another is modern hives. Traditional hives encompass various designs like Mud hive, Clay hive, Skeps hive and bee gums which are no longer commonly used. On the other hand, modern hives include Top-bar hive, Langstroth hive and Warre hive. The Langstroth hive was invented by L. L. Langstroth in 1851 and is the most common type of hive worldwide. This design quickly gained popularity, and it is used by 75 percent of beekeepers [39, 41]. The Langstroth hive consists of either 8 or 10 frames with a specific spacing between frames within the hive. A Langstroth with 10 frames gives more

space for honey and brood. 10-frame hives are heavier in weight than the 8-frame version, increasing the risk of injury for beekeepers when lifting the setup [41, 43].

2.6.1 Hive Boxes

The hive structure includes various boxes which are used for specific purposes, as shown in Figure 2.1. As mentioned in references [44, 45], the hive includes a hive stand which supports the hive under the boxes and includes a hive entrance, facilitating the entry and exit of bees. There is a bottom board, which consists of several rails to safeguard the colony from the damp ground. Nowadays, apiarists substitute a screened bottom board with the standard one, as it allows them to monitor and control the population of Varroa mites within the colony. Moreover, this screen aids in ventilation and airflow, providing beneficial air conditioning for the hive. Additionally, there is also an entrance reducer to control and limit bee access to the hive.

The standard brood box, also known as the deep super, is an essential component that contains some frames of comb and functions as the brood chamber to raise larvae and can have 8 or 10 frames. A queen excluder is typically placed on top of a deep super, which is a flat rack of metal or plastic and serves to prevent the queen from entering and laying eggs inside the above honey super boxes. Honey super boxes are medium depth supers and shallow supers, and consist of 10 frames for each box, and are where the bees store pollen, nectar and honey. An inner cover and outer cover are employed on the top of the colony to provide ventilation and protect the hive from external destructive elements respectively. The outer cover is typically constructed using of a waterproof material such as aluminum flashing, asphalt tiles, cedar shingles or other similar materials to cover the colony and protect it from various environmental factors.

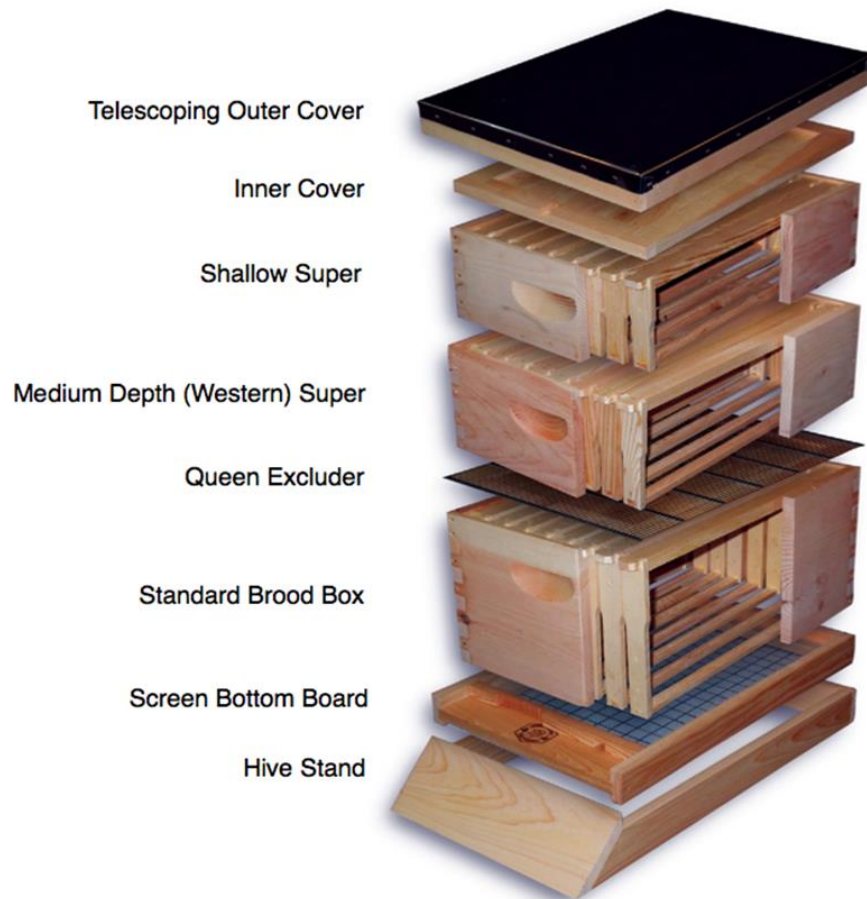


Figure 2.1 Example of hive setup with one brood box and two honey supers.

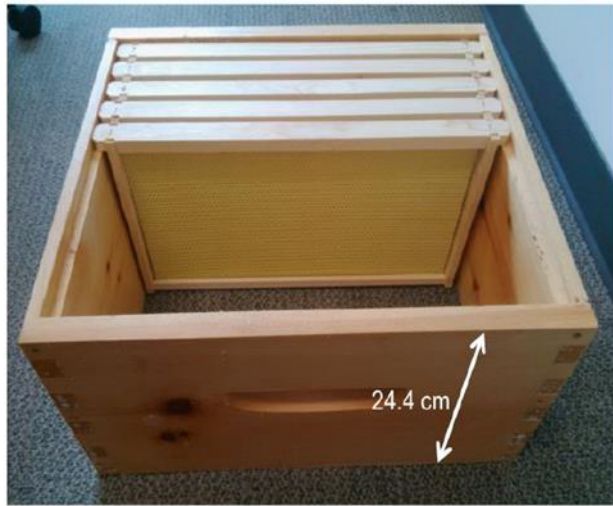
Depending on the type of box, appropriate frames should be chosen for the honey super boxes, and there are some advantages and disadvantages in the various frames. In reference [46], Conrad states that the initial hive style invented by L. L. Langstroth in 1852 was the deep hive, which contains 10 frames, and had a height of 9-5/8 inches. An advantage of using this hive was it allowed for ample space, enabling the queen to lay more eggs and bees to store more honey. However, due to its excessive weight, weighing over 80 pounds, this hive style is not as common and conventional today, despite its suitability for both southern and northern regions. Another hive style that is more commonly used now uses medium sized boxes, which stand at 6-5/8 inches in height. This type of box is called Western or Illinois super and is approximately two-thirds the

weight of a comparable full deep hive. However, beekeepers should add more boxes for super and brood boxes with some equipment in this style if they want to achieve the same honey yield as the deep hive style. Another style that is lightest option for regular use is the shallow style, which measures 5-11/16 inches in height, and is primarily utilized as a honey super.

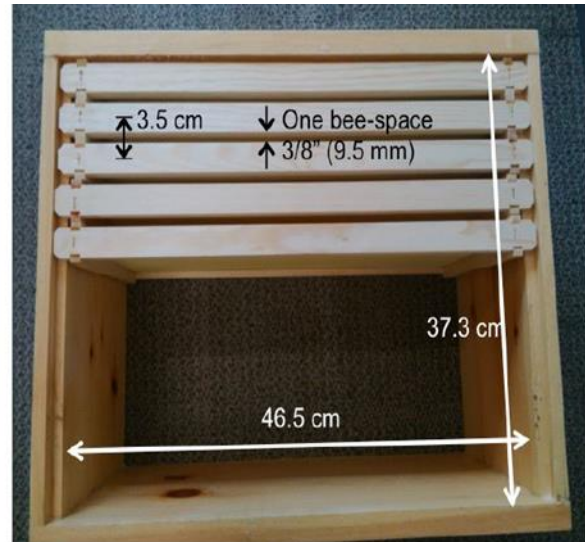
2.6.2 Hive Frames and Foundation

In 1851, Lorenzo Langstroth discovered that bees create a gap between the combs, which they do not fill with honey. If there is a space less than 1/4 inch. Bees will fill this space with propolis. Conversely, bees make another comb if the space is larger than 3/8 inch [48]. Hence, it is recommended that the frame space should be between 3/8 inch and 1/4 inch. The advantage of this size is that, beekeepers can remove combs without enraging the bees, frames do not stick together, allowing for easy removal, and bees can move freely between the combs. This size of bee space has become widespread among beekeepers worldwide. It ensures the combs do not become stuck together, facilitates easy removal of the combs, and there is no obstacle for bees to travel [47, 49].

As mentioned earlier and depicted in Figure 2.2, each hive box typically accommodates between 8 and 10 frames, with a spacing of 3/8 inch between them. If beekeepers use eight or nine frames in honey super, bees are able to extend the cell walls, leading to increased honey production compared to when 10 frames are used [50]. The remote hive system that is presented in this thesis is based on the standard deep frame; however, it should be noted that it can be adapted to various frame shapes.



(a)



(b)

Figure 2.2 Sample hive box (a) front view and (b) top view with half of the frames and dimensions.

As stated in [52], frames can be made from either plastic, which contains a built-in foundation, or wood, which requires beekeepers to add separate foundations on it. Foundation serves as a guide layer that fits into the beehive frame, directing the bees on where to construct their combs. There are two types of foundation that beekeepers use. One type of foundation commonly used by beekeepers is beeswax foundation, which is made of high quality refined beeswax, and it is especially utilized with wooden frames. The other foundation is plastic foundation that is easy to install and stronger than beeswax foundation. However, it requires a wax coating for bees to draw comb on it. While plastic frames have the advantage of being lighter, resistant to high temperatures, and impervious to decay, beekeepers commonly use wood frame due to their natural origin and compatibility with the beekeeping tradition [51]. Consequently, in modern beekeeping, most apiarists and especially beginners utilize foundation to assist bees to make straight cell and combs. Combs built on foundation are always stable, and beekeepers can easily extract honey from the combs by using centrifugal methods and they can reuse the comb

frames multiple times [52]. The other advantage of using foundation is that bees do not need to make the base for each cell, and some of the honey and more labor will be saved. Additionally, producing wax from honey would be a resource expensive process for bees, as it takes approximately 1 kg of honey to produce about 60 g of wax. The other important advantage of using foundation is that beekeeper can control male drone population by decreasing drone cells in the beehive, a benefit since drones consume substantial amount of honey and do not contribute remarkably to the hive [54].

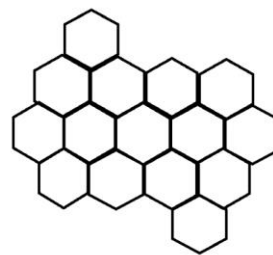
Recycled wax is commonly employed in the production of foundation; however, it does come with certain drawbacks. One such drawback is they are not stable at high temperatures, and they can be harmed by moths and other pests [40]. Various materials, including aluminum, tin, zinc, and paper have been attempted for foundation production, but they require significant financial investment from beekeepers, and they have proven to be unsatisfactory [56]. In 1921, Dandant and sons introduced the use of wires added to the wax sheets to strengthen them from reclining. Later in 1963, Dandant and sons developed the foundation by using plastic, which is widely used today. This plastic foundation includes a layer of thin film covered by two layers of beeswax, with an attached hexagon pattern on it [50]. As previously mentioned and referenced in [57], some beekeepers choose not to use plastic foundation, believing that bees should have freedom to construct various size of cells naturally. However, the majority of beekeepers commonly use plastic foundation due to its ability to maintain straightness over an extended period.

Plastic foundation also guides bees in building cells at defined sizes. Moreover, this type of foundation can protect the hive against pests and parasites. Due to the structure of the plastic foundation, in the center of the frame, pests and parasites that are attached to one side of the frame

cannot cross to the other side. Moreover, using plastic foundation protects the hive from the issue of cross comb, so beekeepers only need to scrape cross comb that forms on the foundation. Plastic foundations are available in various colors, with black being commonly used for brood boxes. The dark color aids beekeepers to identify eggs and larvae more easily. White plastic foundation commonly is employed in honey super boxes, and it allows beekeepers to observe honey easily. However, there are some disadvantages with using plastic foundation. Research indicates bees may not be naturally inclined to build cells on the plastic foundation, and beekeepers must add a layer of beeswax, as a base on plastic foundation to attract the bees. However, in cold temperatures, both beeswax and plastic foundation can become cold and easily separate. Beekeepers also need to ensure the quality and safety of the honey produced on the plastic foundation before consumption. There is a concern that residues of plastic may enter honey and wax, which could pose potential health risks. On the other hand, there are two significant advantages for using plastic foundation. Plastic foundation can be utilized for multiple years if it is not damaged, and beekeepers can save a lot of money. In addition, the use of plastic foundation allows for the easier incorporation of sensors to monitor the colonies, providing a convenient and easy method to check on their colonies.



(a)



(b)

Figure 2.3 Sample of hive frame (a) front view and (b) hexagonal-shaped tubes.

The original size of the frame measures 430 mm x 210 mm, and the cells are shaped by bees in a specific manner. Cells are hexagonal-shaped tubes, with an angle between 9° and 14° and a thickness of 0.08 mm, and they allow bees to optimize space by attaching cells to one another. The angled shape of the cells prevents eggs, larvae, honey and pollen from falling out of the cells. To save time and honey, companies typically manufacture cells with a thickness of 0.0635, and bees only need to cover them with a thin layer of beeswax [50]. As mentioned earlier, there is a distinction between honey cells and brood cells. Honey cells, used for honey production and storage, have a diameter of 5.1-5.5 mm. In the brood cells, the cell size varies depending on the type of larvae (worker, queen). Brood cells are generally larger, ranging from approximately 6.7-7.1 mm [55, 58, 59].

2.7 Existing Remote Hive Monitoring Systems

The development of precision apiculture technologies has allowed scientists to monitor beehives for a wide range of purposes. Nowadays, various types of remote hive monitoring systems have been developed, and they are making beekeeping more convenient than ever before. Notable systems include WBee [60], Arnia [61], B-ware [62], Smarthive [63], APiS [64], IoBee [65] and Hivemind [66]. While all these systems share similarities and measure and monitor specific parameters, there are some differences among them. The aim of employing remote control systems is to reduce labor and enhance hive management. This means that beekeepers no longer need to physically visit the apiaries, and instead can monitor colonies by smartphone, laptop and other devices. In fact, these systems serve a wealth of information that beekeepers can utilize to protect their colonies, optimize production, and even prepare for future seasons.

The WBee system, initiated by AGR-218 Research Group at University of Córdoba in 2015, was designed to collect data on humidity and temperature in order to explore how honeybees regulate these factors. Furthermore, this system allows beekeepers to examine the relationship between these environmental factors and the health and productivity of bees. Moreover, measurement of weight can give some information about effects of different flowers on honey production [60].

The Hivemind system, developed by Bryan Hoyt in New Zealand, is similar to other remote hive monitoring systems. This system measures temperature and weight under the hive every six hours, and humidity is measured every three hours within the hive. In addition, the Hivemind system incorporates three special features that set it apart from other systems. Firstly, it includes a bee counter, which can report the number of bees entering and exiting the hive every three hours. Secondly, a rain gauge is integrated into the system to measure and monitor rainfall, and beekeepers can monitor impact of rainfall on hive condition. Lastly, the Hivemind system has a theft alert sensor, which promptly notifies beekeepers when theft or unauthorized access occurs [66].

Arnia is another remote hive monitoring system that was started in 2009 [61]. This system offers a range of measurements, including hive height, humidity and temperature inside the hive. In addition, the Arnia system incorporates an acoustic sensor to provide valuable insights into colony behavior. This system also includes a sensor to gather data on ambient weather conditions. To monitor hive weight, Arnia system utilizes a weight scale placed beneath the hive. This system provides a feasibility for beekeepers to set a maximum threshold, triggering an alert when the hive becomes full of honey. This data can also be used to determine the amount of nectar in different seasons and to warn when theft occurs. In addition, a temperature sensor is placed within the brood

cells to monitor temperature fluctuation, enabling beekeepers to observe the queen's egg-laying activity remotely. This system utilizes acoustic sensor to track bees activities and their movement inside the hive. Any disturbances detected by acoustic sensors will immediately notify the apiarists. This aspect of the Arnia system is useful to interpret the colony behavior and their health especially during winter to detect the movements of the bees and their health remotely. Beekeepers can conveniently access the data from the Arnia system using any internet-enabled device, eliminating the need for physical presence, and allowing remote monitoring. [61].

The B-ware system, developed by Solutionbee, offers a more streamlined approach with a focus on essential measurements. What sets this system apart is its long-life battery, ensuring prolonged functionality without frequent replacements. This system primarily emphasizes ambient temperature and hive weight, utilizing a weight scale and temperature system positioned beneath the hive. These measurements provide regular updates on hive weight and temperature conditions every 15 minutes for beekeepers. Despite its limited scope, the B-ware system provides valuable system insights into these key parameters, allowing apiarists to monitor the honey's weight and assess the temperature conditions within the colony. The B-ware system employs a gateway device, known as the HiveHub, to collect the gathered data and transmit it to the internet via Wi-Fi connectivity. To access the data, customers simply only need to download the B-ware Mobile App onto their smartphones or devices. This setup enables customers to easily receive updated data every 15 minutes from the comfort of their homes. On the other hand, this system cannot provide any information about bees' health and their activities in the colony [62].

Another available system is Smarthives, which has some sensors to measure weight, ambient temperature, temperature and humidity within the brood cells. In addition, this system is equipped with motion detection capabilities. This feature serves as a protective measure against

potential threats from humans. When triggered, the system promptly alerts beekeepers through email or SMS notifications, allowing them to take immediate action [63].

IoBee is a unique remote monitoring system that sets itself apart from other systems. This remote system does not include any temperature sensor or weight scale. Instead, it has a bee counter at the hive entrance to track bee traffic and detect any potential intrusions by pets or other animals. Moreover, IoBee has developed a specialized sensor to measure and control the density and diversity of pollinators within the hive. The purpose of integrating this sensor into the IoBee system is to decrease the need for manual labor by minimizing the need for frequent hive inspections. The collected data is then uploaded from the hives to the internet for easy access and analysis [65].

The seventh remote control system is APiS. This system is a comprehensive and advanced solution that includes multiple sensors to gather a wide range of data from beehives. This remote system offers extensive monitoring capabilities by having temperature sensor placed both inside and outside of the hives, humidity sensor and bee counter sensor. Some significant features of the APiS system include the ability to detect insufficient space within the hives, determine if larvae require additional food, track bee movements between apiaries, assess honey production levels pre- and post-harvest, monitor daily foraging activity, provide insights into queen behavior and egg-laying patterns, and even detect potential theft incidents from the colonies. The APiS system aims to provide apiarists with detailed information to support effective hive management and ensure the well-being and productivity of their colonies. [64].

In summary, the available remote monitoring systems offer similar functionalities and provide some useful information about temperature, humidity, and weight of honey in the hive. As previously discussed, most of these systems utilize some sensors to measure temperature and

humidity in colonies [60, 63, 64], while some systems incorporate additional sensors to detect bee movement, monitor bee population, and identify potential threats to the colonies [61, 62, 65, 66]. Temperature control is a crucial aspect of beekeeping, and it will be further discussed in Chapter 4, allowing apiarists to gather information about the brood nest and bee health based on temperature readings.

Some of the remote monitoring systems utilize specific sensors to count bees and detect their movements. In [61] and [65], a bee counter is applied at the hive entrance to count the bees and control bee population. In addition, Arina system [62] utilizes an acoustic sensor to determine bee activities precisely and safeguard colonies from swarming by notifying beekeepers of any irregularities. The APiS system [66] takes advantage of the newest technology and multiple sensors that provide a wide range of information. This enables beekeepers to stay informed about various aspects of colony, including queen egg laying and foraging level.

Another factor that some of the mentioned systems can monitor is ambient temperature around the colonies [63, 64]. These sensors measure the temperature, and if it falls outside of the desired range, the systems will send an alert to the beekeepers. This feature is particularly valuable during cold weather and winter months. When the temperature drops too low, bees tend to stay inside the colonies, and the level of the nectar decreases. In such cases, beekeepers need to provide food sources for the bees within the colonies.

The components developed in this thesis introduce new capabilities to the field of beekeeping. The capacitive sensing method outlined in Chapter 3 of this thesis can directly measure the level of honey on frames, potentially yielding more accurate results compared to the aforementioned systems. The presented sensor is also capable to measure the honey production at specific locations on a frame. The temperature sensor and heater systems discussed in chapter 4

enable precise temperature measurement and control on each comb, representing an advancement over previous systems that applied heat to the entire colony and relied on a single temperature sensor. An additional benefit of the system proposed in this thesis is its capability to assist in treating colonies against Varroa mites, by allowing beekeepers to raise the temperature in specific regions to kill the mites remotely. Honey can be produced naturally in this method, and beekeepers do not need to use any chemical pesticide.

2.8 Varroa Mite Background

The Varroa mite, formerly known as *Varroa jacobsoni*, was first discovered by A.C. Oudemans in 1904 within Western Honeybee colonies in Southeast Asia [91]. *Apis cerana* was a type of bees in Asia, and Varroa mite was a parasite of it. In the 1940s, the western honeybee, *Apis Mellifera*, was transferred to Asia, subsequently becoming infested with the Varroa mite [90, 91]. Initially, the Varroa mite was established in Africa and Europe, quickly spreading across the globe [90]. Dr. Denis Anderson has identified at least five species of Varroa mites, including Varroa destructor and Korean Varroa mite [90]. Scientists did an experimental study to find how Varroa mite spreads in beehives, by using of some colonies and monitored them for four years. The finding revealed a gradual increase in the number of Varro mites if preventive measures were not implemented, ultimately leading to widespread infestation across the colonies [92]. Notable behavioral differences between *Apis mellifera* and *Apis cerana*. While *Apis mellifera* bees are not able to fight with Varroa mites, *Apis cerana* worker bees possess the ability to confront, remove, and eliminate adult Varroa mites [93]. As discussed in [40], the developmental stage of *Apis cerana* worker bee is shorter compared to that of *Apis*, resulting in limited damage caused by Varroa mites. Varroa mites can only reproduce within the drone brood of *Apis cerana*, due to the shorter

developmental stage of worker bees, while the mites can reproduce rapidly in any brood cell in *Apis mellifera*. This allows Varroa mites to rapidly increase their population within beehives, causing remarkable damage to drone brood of *Apis mellifera*. In addition, the life cycle of Varroa mites depend on bees and their products. They cannot survive without the presence of bees.

2.9 Existing Methods for Treating Colonies Against Varroa Mites

Varroa mites, despite their small size, are visible to unaided eye, so beekeepers can see them when they attach to bees within the colonies. The number of mites inside of the colonies cannot increase rapidly after infections, and it will be slow in the first three years. However, after the third year, their life cycle accelerates, leading to a multiplication of their numbers [96]. The life cycle of Varroa mites is intertwined with that of bees. Adult female Varroa mites enter to both drone brood and worker brood to lay eggs, with each female capable of laying an egg as frequently as every 10 minutes. The female Varroa mite lays two to five eggs after bees seal the brood cell. The first egg laid by Varroa mite is a male, while the subsequent eggs are females. These mites feed on the bee pupae, and it takes around 5 days for the male Varroa mite and 7 days for female Varroa mites to develop. Mating occurs within the brood cell, and after a few days, the male Varroa mite dies. When the larvae are ready to emerge, mother and young female Varroa mites will emerge with it. The young female Varroa mites then move to other brood cell and lay eggs after around two weeks. Although adult Varroa mite can only survive for two months, they can destroy the honeycomb by their reproduction [97]. The mites can harm bees, and the resulting damages, as quoted in [102] includes:

- Reduced size and weight.
- Reduced life-span.

- Poorly formed wings.
- Reduced immunity to disease.
- Reduced resistance to pesticides.
- Reduced ability to feed.
- Reduced capacities for males to efficiently mate with queens.
- Reduced ability to perform their duties in the colony.

As previously discussed, safeguarding beehives from Varroa mites is crucial due to their ease of spread. Numerous methods have been developed to reduce mite population and eliminate them. Some methods are chemical and some are non-chemical. It is clear that non-chemical methods are preferable as they promote a healthier beekeeping environment. Some of these non-chemical methods are drone trapping, mesh bottom hive boards, splitting colonies, and using small cell size [16, 17, 98]. Methods to detect Varroa mites include the sugar shake method, sticky board method, alcohol wash, and drone brood inspection are commonly used to detect the presence of Varroa mite in beehives [99].

As discussed in [98], there are some non-chemical methods available to control the number of Varroa mites inside of the colonies. One of these methods is using a screened bottom board, which involves replacing the wooden bottom of a standard beehive with a wire mesh screen. Several studies have demonstrated a significant decrease in the number of mites when this method is employed [99].

Another effective non-chemical method is drone brood trapping. Drones are larger than worker bees and their development cycle takes longer. Beekeepers can leverage this advantage by placing special combs with drone-sized cells in their hive to attract mite to infest these cells. This method has shown significant success in reducing mite population within colonies [100].

Another non-chemical method is selecting bee breeds that exhibit greater resistance to mites. In this method, Beekeepers can assess their local conditions and carefully choose bee species that are better adapted and more resilient to Varroa mites. [101].

While beekeepers prefer to use non-chemical methods to protect colonies from the mites, there may eventually come a point when chemical treatments become necessary if the mite population reaches a critical threshold. Using chemical treatments are the last resort for beekeepers due to their negative impact on honeybees. It is important to note that while some chemical treatments break down relatively quickly within weeks to months, many of them can leave residues that persist for a long time, posing risks to the health and well-being of the colonies [102]. One of the chemical methods discussed in [99] involves the use of soft chemicals such as organic acids, essential oils, and hop beta acids. These substances are considered “soft chemicals” because they are naturally derived and can be used by beekeepers as a wax treatment. Soft chemical acids, such as organic acids and essential oils, offer a less harsh approach compared to synthetic chemical treatments, while still exhibiting efficacy in reducing Varroa mite populations. The advantage of using them is they do not have any chemical effect on honey production. One acid that can be utilized as a chemical treatment is formic acid. It occurs naturally in the venom of honeybees and can be applied in wax form to kill mites. However, there is a limitation to its use, as it can increase brood mortality if used at temperatures higher than 85°F [99]. Other acids that have been used are Oxalic acid and Thymol. Beekeepers typically use these acids when their colonies are empty, and excessive use can have detrimental effects on both bees and larvae [99, 100]. Potassium salts of hops beta acid, derived from the hops plant, can also be utilized as a treatment option throughout the year. Unlike other soft acid treatments, this acid does not penetrate the cells, and its impact on colonies is not as pronounced [99].

While chemical treatment can protect colonies from Varroa mites, they come with drawbacks such as cost and potential negative effects on bees and honey production. Due to these concerns, beekeepers are increasingly inclined to explore non-chemical treatment for eradicating Varroa mites. However, non-chemical methods do not result in all Varroa mites being eliminated. An alternative method is heating treatment, which can be considered a non-chemical method. Heat can be used to kill Varroa mites, by raising the temperature above 47°C, as the mites are unable to survive under such conditions. In this method, hives are placed in a heat chamber one time per year to eliminate the Varro mites by increasing the temperature over 47 °C [101]. However, there is a problem in this method, as adult bees are unable to withstand temperature exceeding 45°C, and brood mortality occurs around 38°C. Therefore, all bees and larvae will be destroyed by increasing the temperature of 47°C. Despite this drawback, heat treatment is a natural treatment, and beekeepers prefer to use this rather than chemical methods [40].

One of heating method for killing Varroa mites within colonies is using Linhart's thermosolar. This method involves the use of a multiple-story hive that is sealed using wood and glass, and two heating systems to warm the colonies up. Two temperature sensors are utilized to control the temperature within brood cells. In this method, once temperature reaches to 47 °C, the roof is put in place to maintain the temperature at 47 °C inside of colonies for a duration of 150 minutes. Following this step, the colonies are inspected, and if there are any Varroa mites left, a fumigation process is implemented to eliminate the remaining mites [103]. Heating has proven to be an effective natural method to control Varro mite, as it has been used for more than 20 years in Eastern Europe. In 1987, Karpov and Zabelin conducted a study where bees were removed from colonies, and the combs were placed in a chamber. The temperature rapidly increased to 46-48°C for a duration of 2-15 minutes to kill the mites. According to a study that has been done by Hoppe

and Ritter, this method can only eliminate 23% of the mites population, and between 85-95% of the mites fall from bees. This method is useful in beekeeping because it restricts the movement of mites within the combs, limiting their ability to spread throughout the colony [104].

MiteZapper® is an innovative heating treatment method that has gained popularity worldwide. This method combines a heating element and mite biology within the comb to eliminate Varroa mites. Unlike traditional heating chambers, the MiteZapper method utilizes an electrically heated frame of drone comb with a foundation, which is strategically placed within the brood box of the colony. This frame contains built-in heaters and is connected to an external 12V battery located outside the colony. This battery is enough to increase the temperature around 47°C to kill the mites. This process typically takes 1-5 minutes to effectively eliminate the mites and drone pupae. This process should be repeated approximately five times during the brood rearing season, which occurs every 18-23 days. One notable advantage of using MiteZapper is that beekeepers do not need to invest a significant amount of time, as it is comparatively shorter treatment compared to other method mentioned earlier. After using MiteZapper once, it can be used again to achieve a further reduction in the mite population. Subsequent applications of MiteZapper have been shown to effectively eliminate approximately 89-95% of the mites without the need of additional chemical or non-chemical methods [105].

Heating methods prove to be more advantageous compared to other natural and chemical methods. Chemical treatments can have adverse effects on honey production and may persist in beeswax, potentially causing some problems and diseases for bees. On the other hand, heating methods do not interfere with honey production, ensuring a natural and uncontaminated product. The only disadvantage of using heating method is beekeepers need to do it regularly during

seasons. For instance, beekeepers need to insert MiteZapper into each hive two or three times per year, requiring connection to electrical power for around eight minutes to eliminate the mites.

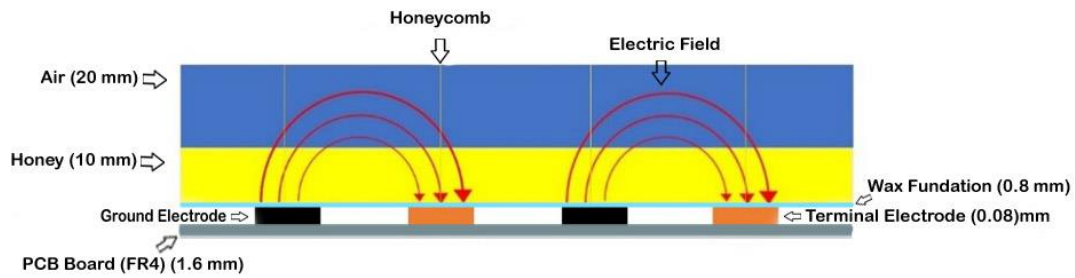
Therefore, the use of heating methods can be time-consuming, especially for beekeepers with larger numbers of colonies. Another disadvantage of using MiteZapper is that when the system starts to eliminate the mites, it will destroy all things on the frame while the mites were not in all regions of the frame, and the system does not necessarily need to heat all regions [105]. To address this issue, it is crucial to implement individual control measures for each region of the hive frame. For instance, if beekeepers identify Varroa mite on one side of the frame, they only need to focus to increase temperature on that specific side and leave the other regions without any changes. Therefore, implementing localized temperature control by using an array of heaters on the beehive frame can offer an optimal solution for beekeepers. This approach ensures that bee health and honey production are safeguarded. By using this system, beekeepers can save time to detect and eliminate Varroa mite. Whenever the system detects the presence of mites, it could immediately raise the temperature in that specific area to 47°C, effectively killing the mites and preventing their proliferation.

Chapter 3: Cell Contents Monitoring within the Hive Supers and Brood Nest

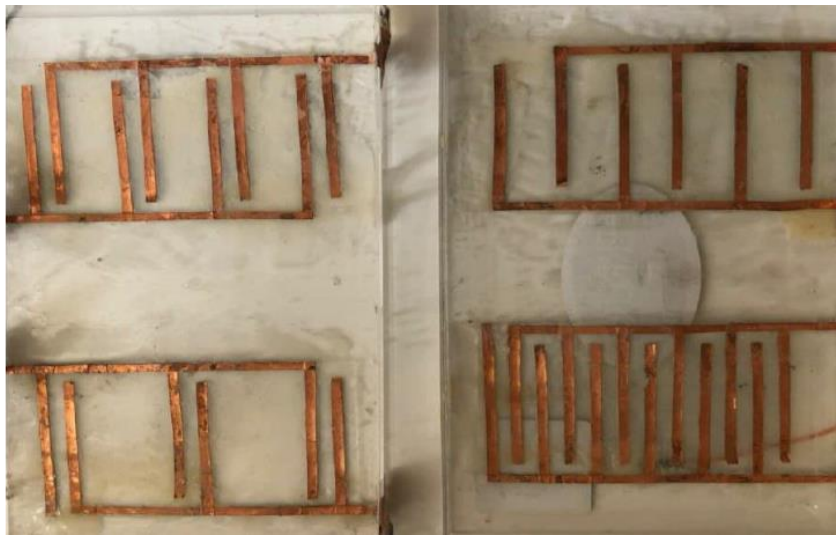
This chapter discusses the use of a capacitive based sensor system to measure honey level in hives and to monitor the growth of the brood. The system employs an interdigitated capacitance sensor (IDC) arrangement on the surface of the frames inside the hive. It is designed and tested to explore remote monitoring applications:

1. The thickness of the honey can be measured with this remote monitoring system. This will assist beekeepers to determine when the combs are full of honey so that they can harvest the product.
2. This system also enables the monitoring of the growth of larval brood within the brood box as they develop. This information can help to assess the overall health of the bee colony and future population.

The IDC sensor is composed of arrays of conductive wires separated by an insulating material. This sensor is fabricated on the surface of the frames. When the frame is empty of honey, a distinct capacitance is present. As the bees deposit honey on the frame's surface, the capacitance changes, enabling beekeepers to monitor colony activity. Figure 3.1 illustrates the utilization of copper tape in creating the IDC sensor. Sensor performance was evaluated through simulation and experimentation by using honey and air to cover the surface of the frame.



(a)



(b)

Figure 3.1 (a) Side view relative to the honeycomb. (b) Top view of prototype IDC boards.

Section 3.1 provides some background about the process of producing honey, and factors that can affect this process. It discusses physical and electrical properties of honey that can cause change in capacitance. In addition, this section introduces existing capacitance sensors used. Section 3.2 contains initial simulations and designs of prototype boards along with the results obtained from the lab tests. This part presents the outcomes from a small prototype of IDC sensor system, which employs 12 separate sensing regions across the IDC sensor board. Section 3.3

focuses on the design of the 12 capacitive sensors of the IDC sensor board prototype and shows the results of lab tests conducted.

3.1 Background

With the expanding human population, apiarists are compelled to enhance both bee and honey production to meet the growing demand for human sustenance. A remote-control hive monitoring system emerges as a valuable tool to alleviate the necessity for constant human oversight of beehives. This system reduces labor time and cost by implementing sensor systems.

3.1.1 Honey Production Process

Honey processing is a difficult operation, in which time and patience are required to achieve the best results. First honeybees fly out of the hive in pursuit of nectar from rich flowers. Subsequently, they ingest the liquid nectar from flowers and deposit it into their specialized organ known as the honey stomach. Bees continue to drink liquid nectar until their honey stomach is fully laden. Bees are remarkable flyers with the ability to transport a nectar payload equal to their own weight. They need to visit approximately 50 to 100 flowers per trip from the hive. In times of hunger, they can rely on the nectar stored in their stomachs as a food source. This is facilitated by a valve situated in the nectar sac, which can be opened to enable a portion of the nectar to flow into their personal stomach. The collected nectar has a sugar concentration of around 30 percent, and it can provide enough energy for bees to make their way back to the hive. When the nectar is in the honey stomach, it will mix with the bee enzymes and the enzymes begin to break down the complex sugars of the nectar into simpler sugars. This process is known as inversion. When bees

return to the hive, the nectar will be passed to another bee by regurgitating into the other bees' mouth. This cycle continues as bees collaborate to convey the nectar to the honeycomb. The stored nectar contains a certain water content. Bees engage in a process of water evaporation, reducing the water content from 70 percent to 20 percent by fluttering their wings. Another advantage of fanning is to increase the hive temperature between 33°C and 36°C, which is essential for sustaining ongoing honey production. When individual cells are full of honey, the comb cell will be meticulously sealed with a secretion of liquid from the bee abdomen to protect the honey from air and water [67 – 68].

Numerous factors can effect the amount of honey production, and these factors can be categorized into two main groups. The first category is Anthropogenic and climatic factors such as depletion of honeybee fodder, colony losses, dwindling of water sources and decreased honey output. The second category pertains to environmental elements, including access to water sources, appropriate rainfall levels, Varroa mite infestation, and variation in temperature and humidity [69]. As discussed in [69], alterations in temperature and humidity can affect the honey production process. The humidity level within the hive can fluctuate within the range of 20-80 %, leading to challenges in honey production. In addition, if the temperature drops, bees need to intensify their wing-fanning activity to elevate hive temperature.

Once nectar is transferred into honey and securely sealed with beeswax, beekeepers can harvest the production. They extract the complete frame from the hive and remove the wax cap and collect the honey from cells. These combs have capacity for multiple uses, providing beekeepers with the opportunity to economize on production time. Another advantage of reusing these combs is bees do not need to make the comb base, and they just need to spread out unripe honey to increase the ripening rate.

The processing of harvesting honey introduces stress for the bees and temporarily halts honey production. Beekeepers need to consistently inspect the hive to remove frames filled with honey. Nonetheless, situations may arise where frames are either empty or only partially filled, further exacerbating stress on honeybees. Therefore, a remote control monitoring system presents itself as a practical solution to assist both beekeepers and honeybees. This technology can detect when the combs reach full capacity and subsequently send an alert to beekeepers for harvesting the production. This approach empowers beekeepers to remotely track the level of honey, thereby minimizing their physical presence at the apiaries until the honey is fully rip and ready to harvest [70].

3.1.2 Physical and Electrical Properties of Honey

While bees prefer to drink nectar with higher sugar concentration level, they encounter a diverse array of plants with different level of sugar and water concentration [40]. Honey is composed of fructose (38%), glucose (31%), water (17%), maltose (7%), and small amounts of trisaccharides, other higher carbohydrates, sucrose, minerals, vitamins, and enzymes [71].

The Canadian Food Inspection Agency has established three honey grades in Canada, designated as Canada No. 1, Canada No. 2 and Canada No. 3. In order to guard against fermentation, Canada No. 1 grade must not exceed 8% of moisture (water) or not more than 18.6% of moisture if it is pasteurized. Canada No. 2 grade should not surpass 18.6% of moisture and not more than 20% if subjected to pasteurization. The third grade must contain no more than 20% of moisture [72]. As stated in [69] that honeybees are capable of producing honey only from nectar with a sugar concentration of 80% or higher, because of the chemical reactions of their enzyme

with nectar. In addition, the honey should not be exposed to humidity levels over 60%, because it will absorb water, consequently leading to a reduction in its concentration.

There are various types of honey with differences sugar concentration, which subsequently impact their electrical traits. Relative permittivity (ϵ_r) is distinct for each substance, and it is an indicator of the relative amount of charge that can be held by the material compared to a vacuum [74]. As mentioned, IDC sensor incorporates a dielectric between its conducting wires. The amount of charge stored on a capacitor is related to the dielectric material's properties. More charge accumulation occurs when materials have a higher relative permittivity [74]. The relative permittivity of air is 1, while water has a relative permittivity of around 80. Honey has relative permittivity of 23 [75]. When the honeycomb cells are empty, the space above two sensing wires on the IDC is air and a low capacitance will be measured. As bees gradually bring some nectar and make some honey in the honeycomb cells, the capacitance will increase step by step until the cells are full. After this, the bees start to evaporate water from the honey, and the capacitance will decrease. Therefore, beekeepers can monitor many processes as this system can report when the cells are empty or full, and beekeepers are able to also observe the ripeness of the honey. This sensor system could send an alert to beekeepers when the cells are full, and beekeepers can harvest the production.

3.1.3 Capacitance of Brood Cells

The IDC sensor can also be used in brood cells to monitor larva and eggs remotely. Before the queen lays eggs, the cells are empty, and most spaces are full of air, and the capacitance is in the lowest possible amount. When the queen starts to lay eggs in the cells, the relative permittivity

in the cells changes and increases. The next step is growing larvae in the cells, which will further increase relative permittivity. The relative permittivity of larvae is unknown, but it is more than the relative permittivity of air and closer to water. Another change in relative permittivity is when the cocoon becomes pupa, which is the last change in the brood cell before the adult bees emerge from the cells. Although the capacitance of eggs, larvae and pupa are unknown, bees have a constant timeline for each growth step, and beekeepers can determine the situation in the hive based on the timeline and change in the capacitance.

3.1.4 Existing Capacitance Sensor Systems

In this thesis, an IDC capacitance sensor was chosen to monitor level of honey and growth of larvae in the hive remotely. This type of sensor was used for many other purposes in the past. Some examples are given below.

An interdigitated capacitance sensor similar to the sensor described in this thesis is used in food applications. For example, Phimphisana and Sa-ngiamvibool used an IDC sensor inside of a glass of milk to determine the water content of the milk [76]. In addition, Lawton and Pethig used capacitance sensors to determine the fat content of milk [77], and Felice et al. used capacitance sensor to measure the bacterial content of milk [78]. All these papers are based on the fact that the relative permittivity of liquid changes when its composition changes. Therefore, IDC sensors would be useful to detect the level of honey for beekeeping. They can also be used to detect the water content in honey, which decreases as the honey ripens, and so changing its relative permittivity.

In [80], an interdigitated capacitance sensor similar to the sensor described in this thesis was designed by Angkawisittpan and Manasri to determine sugar content in a solution. They placed the sensor inside of a beaker, which contains solution, and for the first try, a high-pass filter was used to measure the capacitance. They tried this process with different frequencies to determine which frequency can give the most accurate result, the concentration of sugar in this method was between 10 and 50 percent, and it was found that the capacitance decreased by decreasing the sugar concentration.

In [81], Guo et al. investigated the effects that water content had on the dielectric constant of different types of honey. They tested various types of honey and found that the dielectric constant increases linearly with water content when measured at the same frequency [12].

Another IDC sensor was built by Beynon in 2017 [106], which was similar to the method in [85] and [86] with a specific electrode width and gap between the electrodes. 5 mm was set for width of the electrodes and the gap between them, and capacitance was measured when the level of nectar and honey were increased.

As mentioned before, capacitors have specific saturation levels based on width of the electrodes, gap between them and materials between the electrodes (Figure 3.2). Early designs faced challenges as they were unable to detect changes in the level of honey when they reached 8 mm or more. Instead, they showed a constant capacitance reading, and there was not any variation. In these early designs, a specific electrode spacing was chosen, and it had a resolution problem in the capacitance signal, and for larger honey thickness there was a signal drop-off. This thesis addresses this issue by designing a new IDC sensor with a different shape that does not suffer this problem. This is discussed in section 3.2.1.

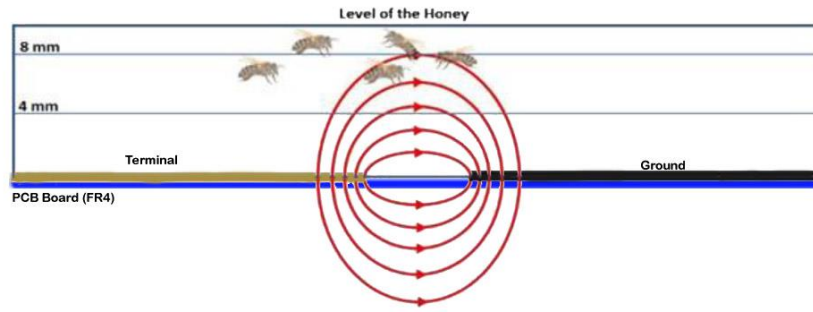


Figure 3.2 Electric field due to stored charge between the electrode terminals.

3.1.5 Interdigitated Capacitor Sensor

Capacitance is a measure of electrical energy stored in an electric field between its plates. In general, the formula $C = Q/V$, can be used to determine the amount of charge (Q) that can be stored on each capacitor plate per unit of voltage difference between the plates [84]. Figure 3.3 shows a parallel plate capacitor design, where the following equation can be used to measure its capacitance:

$$C = \frac{\epsilon_r \times \epsilon_0 \times A}{d} \quad (3.1)$$

where A is the area of the two plates, ϵ_r is the dielectric constant of the material between the plates, ϵ_0 is the permittivity of free space ($8.85 \times 10^{-12} \text{F/m}$) and d is the distance between the plates (in meters).

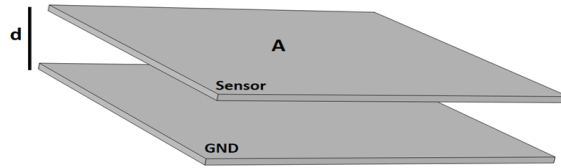


Figure 3.3 Parallel Plate Capacitor

The fabrication of interdigitated capacitor sensors is easy because of their planar structure. It can be easily integrated with other sensing components and signal processing electronics. As shown in Figure 3.1 and Figure 3.3 an interdigitated capacitor sensor contains two electrodes (ground and terminal) with a main line and electrode fingers that extend producing electromagnetic fields between each of the electrode fingers.

In [85], Endres and Drost developed the formula and the total capacitance of interdigitated capacitor sensor:

$$C_{IDC} = C_{UC}(N_E - 1)Lq \quad (3.2)$$

- C_{IDC} = The capacitance of an interdigital capacitor
- N = The number of electrodes (terminal and ground)
- L = Length of the electrodes
- C_{UC} = capacitance of a two-dimensional unit cell

C_{UC} is composed of three partial capacitances C_1 , C_2 and C_3 by permittivities ϵ_1 , ϵ_2 and ϵ_3 respectively. The upper and the lower capacitances can be calculated by using a complete elliptic integral, as the transformation:

$$C_1 + C_2 = \varepsilon_0 \frac{(\varepsilon_1 + \varepsilon_2)}{2} \frac{K[(1 - (\frac{a}{b})^2)^{\frac{1}{2}}]}{K[\frac{a}{b}]} \quad (3.3)$$

- C_1 = Capacitance above the electrodes.
- C_2 = Capacitance below the electrodes.
- ε_0 = Free space permittivity constant.
- ε_1 = Relative permittivity of the material above the electrodes.
- ε_2 = Relative permittivity of the material below the electrodes.
- K = A complete elliptic integral of the first kind.
- a = Distance between electrode fingers.
- b = Distance between the center of one electrode and center of the next electrode.

The volume between the electrodes is treated, as C_3 with permittivity of ε_3 :

$$C_3 = \varepsilon_0 \varepsilon_3 \frac{h}{a} \quad (3.4)$$

- h = Thickness of electrodes.
- ε_3 = Relative permittivity of the material between the electrodes.

$$C_{UC} = C_1 + C_2 + C_3 \quad (3.5)$$

- C_1 = Capacitance above the electrodes.
- C_2 = Capacitance below the electrodes.
- C_3 = Capacitance between the electrodes.

These equations reveal that capacitance is highly sensitive to the relative permittivity of the material above, below and between the electrodes. Therefore, when nectar and honey deposits onto the cells, capacitance increases due to the elevated relative permittivity. In total, the total capacitance (C_{total}) can be adjusted by varying the gap between the electrodes (C_{uc}). Additionally,

if the unit cell width ($b = \text{gap width} + \text{electrode width}$) decreases, the amount of capacitance between the electrodes will increase.

IDC capacitors will have a saturation level in terms of the distance above their surface that they can effectively measure a change in permittivity. In [86], Kim and Lee investigated the maximum depth to which the electric field can penetrate into the substance above. These equations revealed that anything exceeding this saturation level cannot be detected, resulting in a constant capacitance. Additionally, increasing the gap width will lead to an increase in electrode width, and conversely, reducing the width of the electrodes will decrease capacitance. Therefore, there is a disadvantage in using this method as capacitance will approach a constant value when the material thickness over the sensor increases. Consequently, the sensor becomes limited in its ability to detect levels beyond a saturation threshold.

3.2 Initial Simulations and Prototype Board Design

As mentioned previously, several factors must be taken into account when designing IDC sensors for beekeeping. These factors encompass the number of bees, dimension of IDC sensor, honey production process and other relevant considerations. These initial simulations aimed to establish an understanding about IDC sensor and how beekeepers utilize it to determine liquid level.

3.2.1 Simulations

In this thesis, multiple IDC sensors designs were simulated using COMSOL Multiphysics software to study their performance in measuring liquid on top of the sensor board. A region of a

honeycomb frame (105 mm x71.66 mm) was simulated as a PCB board, utilizing the FR4 material selected in COMSOL, with a thickness of 1.6 mm. Copper tape with a width of 3 mm and thickness of 0.08 mm was employed to make capacitor electrodes. In these simulations, one electrode was grounded, and the other was set to 5V. These simulations focus on the distance between the electrodes and several shapes of capacitors were made to measure the level of liquid from 1 mm to 10 mm. In all IDC sensor simulations, the width of electrodes was set to 3 mm.

3.2.2 2D simulations Results of IDC Sensors

All designs were simulated in 2D using COMSOL Multiphysics to obtain results regarding the capacitance changes with increasing liquid level. In the first IDC sensor design, the space between electrodes was set to 5 mm. As shown in Figure 3.4, 2D of first simulations were performed to get a better understanding of the IDC sensor. The capacitance signal starts to saturate for liquid thicknesses over about 5 mm.

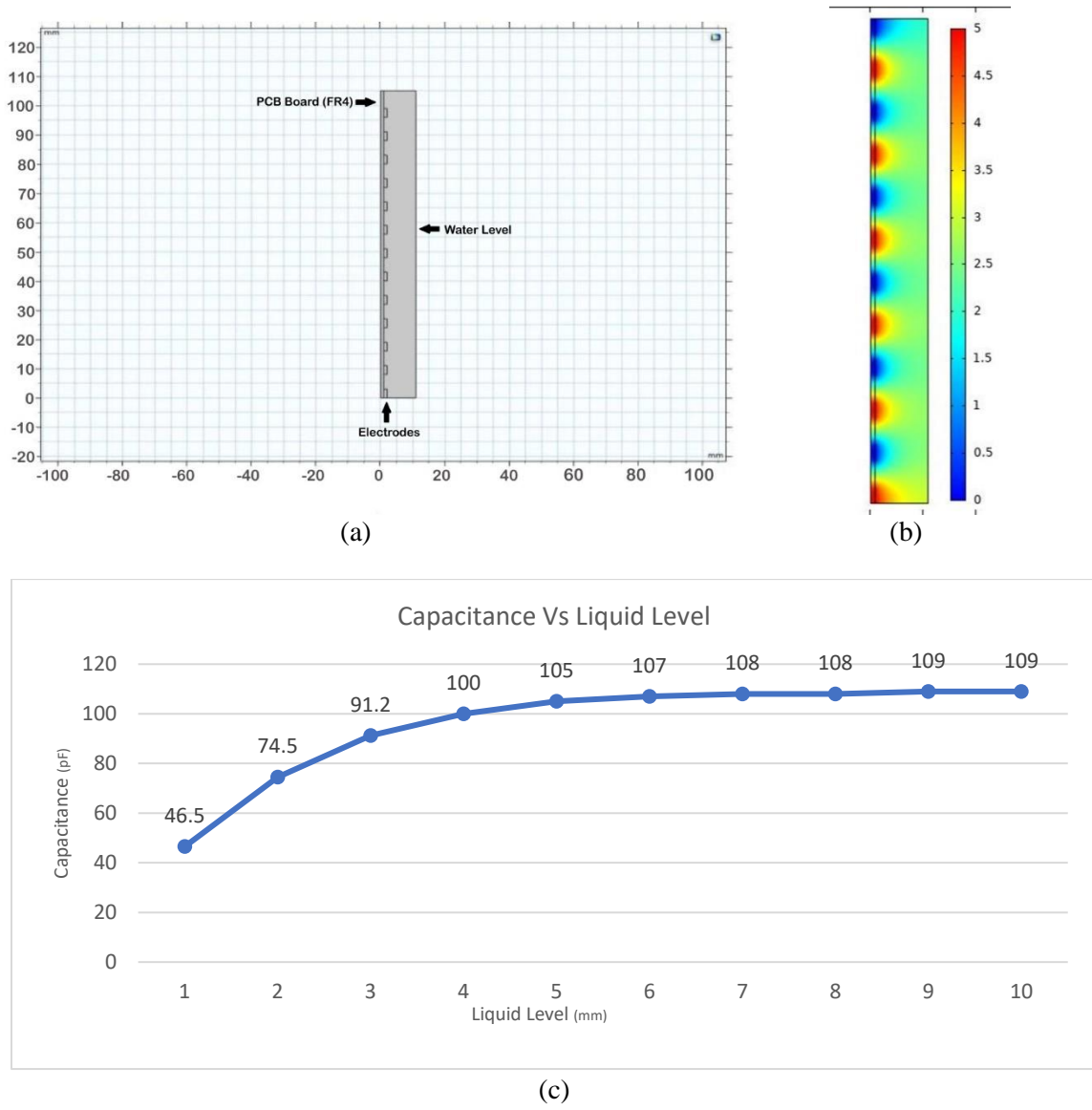
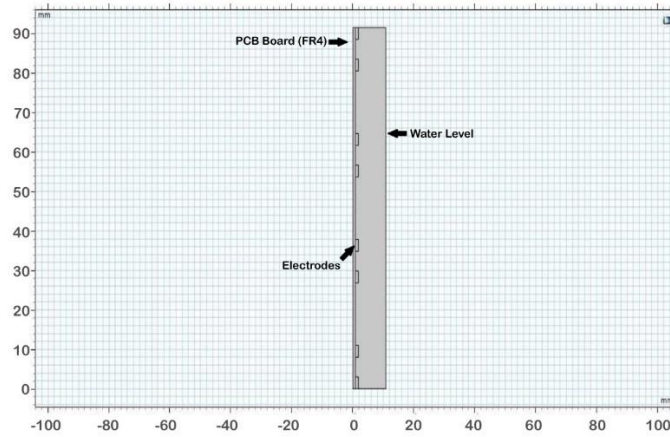
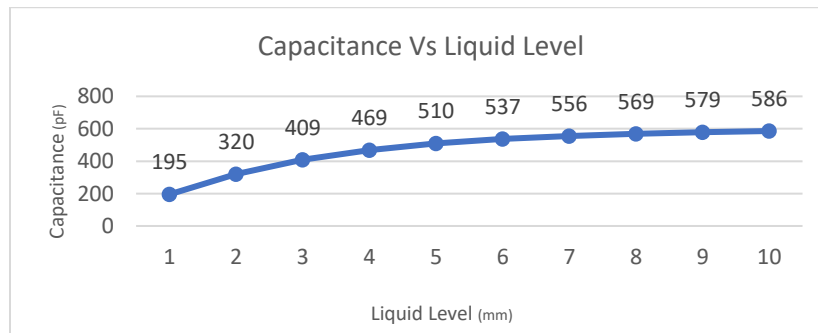


Figure 3.4 (a) 2D simulations of the first IDC sensor with water block on top of the IDC sensor. (b) Heat map of first IDC sensor, showing electric field values in V/m. (c) Capacitance changes when water level goes up from 1 mm to 10 mm.

In the second sensor design as shown in Figure 3.5, the width of electrodes was the same as the first simulation (3 mm), but two different spacings were used between the electrodes, 5 mm and 16 mm. Therefore, this simulation includes two different capacitors spacings and eight electrodes were used in this simulation. The intent of having two separate spacings was to explore the possibility of having good sensitivity as small liquid thicknesses, while reducing signal saturation at larger liquid thicknesses. We can see that signal saturation is reduced significantly, becoming noticeable after about 7 mm liquid thickness, and that there is a more linear response for small liquid thicknesses.



(a)

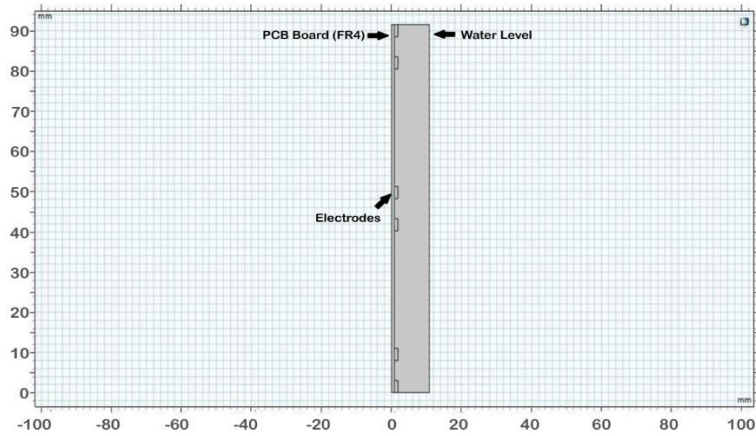


(b)

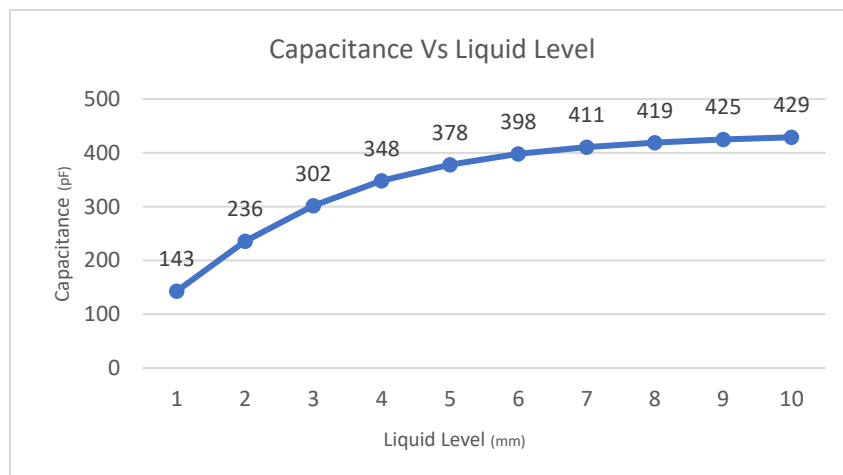
Figure 3.5 (a) 2D simulations of the second IDC sensor with water block on top of the IDC sensor. (b)

Capacitance changes when water level goes up from 1 mm to 10 mm.

In the third sensor design, the distance between the electrodes was increased again. The IDC sensor was simulated for two different electrode distances set to 5 mm and 30 mm, and liquid level increased from 1 mm to 10 mm (Figure 3.6). For this design we can see that there is increased sensitivity at low liquid thicknesses, but saturation effect is noticeable after 7 mm liquid thickness.



(a)

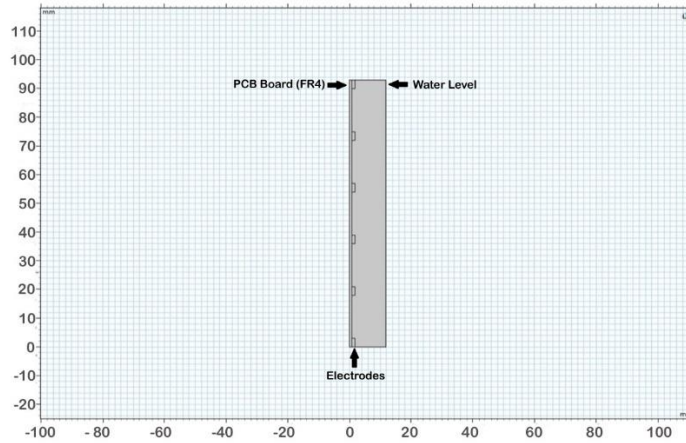


(b)

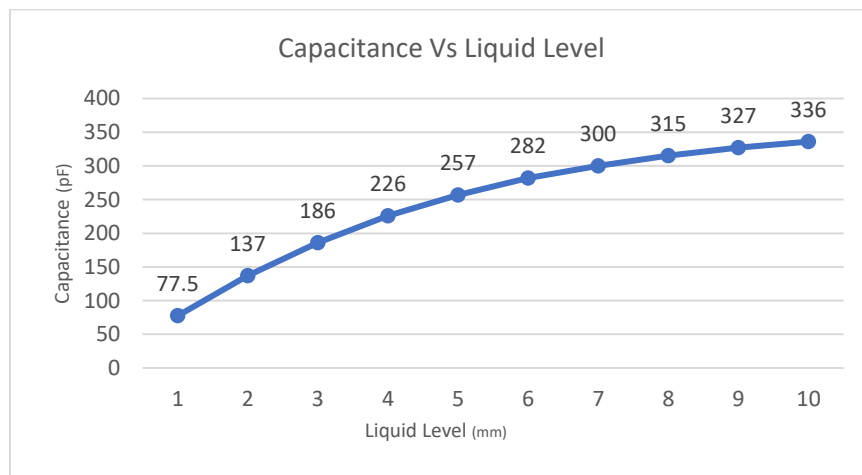
Figure 3.6 (a) 2D simulations of the second IDC sensor with water block on top of the IDC sensor. (b)

Capacitance changes when water level goes up from 1 mm to 10 mm.

Figure 3.7 shows the fourth sensor design and its results as the distance of electrodes was set equal as 15 mm. Six electrodes were simulated for liquid level increased from 1 mm to 10 mm. This design has a more linear response with reduced saturation effect at larger liquid thicknesses.



(a)



(b)

Figure 3.7 (a) 2D simulations of the second IDC sensor with water block on top of the IDC sensor. (b)

Capacitance changes when water level goes up from 1 mm to 10 mm.

In all of these simulations, capacitance was measured when water was added from 1 mm to 10 mm step by step. A noticeable difference would exist between the capacitance measurement when the IDC sensor measures the level of water and the level of the honey due to their different relative permittivity values. The relative permittivity of water and honey is 80.1 and 24, respectively. Consequently, a higher capacitance reading is recorded with water than with honey. Although, the changes in capacitance are minimal, within the picofarad range, the simulations demonstrate the feasibility of employing this method to measure the levels of both honey and water.

As shown in Figure 3.8, there may be some bees around the comb. Although the impact of bees walking above the comb can affect the amount of capacitance, for a small number of bees this effect would be relatively minor compared to the impact of increasing the level of liquid. As previously mentioned, the rate of change in capacitance is much larger when the level of liquid was between 0 mm and 3 mm than between 7 mm and 10 mm. Therefore, the existence of bees, residing on a thick layer of honey, would not have a significant effect on the capacitance result.

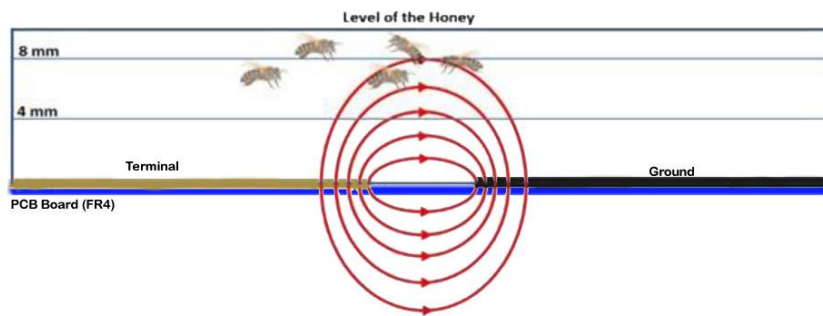


Figure 3.8 Existence of bees on top of come.

3.2.3 Comparison of sensor designs:

Table 3.1 shows simulated capacitance for various water levels for all for sensor designs. We can see that the change in capacitance begins to level off at approximately 7 mm of water for designs 1 and 2 and 3, but less so for design 4. Consequently, for designs 1-3 the signal from the IDC sensor starts to drop-off at larger liquid thicknesses, posing a challenge when measuring progressively higher water levels.

Table 3.1 Results of capacitor simulations for water levels from 1 mm to 1 cm.

Level of Liquid	First Design (pF)	Second Design (pF)	Third Design (pF)	Fourth Design (pF)
1 mm	116.2	80.3	94.2	170.7
2 mm	182	86.7	105	188.3
3 mm	210.1	91	111.5	202.3
4 mm	218.5	94.2	121.4	218.5
5 mm	237.4	97.5	130	237.4
6 mm	248.2	107.1	133.2	248.2
7 mm	249	109.2	136.5	260.1
8 mm	253.1	109.2	140	273.1
9 mm	273.1	109.2	147.6	287.4
10 mm	273.1	111.5	151.7	303.4

Figure 3.9 shows the results for all four designs compared to each other. In Figure 3.10, all simulations are presented with their capacitance values normalized to 1 at 10 mm water thickness to better compare each sensor to the others. While each sensor design demonstrates an increase in capacitance as water is added, the fourth design exhibits a more linear performance curve, showing

that it can more accurately measure the specific capacitance for each level of water compared to the other methods.

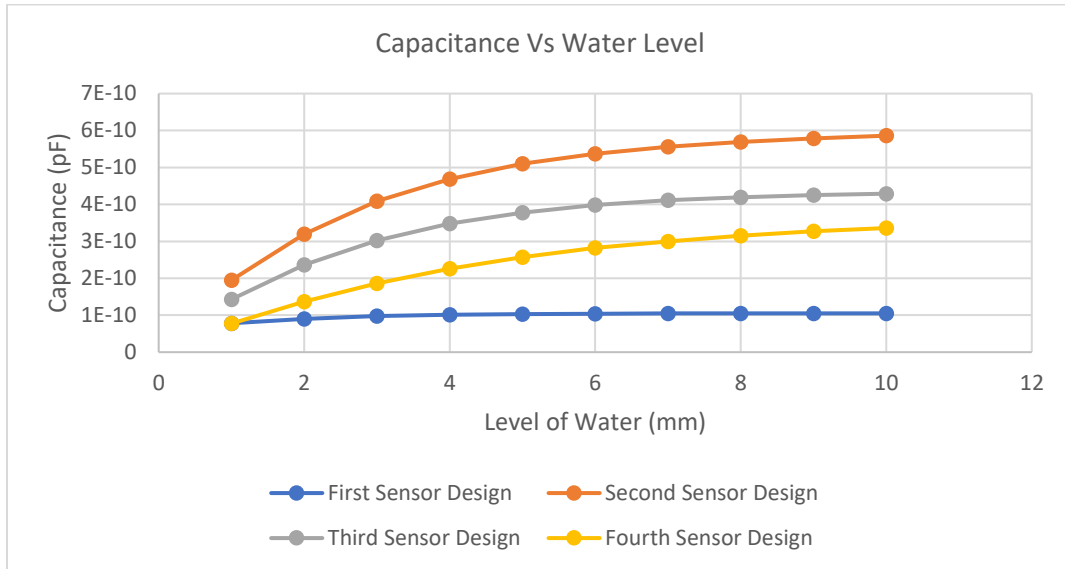


Figure 3.9 All four IDC designs compared.

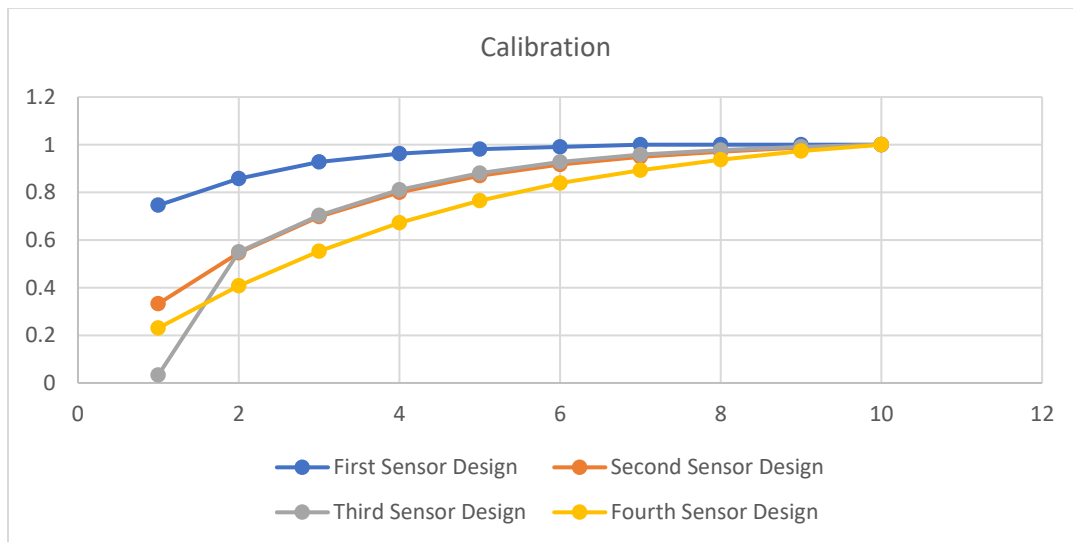


Figure 3.10 Comparison of all designs with normalized data.

In summary, based on these initial simulations, it was determined that the capacitance will change in picofarad range across the IDC sensor by increasing liquid level. Furthermore, it was also discovered that the capacitor sensors exhibit higher sensitivity to a change in liquid thickness when the liquid level is low. The fourth IDC design showed better linearity and reduced saturation effect for liquid levels up to 10 mm.

3.2.4 3D simulations Results of IDC Sensors

The 3D simulations of IDC sensors were conducted in COMSOL to emulate real IDC sensors and corroborate the findings from the 2D simulations. As indicated by the results in Table 3.2, the 3D simulations of IDC sensors yielded results that were very similar with those from the 2D simulations.

Table 3.2 Results of capacitor simulations for water levels from 1 mm to 1 cm.

Level of Liquid	First Design (pF)	Second Design (pF)	Third Design (pF)	Fourth Design (pF)
1 mm	111.8	77.9	92.3	168.2
2 mm	178.8	85.9	101.3	185.5
3 mm	205.8	88.6	106.7	198.1
4 mm	215.2	91.3	115.3	207.9
5 mm	233.5	94.6	126.6	229.3
6 mm	242.8	102.5	129.8	241.7
7 mm	239.9	105.9	131.3	253.9
8 mm	242.8	106.7	136.1	262.5
9 mm	244.2	108.9	140.5	273.9
10 mm	244.2	109.7	145.3	292.9

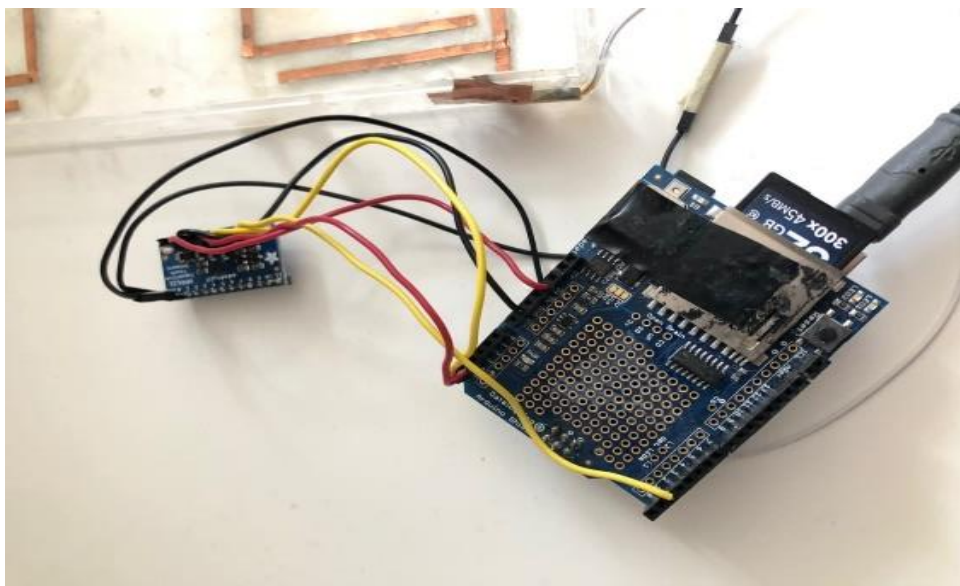
The 2D and 3D capacitance simulations yield nearly identical results. This similarity arises due to several factors. Firstly, in scenarios where the primary capacitance changes mainly occur within the 2D plane, such as variations in a planar surface, both 2D and 3D simulations capture these effects accurately. Additionally, if out-of-plane effects on capacitance are minimal compared to in-plane effects, both methods provide reliable results.

3.2.5 Design and Test of a Small Prototype Board

A small board of IDC sensor for all four sensor designs was constructed to validate the design concepts and obtains results for comparison with the simulation outcomes, as depicted in Figure 3.11. As mentioned before, the width of electrodes was 3 mm for all sensor designs, with one electrode grounded and the other voltage biased to establish an electric field between the electrodes. Copper tape was also employed to create the electrodes, and the distances between them were set as mentioned before for each IDC sensor. An analog IDC sensor could be used to measure the capacitance on the small prototype board, however the whole frame is divided to 12 regions and a separate IDC sensor is needed to measure the capacitance for each region separately. Electronics for 12 analog sensors must be prepared if analog sensing is used for getting the capacitances. An Arduino was used to collect the data from each capacitor sensor. This method costs more due to the need for 12 IDC sensors and associated electronics.



(a)



(b)

Figure 3.11 (a) A small board of IDC sensor for all four sensor designs (b) The IDC sensor with an Arduino UNO.

In order to reduce the number of parts required, a digital capacitive touch sensor, MPR121, was used to measure the 12 IDC electrodes. The MPR121 was chosen because it operates with a supply voltage range of 1.71 to 3.6 V and utilizes an I2C interface, which is compatible with the Arduino UNO platform. This sensor also boasts 12 capacitance sensing inputs with -40 °C to +85 °C operating temperature range which will be suitable in this thesis [87]. Therefore, one MPR121 will be enough for the entire honeycomb frame, eliminating the need for any additional signal conversion electronics. To create the capacitors, a copper tape with 3 mm width was employed. The capacitor board was assembled on a plastic container, allowing for addition of water. These capacitors were then connected to the capacitor sensor. As shown in Figure 3.11, each capacitor is connected to two wires, one is the ground, which is connected to MPR121 ground pin, and the other connected to a pin between zero and 10 in MPR121 to measure the capacitance. A thin layer of silicone was applied on top of the copper tape to simulate beeswax. MPR121 was connected to an Arduino UNO to send measurements to the Arduino and an SD card was connected to the Arduino to store the collected data on it. Capacitance measurements were taken by gradually adding water from 1 mm to 10 mm. As expected, it can be seen that the capacitance increased linearly by increasing the water level.

A program was developed to record the data during capacitance measurements. The program gathered data every 3 seconds and 30 minutes and stored the obtained data on an SD memory. The program used for measuring the capacitance can be found in Appendix A.

The capacitor charging process follows a characteristic exponential curve when charged by a fixed voltage. Initially, when a capacitor is connected to a fixed voltage source, it starts charging rapidly. The voltage across the capacitor increases exponentially, while the current flowing through it decreases exponentially. This initial rapid charging phase is depicted by a steep

slope on the charging curve. As the charging process continues, the voltage across the capacitor approaches the voltage of the source, and the current decreases further. Eventually, the capacitor reaches a state of saturation where it is fully charged and the voltage across it is equal to the voltage of the source. At this point, the charging curve levels off, indicating that the capacitor has reached its maximum charge for the given voltage.

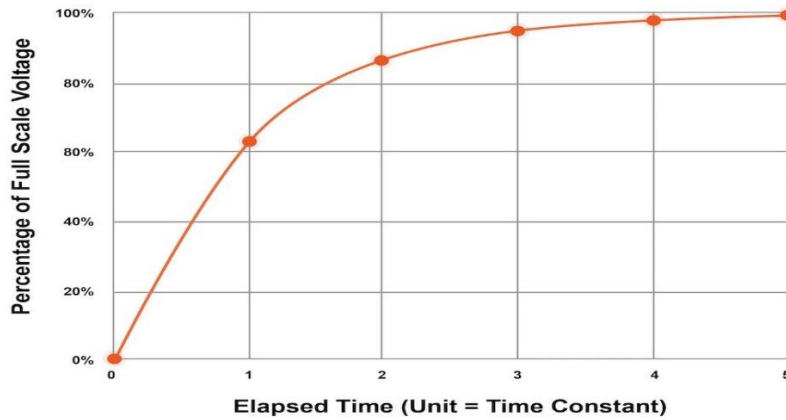


Figure 3.12 A plot of the capacitor voltage over time for the charging circuit.

According to [87], a capacitor’s value can be measured by applying a specific current for a brief duration in the linear charging region of the capacitor’s response curve. Over this amount of time (T), if the current is known and the capacitor voltage is measure, the capacitance C can be found using:

$$C = \frac{Q}{V} = \frac{I \times T}{V} \quad (3.6)$$

where Q is the amount of charge, V is the voltage measured across the capacitor, I is the charge current, and T is the charge time.

According to [88], the valid ADC range can be measured by:

$$ADC_{low} = \frac{0.7}{V_{DD}} \times 1024 \quad (3.7)$$

$$ADC_{high} = \frac{V_{DD}-0.7}{V_{DD}} \times 1024 \quad (3.8)$$

The minimum and maximum ADC values are used to calculate the valid range for capacitance; therefore, the maximum and minimum capacitance values will be:

$$C_{low} = \frac{I \times T}{V_{DD}-0.7} \quad (3.9)$$

$$C_{high} = \frac{I \times T}{0.7} \quad (3.10)$$

Therefore, measurable capacitance can be calculated by:

$$C = \frac{I \times T \times 1024}{V_{DD} \times adc} \quad (3.11)$$

$$C_{low} = \frac{I \times T}{ADC_{high} \times V_{DD}} \times 1024 \quad (3.12)$$

$$C_{high} = \frac{I \times T}{ADC_{low} \times V_{DD}} \times 1024 \quad (3.13)$$

The MPR121 uses a constant DC current capacitance sensing scheme [88]. It can measure capacitances ranging from 10 pF to over 2000 pF with a resolution up to 0.01 pF. The device does this by varying the amount of charge current and charge time applied to the sensing inputs. The voltage measured on the input sensing node is inversely proportional to the capacitance. At the end of each charge cycle, this voltage is sampled by an internal 10-bit ADC. The sampled data is then processed through several stages of digital filtering.

In summary, the MPR121 sensor works with the capacitance curve by monitoring changes in capacitance within its operating range, particularly focusing on the linear region where capacitance changes are more pronounced and easily detectable. This allows the sensor to provide accurate and responsive touch or proximity sensing capabilities for various applications.

As indicated in Table 3.2 and Figure 3.12, it is evident that during lab testing there is a noticeable fluctuation in the capacitance results. This variability may be attributed to factors such as the presence of wires around the IDC sensor and variations in the placement of the comb.

Table 3.3 Results of capacitors when water level rose from 1 mm to 1 cm in lab test.

Level of Liquid	First Design (pF)	Second Design (pF)	Third Design (pF)	Fourth Design (pF)
1 mm	116.2	80.3	94.2	170.7
2 mm	182	86.7	105	188.3
3 mm	210.1	91	111.5	202.3
4 mm	218.5	94.2	121.4	218.5
5 mm	237.4	97.5	130	237.4
6 mm	248.2	107.1	133.2	248.2
7 mm	249	109.2	136.5	260.1
8 mm	253.1	109.2	140	273.1
9 mm	273.1	109.2	147.6	287.4
10 mm	273.1	111.5	151.7	303.4

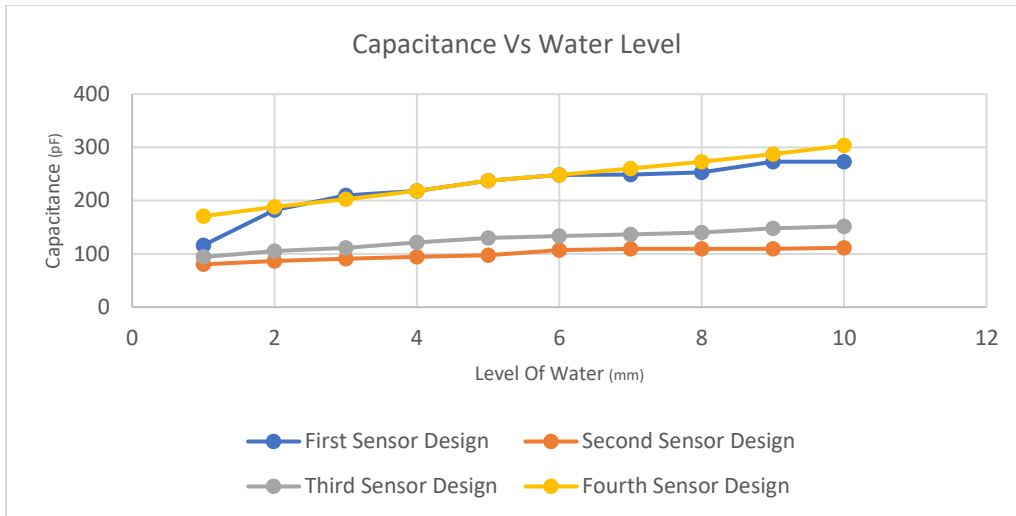


Figure 3.13 Test results for lab trials with small prototype boards.

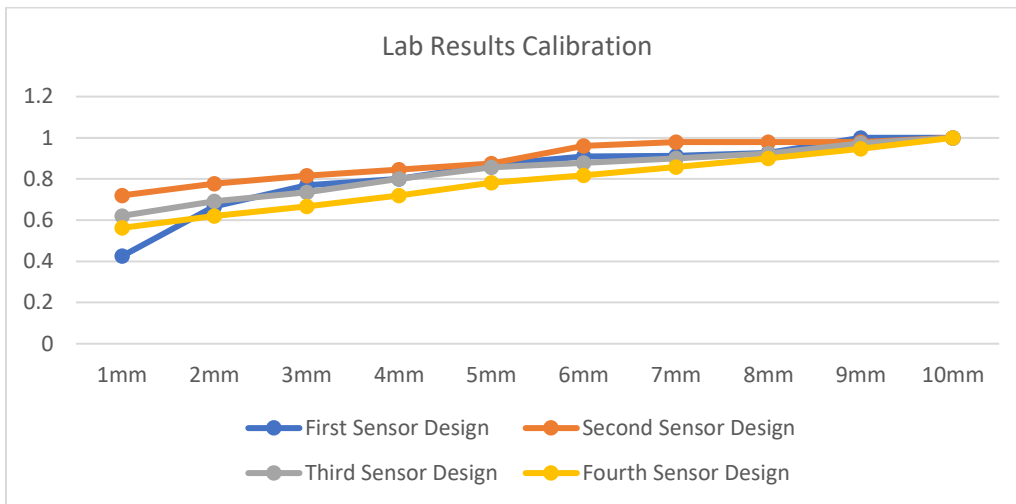


Figure 3.14 Normalization of data from all experimentally tested designs.

As shown in Figure 3.12 and Figure 3.13 capacitance increases by adding water on the board. This same approach can be applied to measure honey on top of the comb, where it is expected that capacitance will increase similarly.

3.2.6 Results and Discussion

As illustrated in Figure 3.14, there are some differences between the simulation and experiment results. Notably, the IDC sensor got more favorable results in simulations than experimental outcomes. These disparities may arise from the lack of precise dimensional matching between the simulated and lab IDC sensors, as well as the omission of wiring connection considerations in the simulations. Based on the results shown in Figure 3.14, the fourth IDC sensor design outperformed the others. Consequently, this type of IDC design will be employed for future steps of the thesis.

The normalized data of Figure 3.15 more clearly shows that while the second and third sensor designs exhibited changes in response to increasing water level, the fourth design displayed a suitable more linear slope in simulation and experimental test. Furthermore, it illustrated a more distinct specific capacitance value for each level of water, particularly noticeable above 7 mm of water as this design shows little saturation effect. This characteristic sets it apart from the other sensor designs.

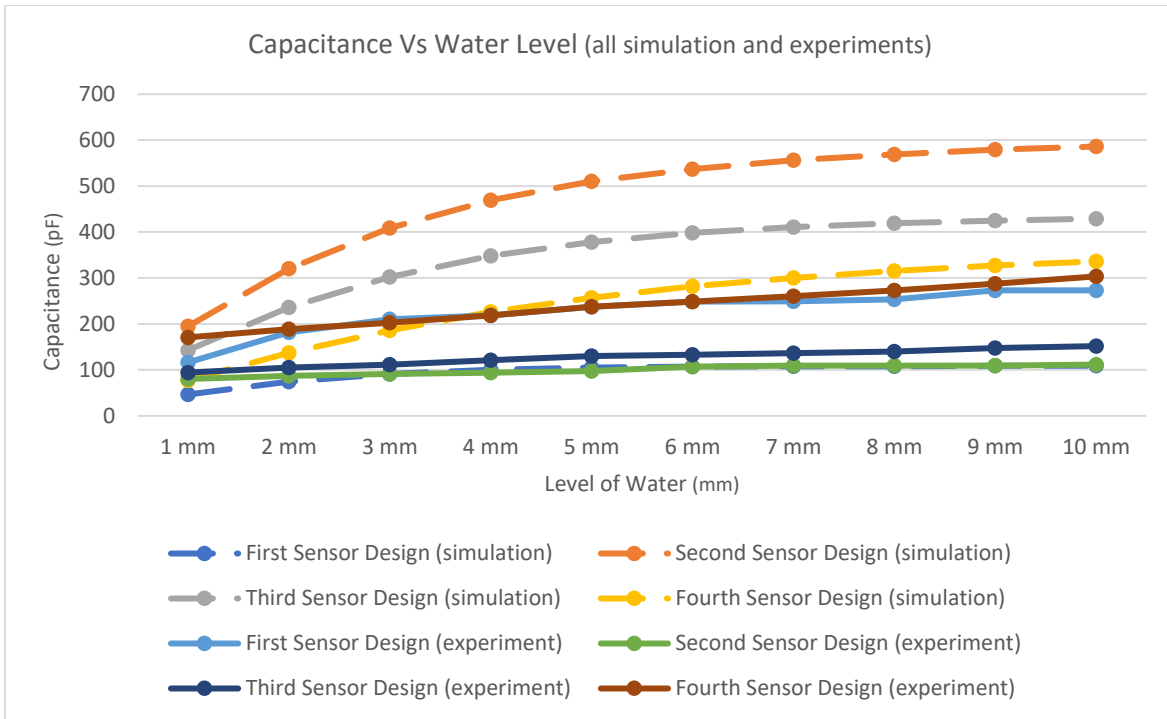


Figure 3.15 Comparison of simulation and experiment results.

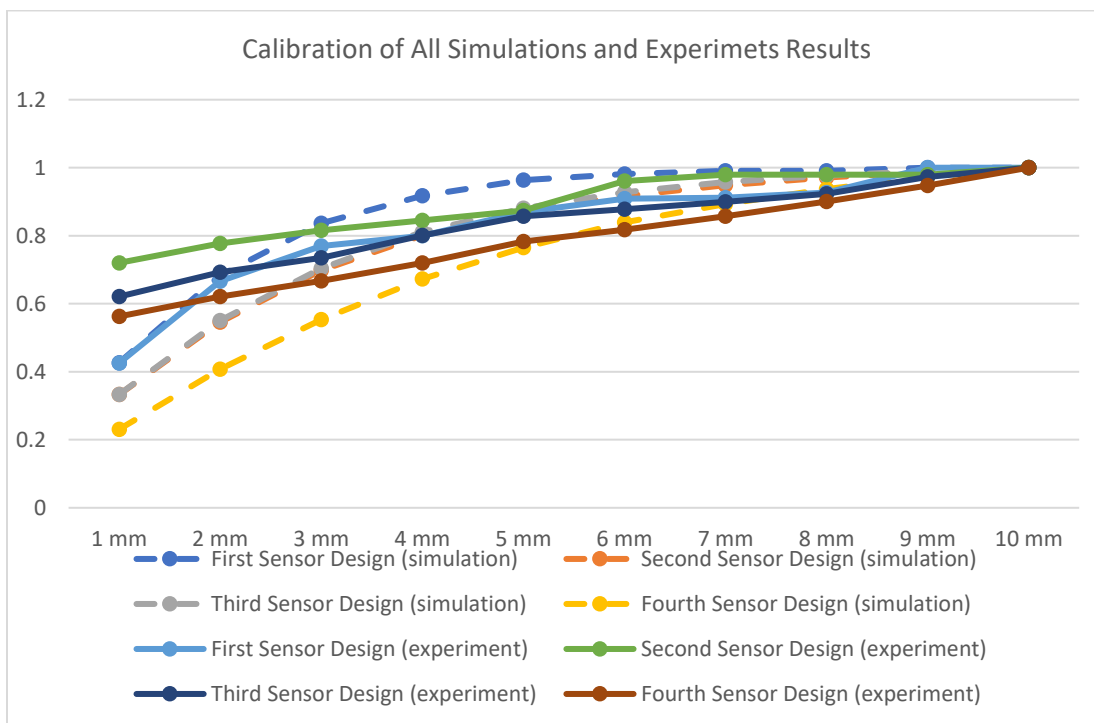


Figure 3.16 Normalized data for simulations and lab test results.

3.3 Chapter Summery

In summary, initial simulations revealed that a detectable change in capacitance, in the order of picofarad, occurred within the IDC when the water level was altered. Four different designs of IDC capacitors were simulated on COMSOL Multiphysics software. The collected results were compared to determine which capacitor could better detect changes in capacitance with increasing liquid height. A small prototype board was built to implement all four capacitor designs for the purpose of capacitance measurement and comparative analysis. Copper tape was employed to fabricate the capacitors, and wax was added on top of the capacitors. A MPR121 capacitive touch sensor was connected to these capacitors to facilitate capacitance measurement. Despite the changes being in the picofarad range, it was observed that the capacitance increased linearly by raising the water level. Data collected from the IDC sensor was stored on an SD card, with measurements recorded at 30-minute intervals.

Four types of capacitors were tested to determine which one could provide better data in each level of water. The study showed designs that were capable of detecting the level of water more than seven millimeters thick, while Beynon's design [106] was unable to do this as the capacitance signal approached saturation.

The fourth design is considered superior to the other designs due to several key advantages. Firstly, it exhibits significantly better linearity compared to the preceding designs. This means that its response is more proportional and predictable, especially in relation to changes in liquid levels. The improved linearity is crucial for accurate and reliable measurements, as it minimizes errors and inconsistencies in the data. Secondly, the fourth design also demonstrates reduced saturation effects, particularly for liquid levels up to 10 mm. By minimizing saturation effects, the fourth design maintains a more consistent and reliable response across a wider range of liquid levels.

Chapter 4: Cell Contents Monitoring within the Hive Supers and Brood Nest

As outlined in Chapter 1, numerous factors can impact the temperature within bee colonies. Bees are highly sensitive to temperature, and a temperature of 35 °C needs to be provided for them throughout the year to ensure their well-being [13, 14]. The temperature control system designed in this thesis is based on the concept shown in Figure 4.1. It can be fabricated on the frames inside the hive box. Section 4.1 presents some information about the influence of temperature on bees and honeycombs. It also reviews some systems previously used to control and monitor the temperature. This section also introduces some methods that have been used to fight the Varroa mites and provides some background information on these pests. Section 4.2 provides some initial simulations to convey a general understanding of heat flow and distribution. Final design is shown in section 4.3, and a PCB board was developed based on this design to conduct laboratory tests.

4.1 Background

4.1.1 Factors that Can Have Effect on Temperature on Honeybees

As discussed in chapter 2, an important factor that can affect bee activities is temperature. An optimal temperature for bees is around 35 °C, and deviations from this temperature can trigger changes in bee behavior. Lower temperatures can also adversely impact bee colonies. In response to low temperatures below 35 °C, bees cease their work and congregate, generating heat by collectively shaking their bodies in order to ensure their survival [29]. In addition, temperatures below 30 °C can cause harm to both the brood and emerging brood. Conversely, elevated

temperatures can also have adverse effects. If the temperature goes above 35 °C, larvae and honey become susceptible to harm, and bee workers need to take action reduce the temperature. Bees reduce the temperature by waving their wings to ventilate the hive. Temperatures above 38 °C may damage the brood. Honey production enzyme can be impaired if the temperature exceeds 40 °C, and worker bees will die in temperature above 45 °C.

Baby bees and eggs exhibit a high degree of sensitivity to temperature fluctuations, necessitating vigilant protection. As previously discussed, bees have temperature sensors on their antennas, and they react quickly to temperature changes by employing their wings or congregating. Many scientists have delved into how bees distribute heat over the honeycomb equally.

4.1.2 Existing Hive Temperature Monitoring Systems

As previously discussed in [5] and [13-15], the monitoring of temperature within colonies is a crucial undertaking. Over time, various methods have been used to measure temperature. For instance a system developed by Kridi [89] incorporated LM35 sensors, which were added on the honeycomb with the assistance of an Arduino platform to measure temperature within colonies [89]. These tests showed temperature variations across different regions of the honeycomb, with temperature being less in the corners of combs. In general, the temperature difference was only a few degrees, and the center of the comb was around 35 °C. Other researchers have employed some sensors for temperature detection, with these sensors were commonly situated directly on the combs. Typically, most studies relied on a single sensor to measure temperature.

This thesis deploys multiple sensors strategically positioned throughout the honeycomb instead of using a single sensor, yielding comprehensive and precise data. This method offers

several advantages, including the potential to provide more data about bee behavior, the precise location of the brood within the comb, and can even provide an estimate of the brood quantity.

As mentioned before, when the Varroa mites infiltrate a beehive, they lay eggs and feed on the larva. To kill Varro mites, the temperature needs to increase to 47 °C. After heating to 47 °C, the board must be kept warm for a certain period to ensure the complete elimination of all mites. Two important things affect the heating process. One of them is thermal mass and the other is thermal conductivity. These two factors are important to heat the board, as well as honey (and in the testing also water) on top of the board. Different amounts of energy is needed to change temperature in different materials. The amount of energy needed depends on [107]:

- 1- The mass of the material.
- 2- The substance of the material (specific heat capacity).
- 3- The temperature changes.

In this thesis, the test liquid employed was water, which is characterized by a specific heat capacity of 4.186 J/g°C. This means that it takes 4.186 joules to raise the temperature of 1 gram of water by 1 °C. The specific heat capacity of honey is 3.05636 J/g°C, indicating its lower energy requirement compared to water. Each material has a specific thermal mass and heat capacity, and in this thesis, copper tape, PCB board, wires, and water are employed, and each of them have a significant influence on the outcomes. The other factor, which can affect is thermal conductivity, which refers to how easily heat can flow through a solid material [108]. In this thesis, both of these elements are two important as the rapid heating of the honeycomb and uniform heat distribution are paramount. In subsequent discussions, these factors will be explored in greater detail.

4.2 Simulations of heat flow within the honeycomb

The heater system design of this thesis is based on the concept shown in Figure 4.1. This design has the heaters placed behind the honeycomb board. A metal heat conductor assists the thermal conduction of heat from the heater to copper tape placed on the honeycomb side. The copper tape assists the spreading of heat under the honey in each honeycomb cell.

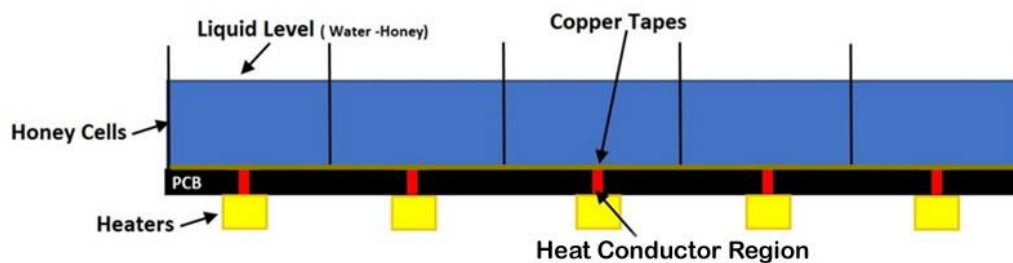


Figure 4.1 General board design indicating the placement of the heaters, heat conductor, honey cells and copper tape to distribute the heat.

The first simulations of the on-comb heater design were done in COMSOL Multiphysics to acquire an understanding of how to use heaters and increase the temperature within the cells in combs. All simulations were 3D to identify optimal heating results. As previously mentioned, a honeycomb was segmented into 12 regions, each with equivalent dimensions, the same number of heaters, and temperature sensors.

- 1- Finding the best way to simulate a resistor as a heater.
- 2- Modeling the heat conductor region.
- 3- Modeling the copper tape.
- 4- Simulation of four heaters.

- 5- Simulation of nine heaters for a region of 100x100mm.
- 6- Simulation of nine heaters for a region of the board.

It should be noted that each material has the specific heat capacity and thermal conductivity that can affect results. According to the formulas below, these two factors can have a significant effect on the heat distribution. One of them is thermal conductivity that can be calculated by [107]:

$$\Delta E = mc\Delta T \quad (4.1)$$

where the change in thermal energy (ΔE) is measured in joules (J), mass (m) is measured in grams (g), specific heat capacity (c) is measured in joules per gram per degree Celsius (J/g°C), and temperature change (ΔT) is measured in degrees Celsius (°C).

The other factor, which is important, is thermal conductivity that is the ability of a given material to conduct or transfer heat and can be calculated by [109]:

$$k = \frac{LQ_d}{A \Delta T} \quad (4.2)$$

where k is the thermal conductivity in W/mK, Q_d is the amount of heat transferred through the material in Joules/second or Watts, L is the distance between the two isothermal planes, A is the area of the surface in square meters, and ΔT is the difference in temperature in Kelvin.

The preferred approach for mite elimination amongst apiarists is through the use of heating methods rather than chemical treatments. This method involves placing heaters on the honeycomb to raise the temperature to 47 °C to kill the mites. In this thesis, some resistors served as heaters by connecting them to an external power source. Various small 5-volt heaters are available in the market that can be employed for this purpose. In the simulations of this thesis, the heater is modelled as a resistor, and can be represented as a block, line or point in COMSOL. Theoretically,

an Arduino UNO can be utilized to control these heaters, and this Arduino can provide a 5-volt output that can be used as a power for heaters. The goal of this system is increasing temperature to 47 °C and maintain this temperature uniformly across the entire board, from the surface of the board through 10 mm of honey, for a certain amount of time in order to kill all mites. As we have honey on the board and the level of it might be different, it is necessary to establish an appropriate time for temperature elevation based upon honey level in order to eliminate all mites. In this thesis, a duration of 10 minutes is assumed as a suitable time to uniformly raise the temperature across the board to obtain reliable results. The primary goal of this heating system design is to conserve energy by achieving optimal heat transfer while maintaining uniform heat distribution. In this regard, to enhance heat transfer efficiency, we have incorporated a heat conductor and a copper tape has been employed to distribute heat evenly throughout the board.

As mentioned before, each material possesses a specific heat capacity and Table 4-9 provides some of the specific heat capacities used in the simulations.

Table 4.1 Specific heat capacity for different materials.

Specific Heat Capacity (J/g°C)					
PCB board	Copper tape	Water	Honey	Carbon	Air
0.396	0.385	4.184	3.05636	0.00071	0.001012

The other factor mentioned earlier is thermal conductivity, which can affect heat distribution. Table 4-10 displays the thermal conductivity of materials used in this thesis.

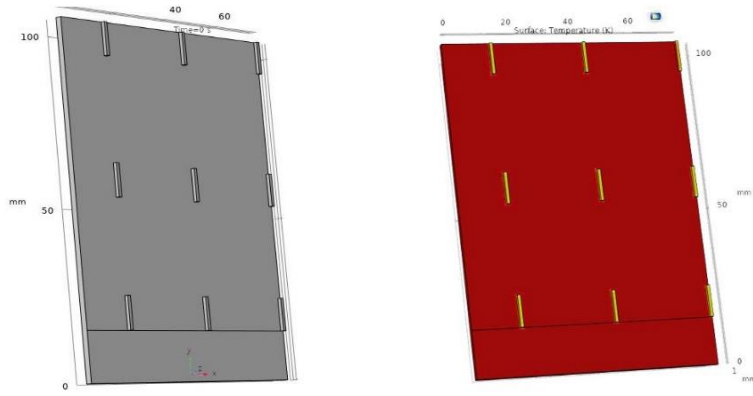
Table 4.2 Thermal conductivity for different materials.

Thermal conductivity (W/mK) in room temperature					
PCB board	Copper tape	Water	Honey	Carbon	Air
0.25	385.0	0.6	0.377	2000~6000	0.0262

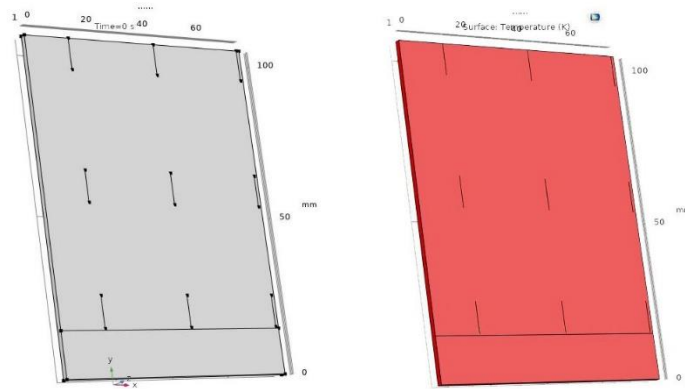
4.2.1 Finding the best way to simulate a resistor as a heater

In COMSOL, various lines, points, and blocks are simulated as heaters to determine the optimal dimensions for better results. Figure 4.2 illustrates the simulations conducted in COMSOL.

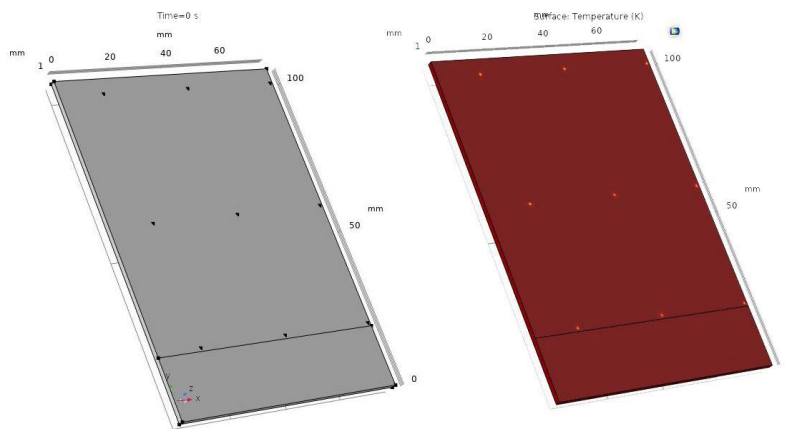
As previously discussed, the honeycomb is divided to 12 regions. Each of these regions is examined for the placement of nine heaters, which can be either block heater, line heater or point heater. The simulated temperature was determined at three locations near the three resistors placed in a line at various time intervals: 1s, 60s, 120s, 300s and 600s. Heat transfer in solid method was used to study the heating of the board with the application of 750 mW power per heater. The results are shown in Table 4.1 and Figure 4.3. Examining the results, it can be seen that the results obtained from point heaters are significantly worse than the other designs, and so they were deemed unacceptable. The choice of heater designs for simulations in subsequent analysis in this thesis could then be either the block heater or the line heater. Since the block heater is more like a realistic resistor, it was chosen for subsequent simulations.



(a)



(b)



(c)

Figure 4.2 (a) Simulation of block heater (b) Simulation of line heater (c) Simulation of point heater.

Table 4.3 The results of different heaters with increasing time.

Time (second)	Block Heater(°C)	Line Heater(°C)	Point Heater(°C)
1	20.12	20.46	28
60	31	29.5	420
120	37	34.5	510
300	46	43	620
600	55	53	710

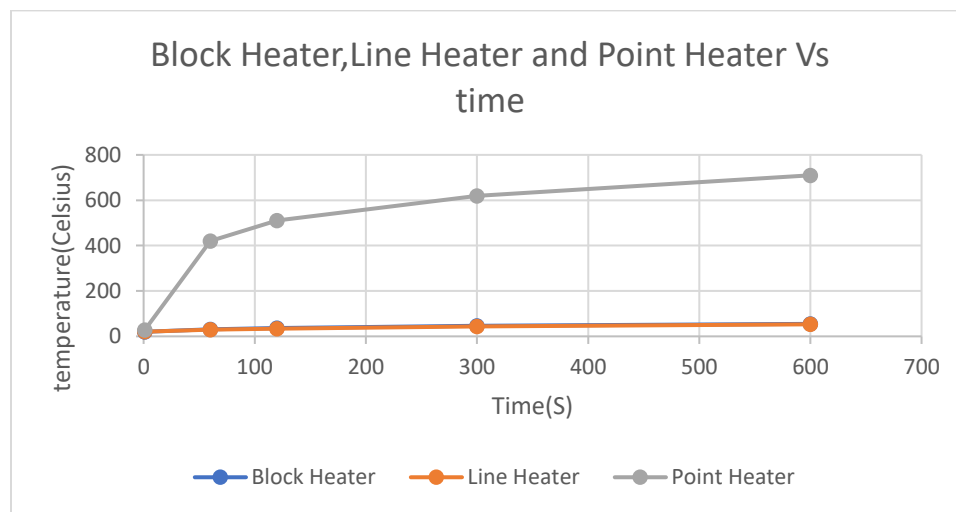


Figure 4.3 The results of the three different heaters between 1 and 600 seconds.

4.2.2 Modeling the heat conductor region

Figure 4.1 illustrates the process of heat transfer to the copper tape and the liquid on the honeycomb side of the board by using a heat conductor. The heat conductor is modelled as an empty square cube that better enables the transfer of the heat from the heater to the PCB board. As previously mentioned, the goal of this heating system design is to conserve energy by achieving optimal heat transfer while maintaining uniform heat distribution. Copper tape was chosen to cover

the heat conductor due to its ability to rapidly transfer heat across the surface of the board, minimizing energy wastage. In this part of thesis, three different sizes of heat conductors were explored to determine which one could transfer heat better to the honeycomb side of the board. For COMSOL simulations, FR4 with thickness of 1.6 mm was utilized as a PCB board, and a 5x5 mm block heater was simulated as a resistor below the board (Figure 4.4). Temperature measurements were taken when the heat conductor sizes were 1x1 mm, 2x2 mm, 5x5 mm to determine which one could more effectively transfer heat to honeycomb side of the board. In addition, the initial temperature of 35 °C was assumed for all simulations.

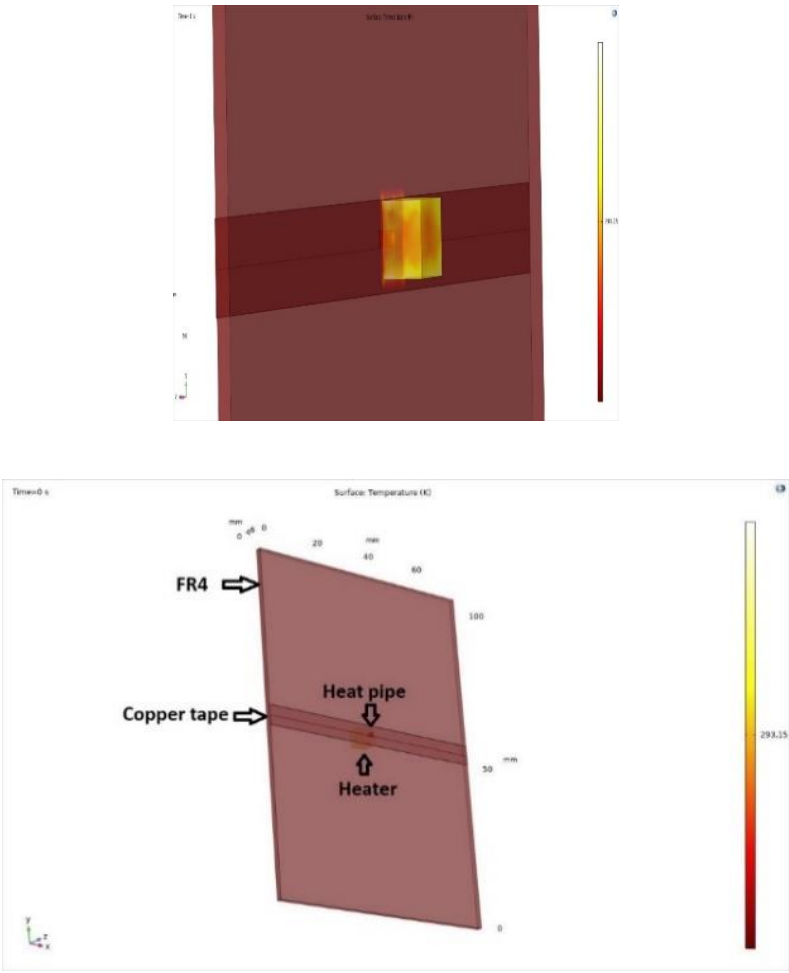


Figure 4.4 Pre-simulation of heat conductor region and copper tape.

Figures 4.5 to 4.7 show the temperature on the honeycomb side of the board when the dimensions of the heat conductors were 1x1x1.6 mm, 3x3x1.6 mm, and 5x5x1.6 mm. In all simulations, the heating time duration was simulated from 1 second to 600 seconds in 60 seconds increments.

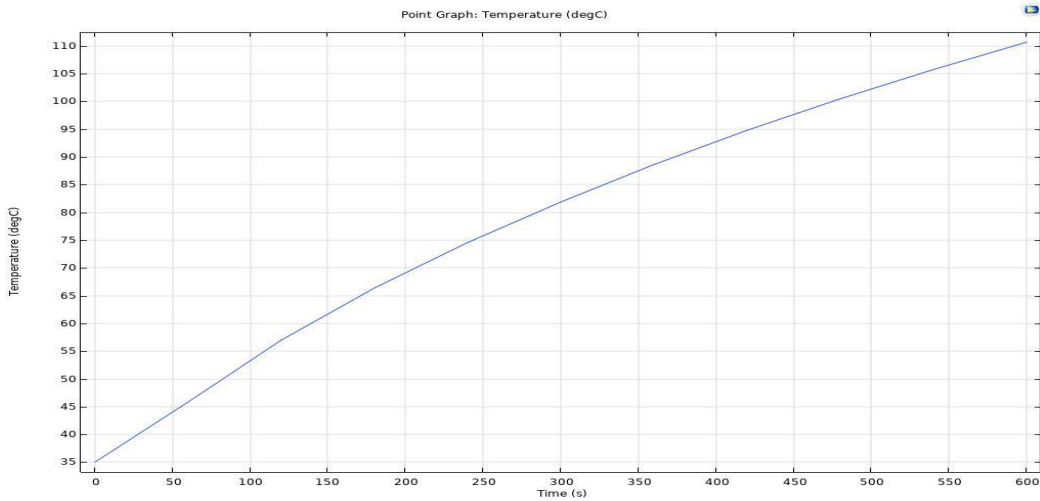


Figure 4.5 Temperature simulation results with the 1x1x1.6 mm heat conductor and different thickness of the copper tape.

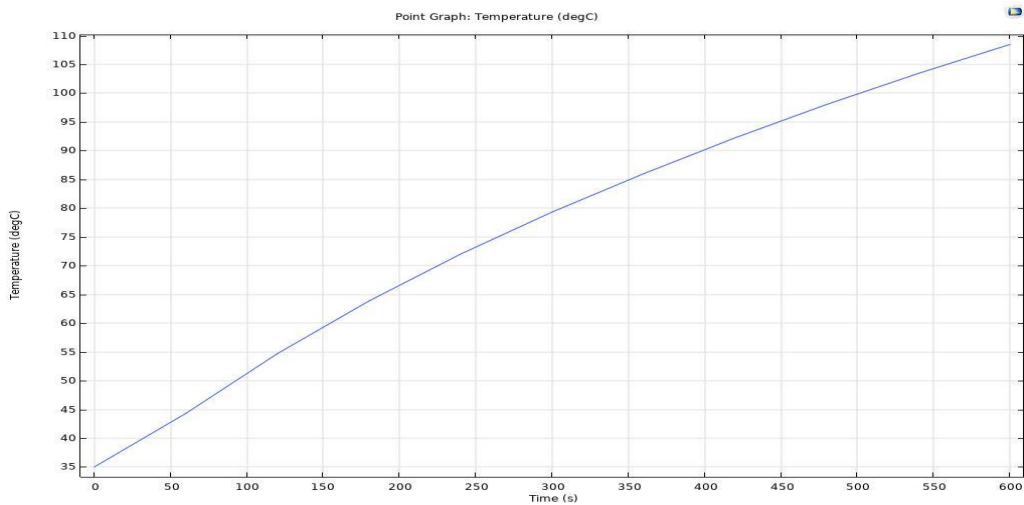


Figure 4.6 Temperature simulation results with the 3x3x1.6 mm heat conductor and different thickness of the copper tape.

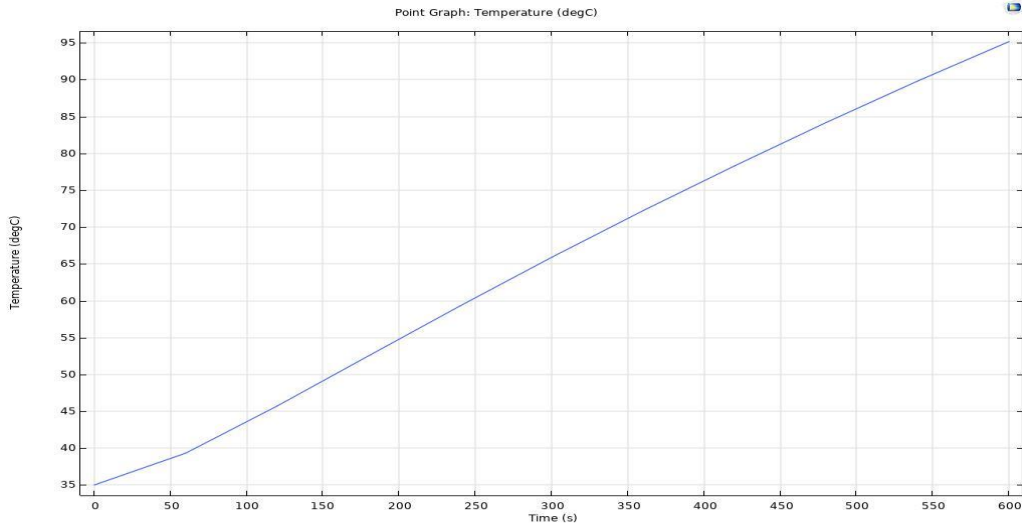


Figure 4.7 Temperature simulation results with the 5x5x1.6 mm heat conductor and different thickness of the copper tape.

Table 4.4 The results of different heat conductor with increasing time.

Time (second)	1x1x1.6 mm heat conductor (°C)	3x3x1.6 mm heat conductor (°C)	5x5x1.6 mm heat conductor (°C)
1	35	35	35
60	45	44	38
120	57	55	45
300	82	79	66
600	110	107	95

According to Table 4-2, these studies show that the best heat transfer result was for the 1x1x1.6 mm heat conductor, as evidenced by the higher temperature observed on the upper surface of the board after 600 seconds. Therefore, the 1x1 mm heat conductor has been selected for use in the upcoming simulations.

4.2.3 Modeling the copper tape

Using copper tape on the surface of the board can be useful to evenly distribute heat. This section of the thesis explores heat distribution by employing a layer of copper tape on top of the heat conductor. As shown in Figure 4.8, a substrate of 100x100 mm of FR4 was used as a PCB board and a 1x1x1.6 mm heat conductor transferred the heat from 5x5 mm heater to the top of the copper tape (50x50 mm). Various thicknesses of copper tape were tested to determine which thickness of copper tape could distribute heat better on the honeycomb side of the board.

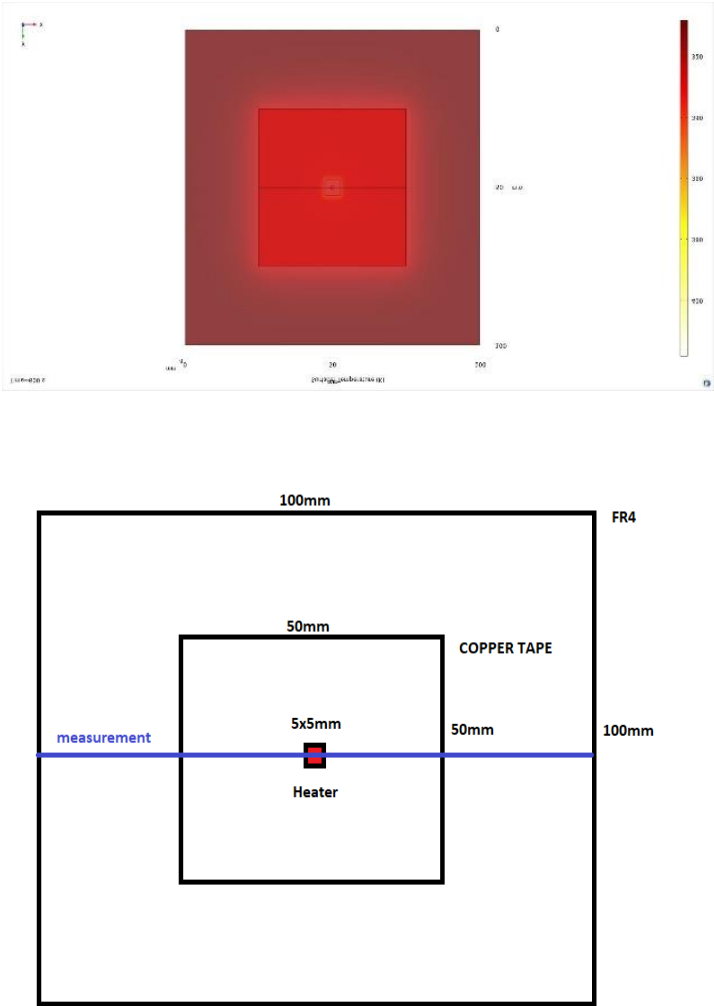


Figure 4.8 Simulation of one heater with 50x50 mm copper tape.

Figures 4.9 to 4.13 explore copper tapes with thicknesses of 0.03 mm, 0.07 mm, 0.1 mm, 0.3 mm, and 0.7 mm. The simulations analyzed temperature distribution across the upper surface of tapes for heating durations ranging from 1 second to 600 seconds, in 60 seconds increments.

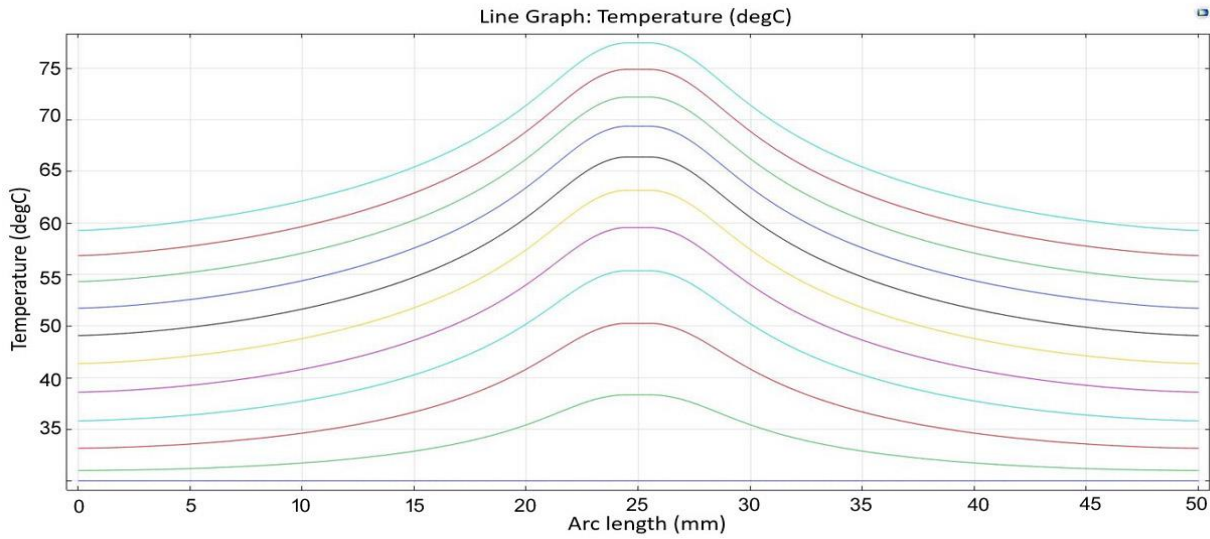


Figure 4.9 Temperature simulation with the 1x1x1.6 mm heat conductor and copper tape with thickness of 0.03 mm.

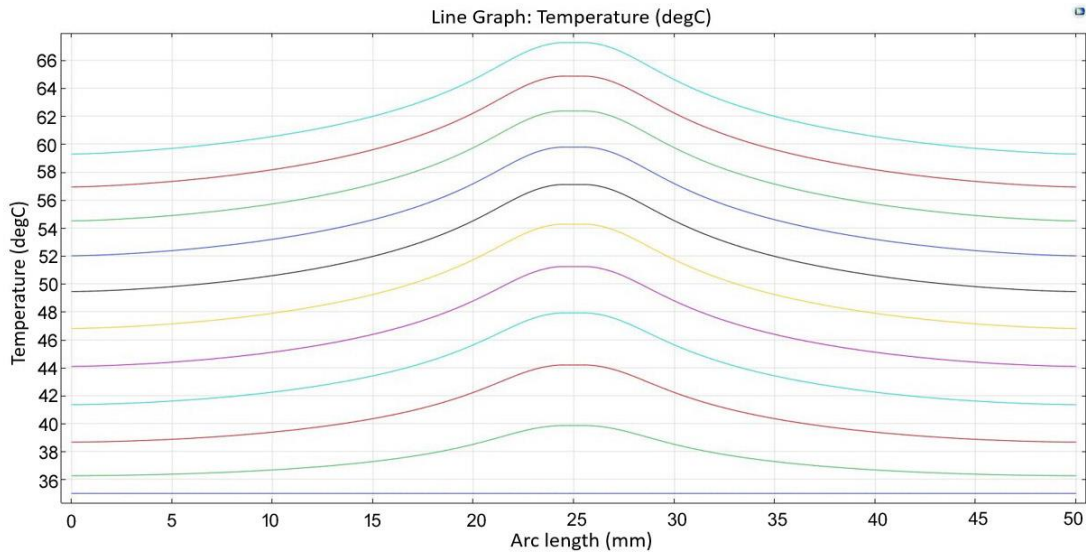


Figure 4.10 Temperature simulation with the 1x1x1.6 mm heat conductor and copper tape with thickness of 0.07 mm.

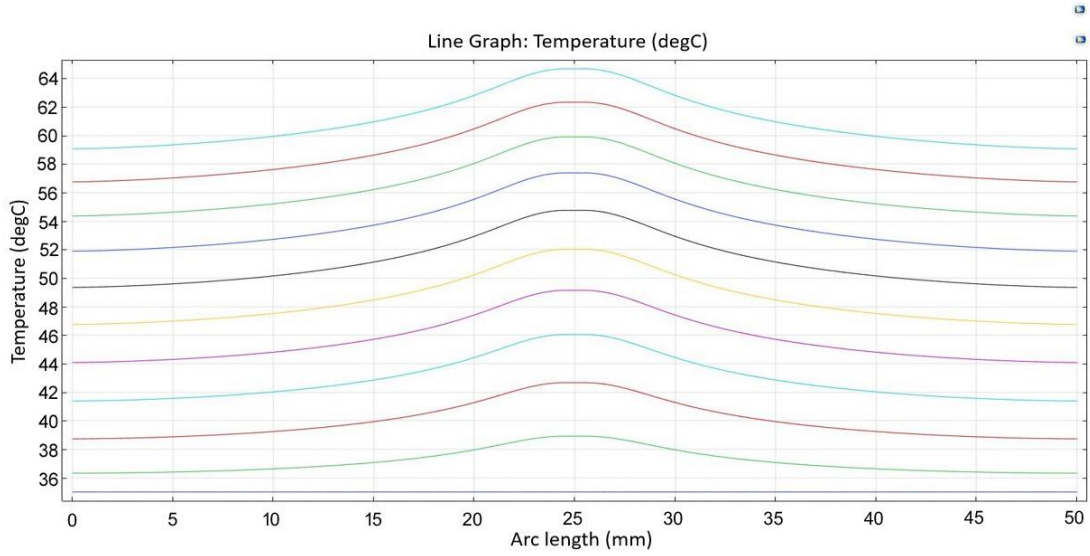


Figure 4.11 Temperature simulation with the 1x1x1.6 mm heat conductor and copper tape with thickness of 0.1 mm.

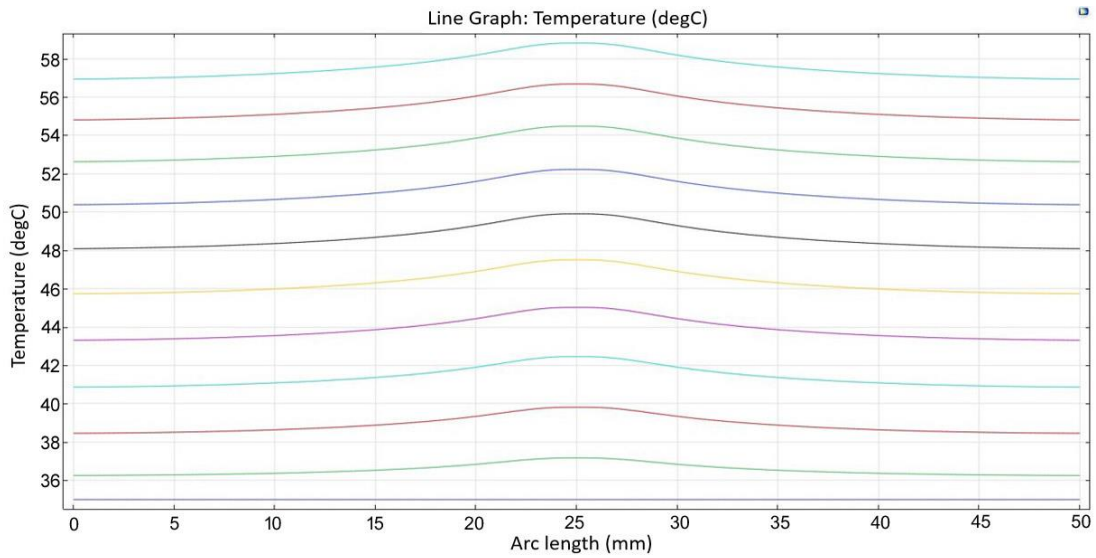


Figure 4.12 Temperature simulation with the 1x1x1.6 mm heat conductor and copper tape with thickness of 0.3 mm.

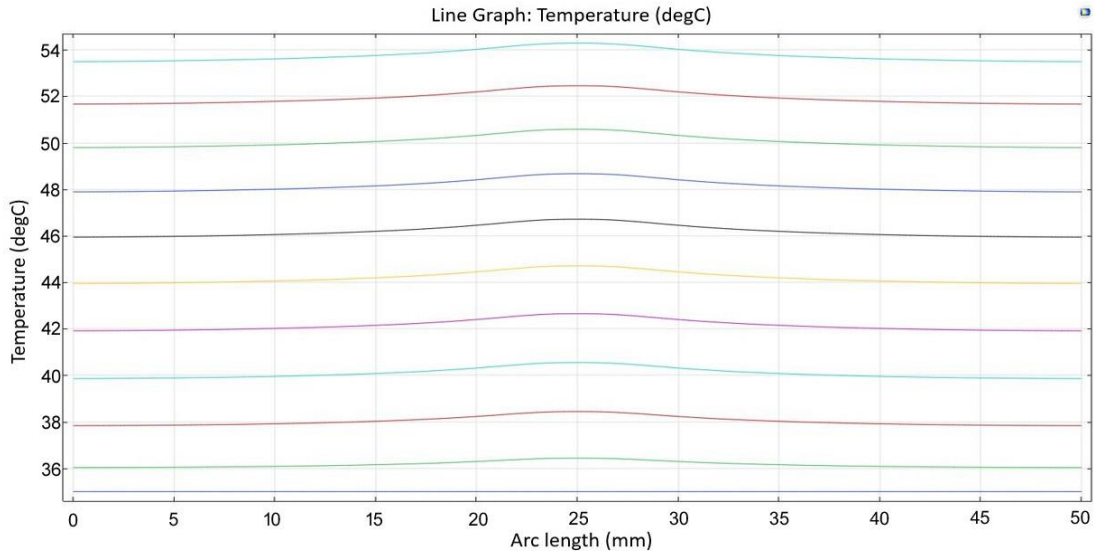


Figure 4.13 Temperature simulation with the 1x1x1.6 mm heat conductor and copper tape with thickness of 0.7 mm.

It can be observed that the thin copper tape heats up better than the thicker copper tape after 600 seconds. The temperature on top of the 0.03 mm copper tape is around 73 °C, while the 0.3 mm copper tape only reached around 57 °C. However, it is observed that while the temperature rise is slower on the thicker copper tapes, they exhibit better heat distribution capabilities.

Two factors are important in this heating study, one is increasing the heat quickly and another is uniform heat distribution. Therefore, it is crucial to determine the ideal thickness of copper tape to achieve both objectives. In order to gain a clear understanding of heat distribution with different copper tape thicknesses, four heaters are simulated in the next section to observe the effects of varying tape thicknesses.

4.2.4 Simulation of four heaters

In this section of the thesis, water and an air block is simulated to exist above the copper tape. Temperature is simulated between two heaters to investigate the impact of varying thicknesses of copper tape on the temperature distribution.

In order to get a better understanding about how the heat dissipates, four 5x5 mm block heaters were explored. The substrate was 100x100 mm of FR4 with thickness of 1.6 mm and was employed at top of the heater as a PCB board, accompanied by 100x100 mm copper tape for heat distribution around the board. In addition, a 1x1x1.6 mm heat conductor was applied to transfer heat to the copper tape. As shown in Figure 4.14, a water block with thickness of 10 mm and an air block with thickness of 100 mm were added on top of the board to study their effect on the temperature across the width of the copper tape between the heaters when the heating time was increased from zero to 600 seconds in 60 seconds increments.

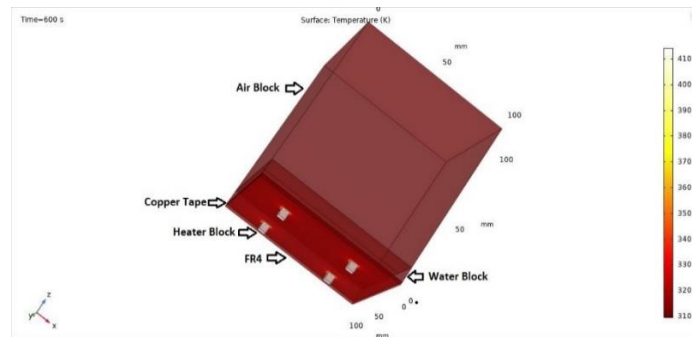


Figure 4.14 Simulation of four heaters with water and air block.

Figures 4.15 to 4.19 explore copper tapes with thicknesses of 0.03 mm, 0.07 mm, 0.1 mm, 0.3 mm, and 0.7 mm. As previously mentioned, 10 mm of water was simulated on top of the PCB board, and temperature simulations are taken between two heaters at three distinct locations: on top of the copper tape; in the middle of water block (5 mm height in the water block), and at 10

mm height of water block. Simulations were for the time increasing from zero to 600 seconds, in 60 seconds increments.

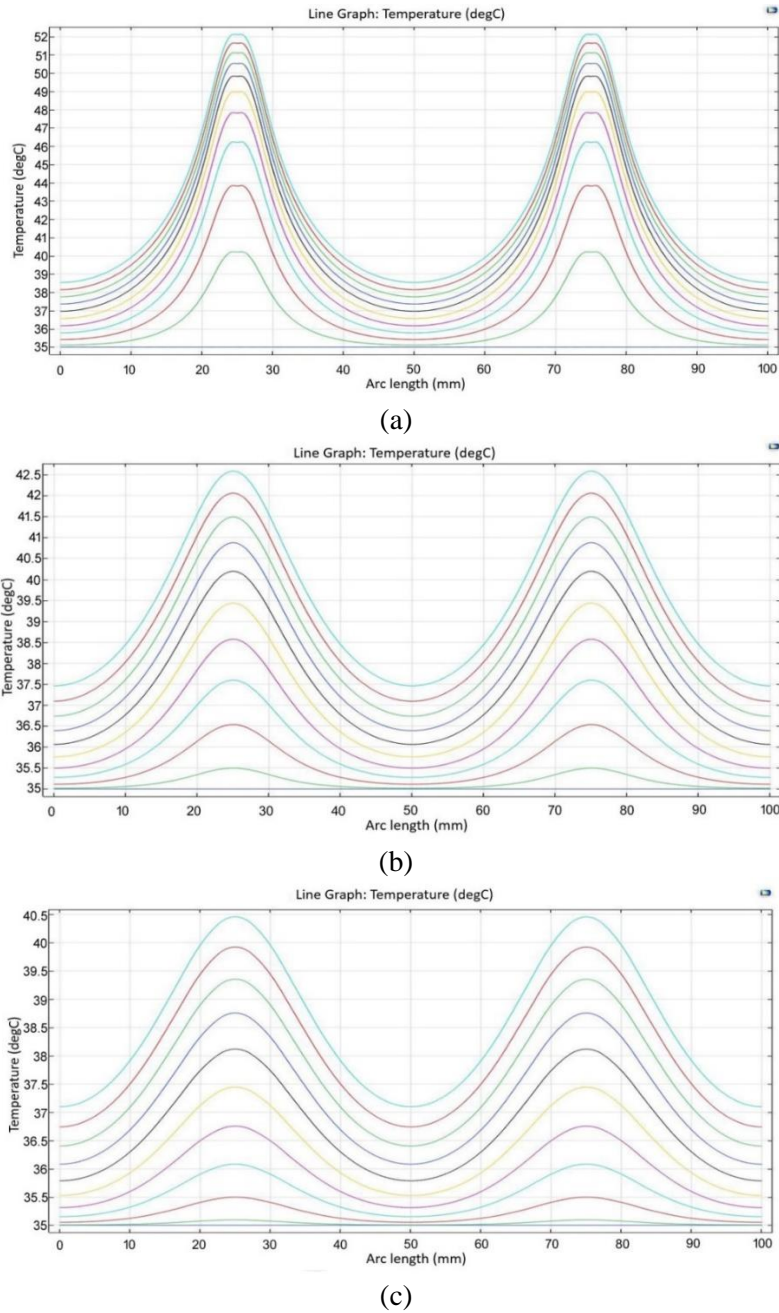
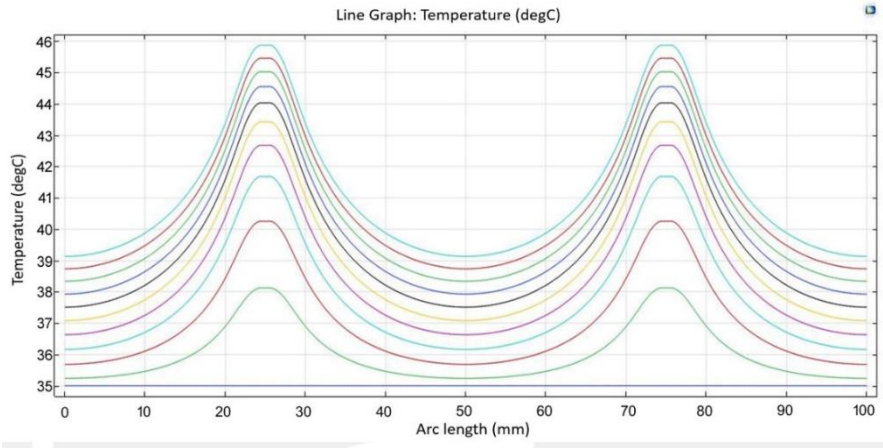
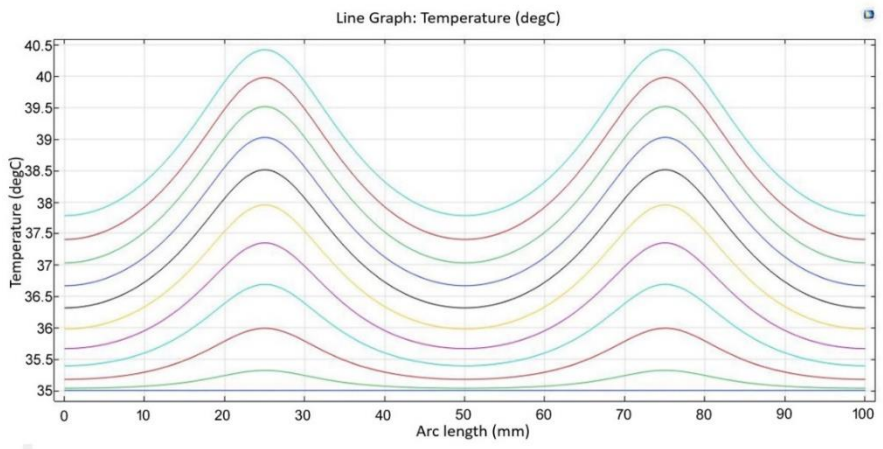


Figure 4.15 Simulation study for 0.03 mm copper tape. (a) Temperature distribution on top of the copper tape. (b) Temperature distribution at 5 mm in water block. (c) Temperature distribution on top of the 10 mm water block.



(a)

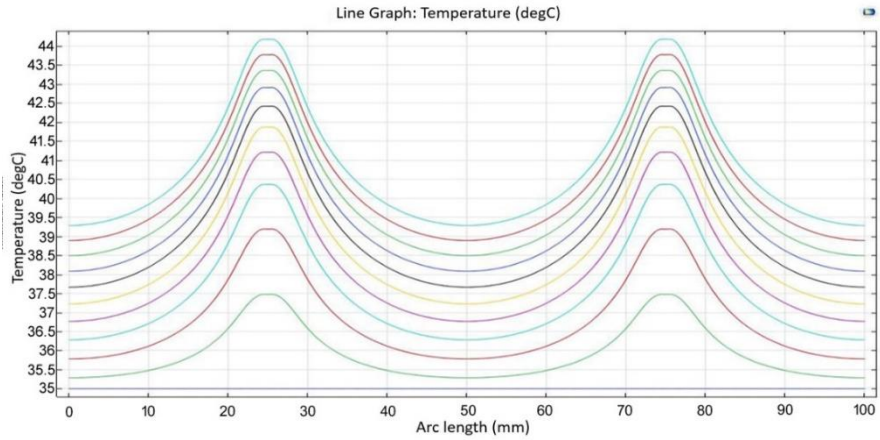


(b)

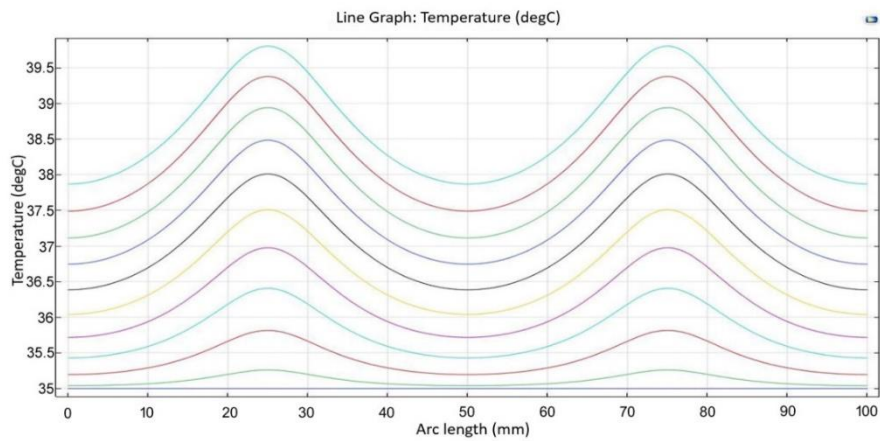


(c)

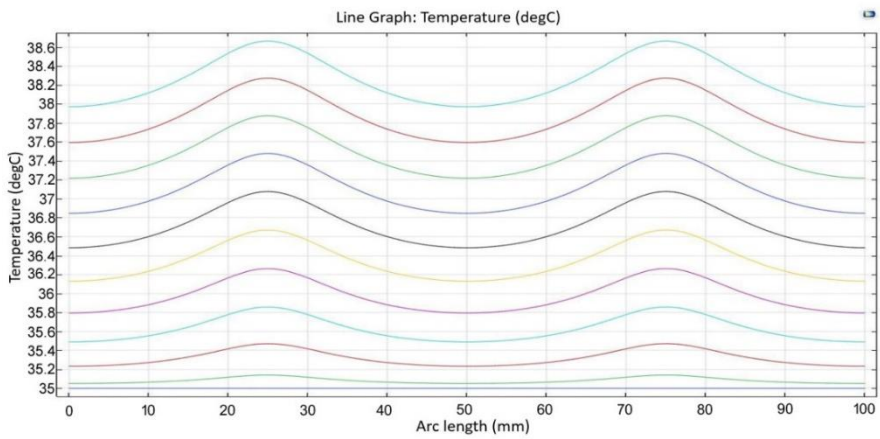
Figure 4.16 Simulation study for 0.07 mm copper tape. (a) Temperature distribution on top of the copper tape. (b) Temperature distribution at 5 mm in water block. (c) Temperature distribution on top of the 10 mm water block.



(a)

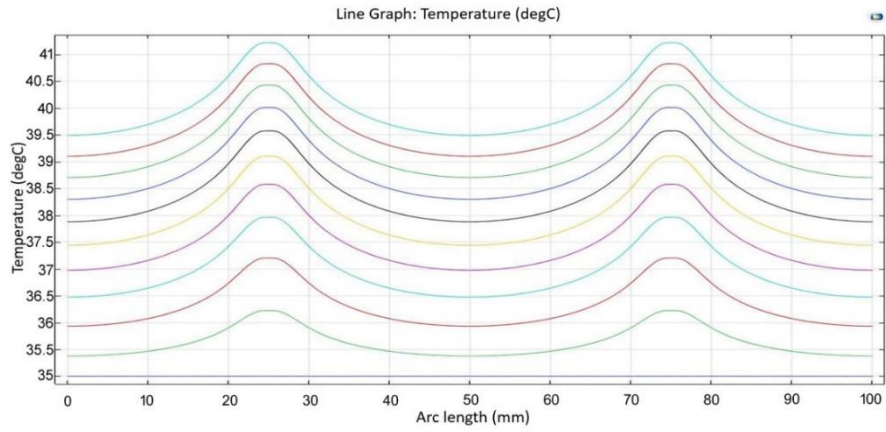


(b)

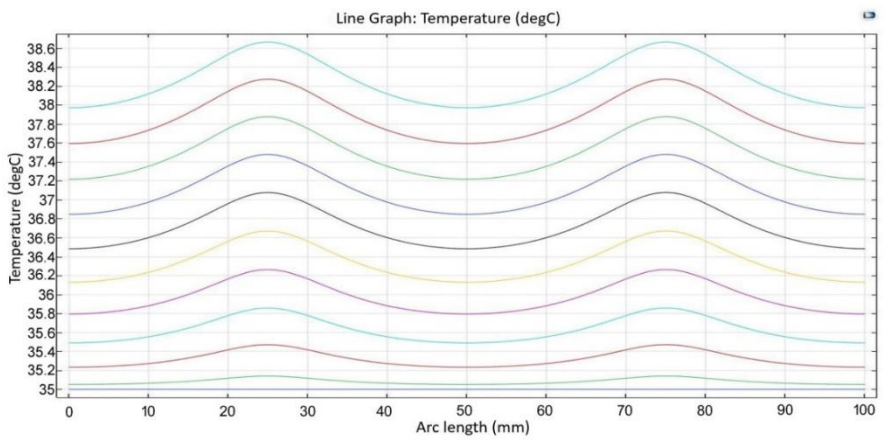


(c)

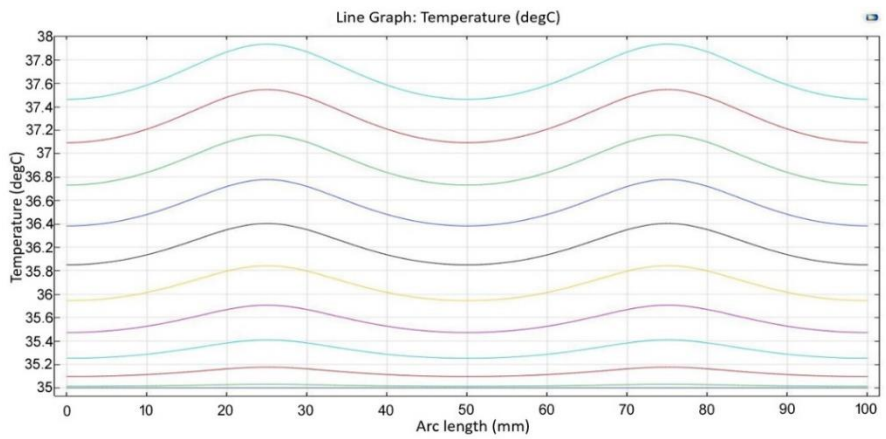
Figure 4.17 Simulation study for 0.1 mm copper tape. (a) Temperature distribution on top of the copper tape. (b) Temperature distribution at 5 mm in water block. (c) Temperature distribution on top of the 10 mm water.



(a)

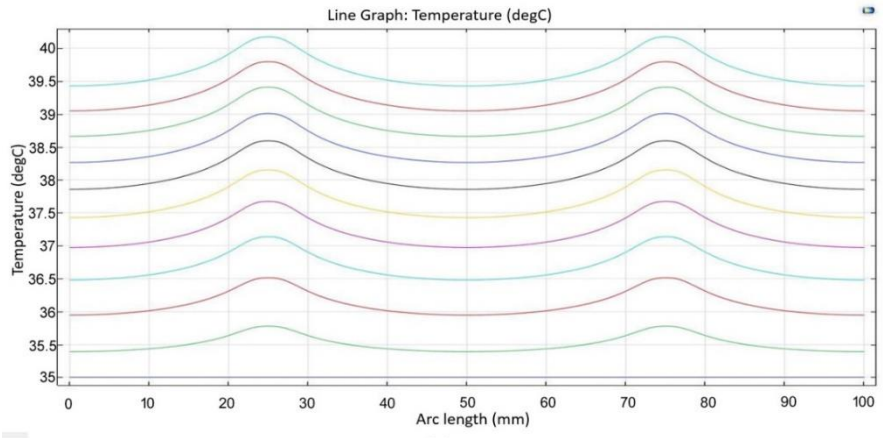


(b)

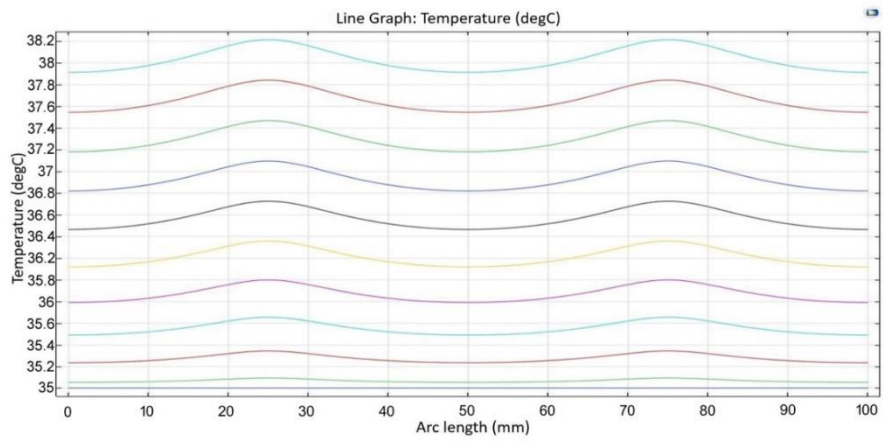


(c)

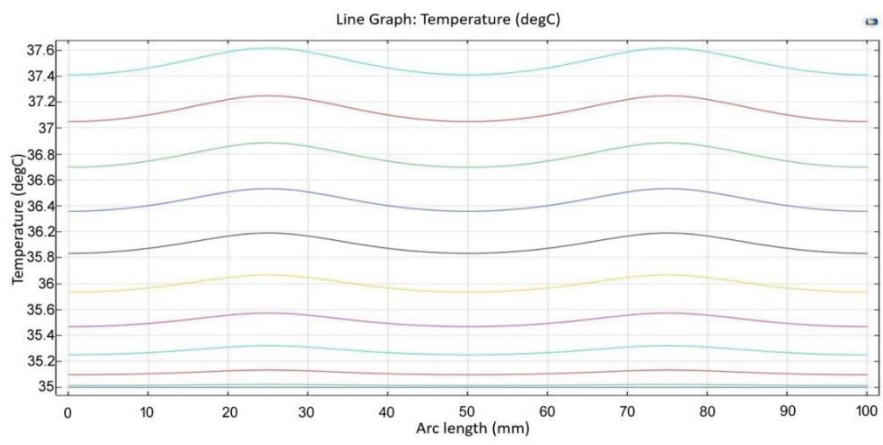
Figure 4.18 Simulation study for 0.3 mm copper tape. (a) Temperature distribution on top of the copper tape. (b) Temperature distribution at 5 mm in water block. (c) Temperature distribution on top of the 10 mm water block.



(a)



(b)



(c)

Figure 4.19 Simulation study for 0.7 mm copper tape. (a) Temperature distribution on top of the copper tape. (b) Temperature distribution at 5 mm in water block. (c) Temperature distribution on top of the 10 mm water block.

Based on the findings from Figure 4.15 to 4.19, thinner copper tape demonstrates faster heating capabilities in comparison to thicker copper tape. However, thicker copper tape excels in the effective distribution of heat. Figure 4.20 compares the results on top of the heaters when the level of water was zero, 5 mm and 10 mm.

Table 4.5 Heat distribution with different copper tape thicknesses.

	Thickness of copper tape				
	0.03 mm	0.07 mm	0.1 mm	0.3 mm	0.7 mm
Top of the copper tape (°C)	52.1	45.8	44.25	41.25	40.25
Top of 5 mm water (°C)	42.7	40.3	39.75	38.7	38.2
Top of 10 mm water (°C)	40.5	39.25	38.7	37.9	37.6

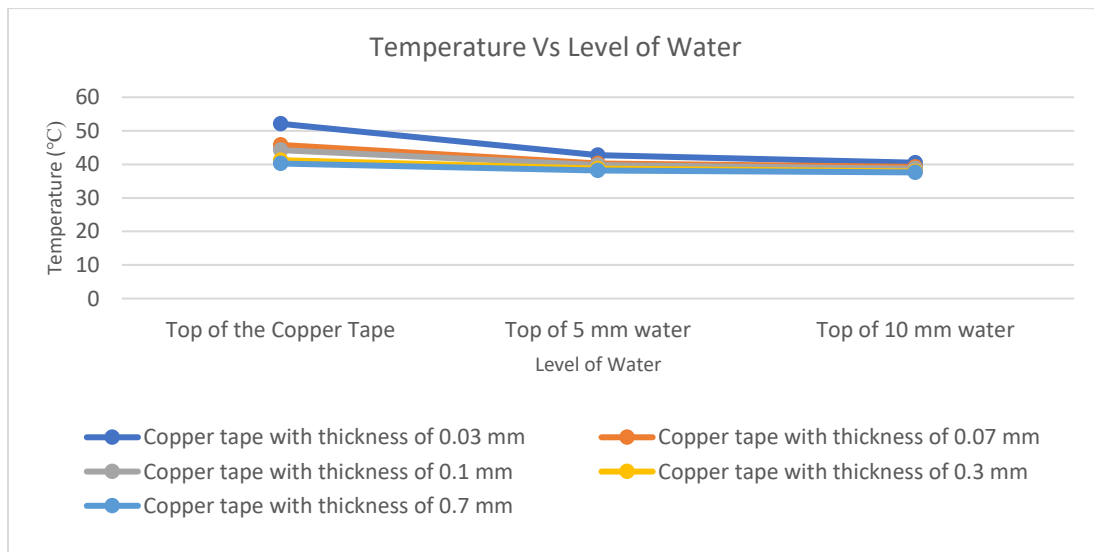


Figure 4.20 Comparing temperature distribution on top of the heaters.

As previously discussed, two factors are important in choosing copper tape. The first factor is the time required for it to attain warmth, while the secondary factor is its heat distribution capability. As shown in Figure 4.20, the copper tape with thickness of 0.03 mm reaches the highest temperature at all water depths. The second factor was heat distribution, and Figure 4.21 compares the temperature at a distance of 10 mm from the heater atop of the copper tapes, with 5 mm and 10 mm of water block. Although thicker copper tape distributes heat smoothly, it can be noted that copper tape with thickness of 0.03 mm possesses a significant peak heat result. As mentioned before, the board needs more heat to eradicate mites. Therefore, the copper tape with thickness of 0.03 mm was chosen for next step of simulations, and the number of heaters was increased to nine heaters to get more heat on top of the copper tape and water block.

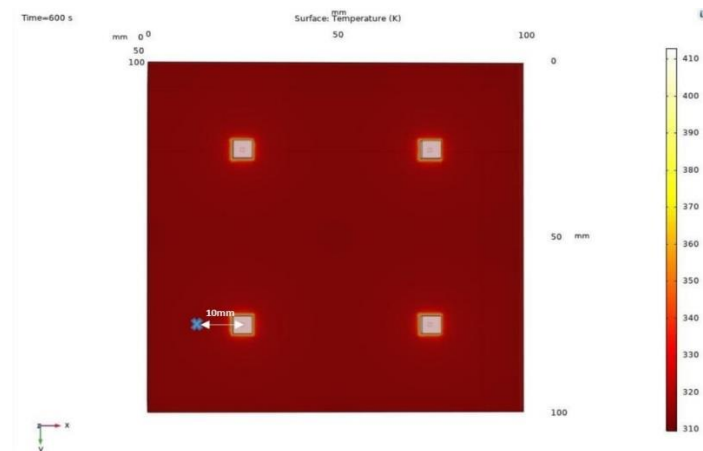


Figure 4.21 Heat distribution around the heaters.

Table 4.6 Heat distribution when four heaters are applied.

	Thickness of copper tape (°C)				
	0.03mm	0.07mm	0.1mm	0.3mm	0.7mm
Top of the copper tape (°C)	41.5	41	40.5	40	39.6
5 mm of water (°C)	39.5	38.75	38.75	38.3	38
10 mm of water (°C)	38.75	38.25	38	37.7	37.5

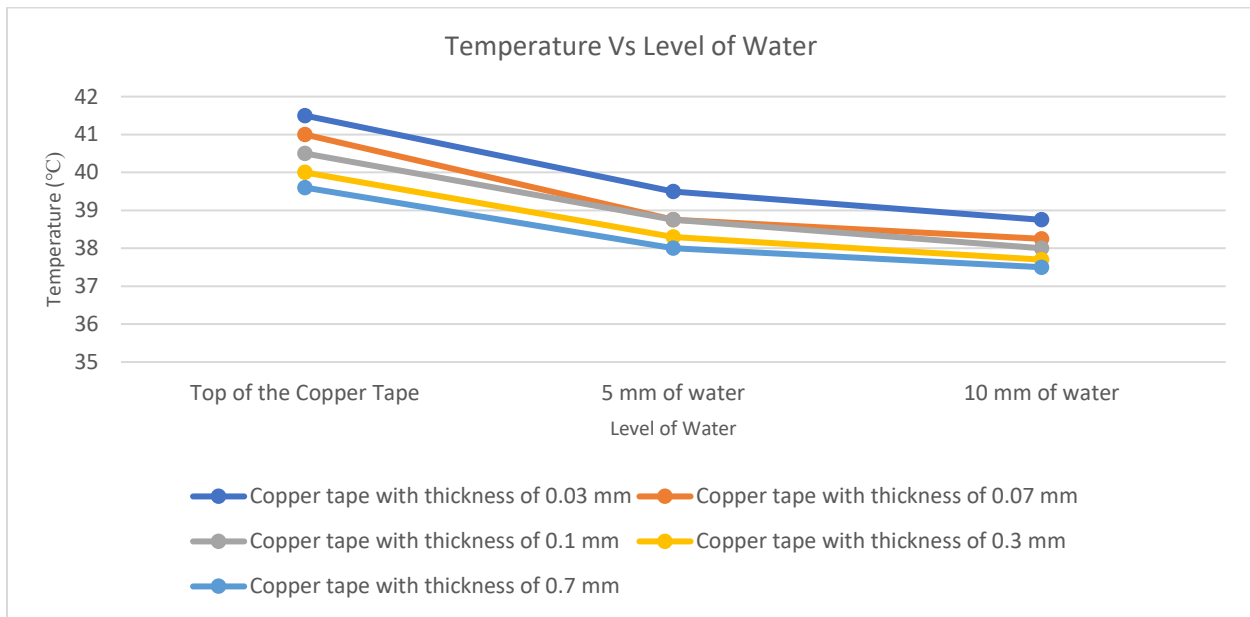


Figure 4.22 Comparing temperature distribution at 10 mm from the heater on top of the copper.

4.2.5 Simulation of nine heaters for a region of 100x100 mm

4.2.5.1 Simulation of nine heaters for a region of 100x100 mm with a copper tape with thickness of 0.03 mm

Nine heaters were employed in this study, as depicted in Figure 4.22, to determine temperature horizontally between three heaters placed in the middle of the board. The substrate

was FR4 with dimensions of 100x100 mm with thickness of 1.6 mm is used as PCB board and 100x100 mm copper tape with thickness of 0.03 mm. 10 mm of water block and 100 mm of air block were employed on top of the PCB board. Temperature simulations are conducted at three different heights: at zero, 5 mm and 10 mm of water level when the time increases from zero to 600 seconds in 60 seconds increments. Figure 4.23 shows temperature dissipation on top of the copper tape, 5 mm of water block and 10 mm of water block.

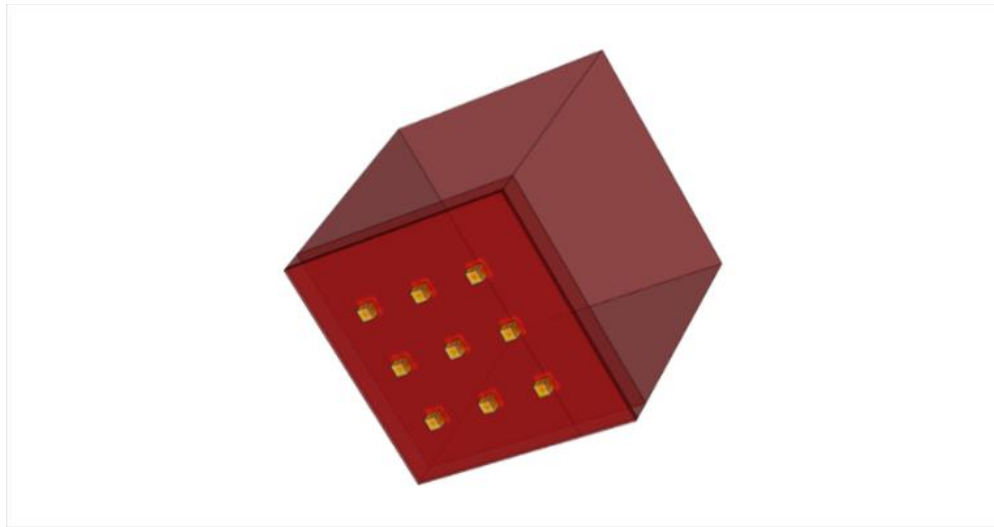
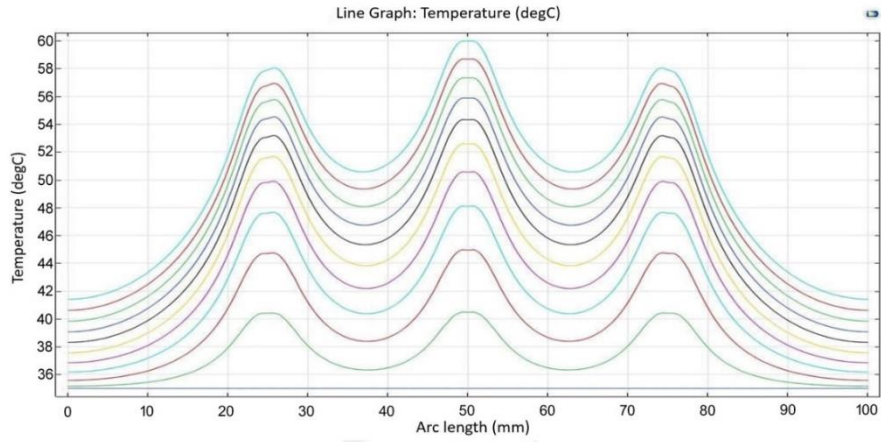
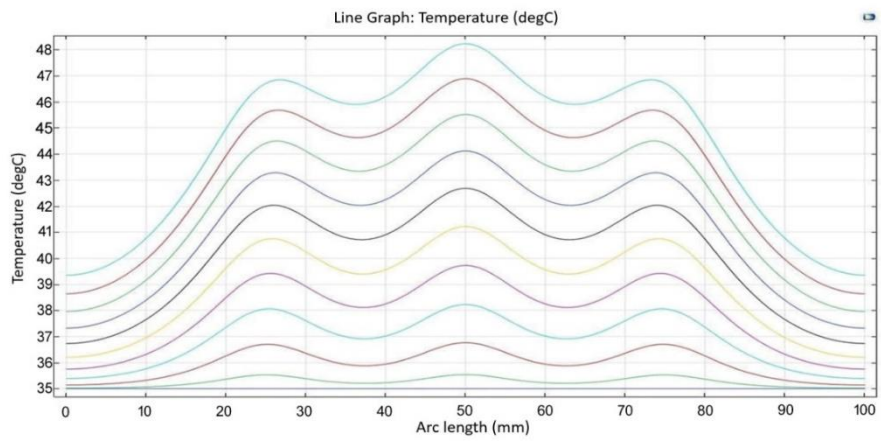


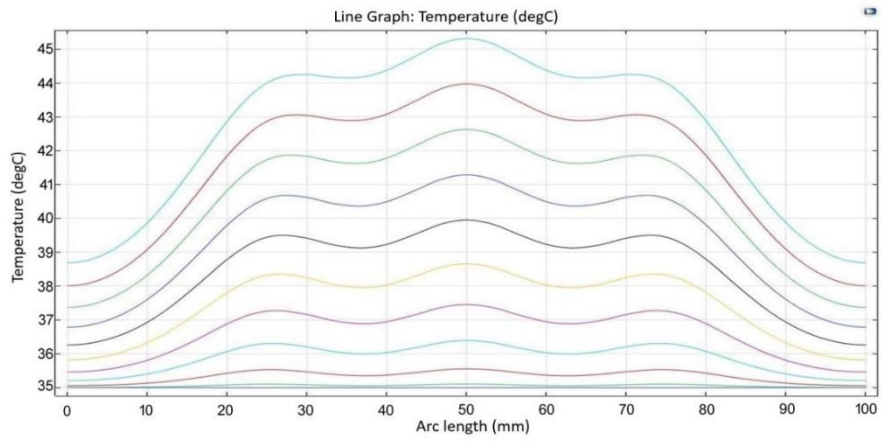
Figure 4.23 Simulation of nine heaters on 100 mm x 100 mm of FR4.



(a)



(b)

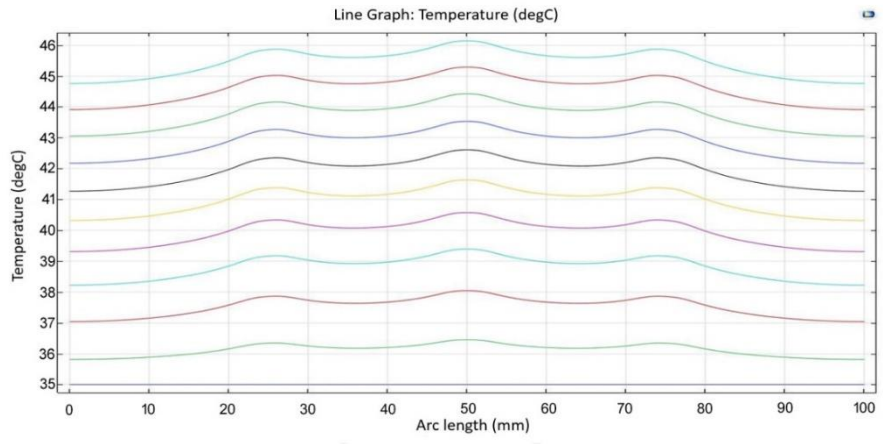


(c)

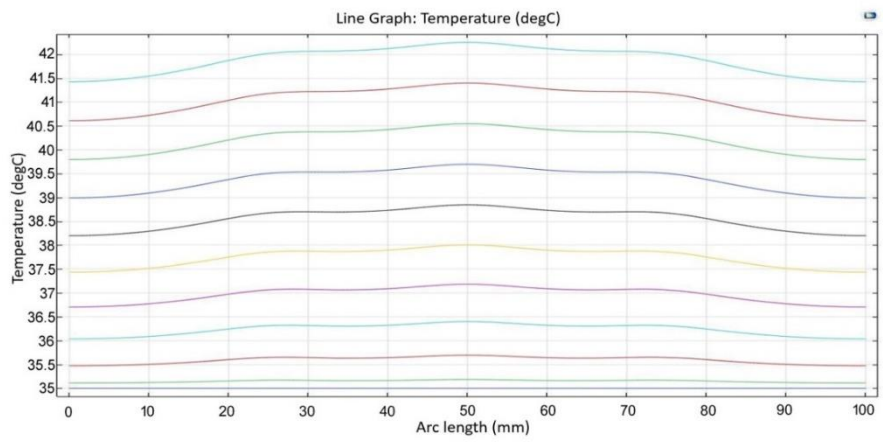
Figure 4.24 Simulation study for 0.03 mm copper tape. (a) Temperature distribution on top of the copper tape. (b) Temperature distribution at 5 mm in water block. (c) Temperature distribution on top of the 10 mm water block.

4.2.5.2 Simulation of nine heaters for a region of 100x100mm with a copper tape with thickness of 0.7 mm

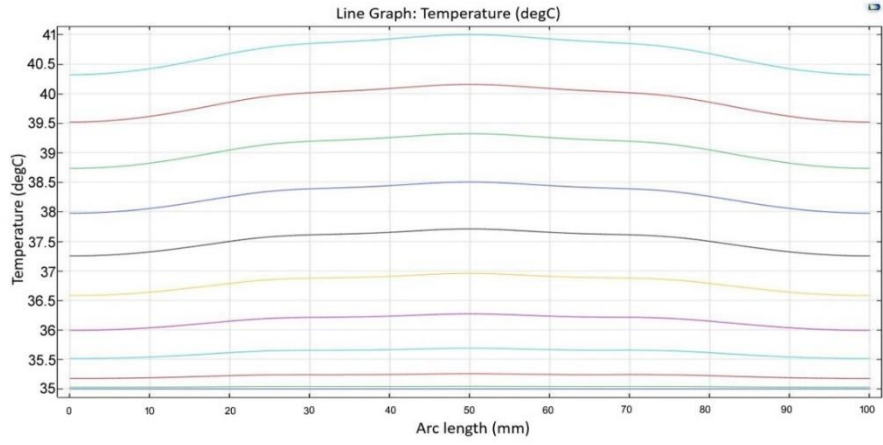
The study of section is similar as that of the previous section, however, the copper tape with thickness of 0.03 mm is replaced by a thicker tape of 0.7 mm.



(a)



(b)



(c)

Figure 4.25 Simulation study for 0.7 mm copper tape. (a) Temperature distribution on top of the copper tape. (b) Temperature distribution at 5 mm in water block. (c) Temperature distribution on top of the 10 mm water block.

Table 4.7 Heat distribution when nine heaters are applied with 0.03 and 0.7 copper tape thicknesses.

	Copper tape with thickness of 0.03 mm			Copper tape with thickness of 0.7 mm		
	Heater 1	Heater 2	Heater 3	Heater 1	Heater 2	Heater 3
Top of the copper tape (°C)	58	60	58	45.9	46	45.9
5 mm of water (°C)	47	48	47	42	42.75	42
10 mm of water (°C)	44.5	45.5	44.5	40.75	41	40.75

Based on the findings from sections 4.2.5.1, 4.2.5.2 and Table 4-5 it is evident that a copper tape with a thickness of 0.03 mm yields higher heat concentration above the heaters at each water level compared to the 0.7 mm counterpart. However, the 0.7 mm copper tape exhibits superior heat distribution, ensuring uniform heating around the heaters. As previously noted, the board is segmented into 12 regions. To deepen our understanding of heat distribution, the simulations were conducted in a single region in the subsequent section for further investigation.

4.2.6 Simulation of nine heaters for a region of the board

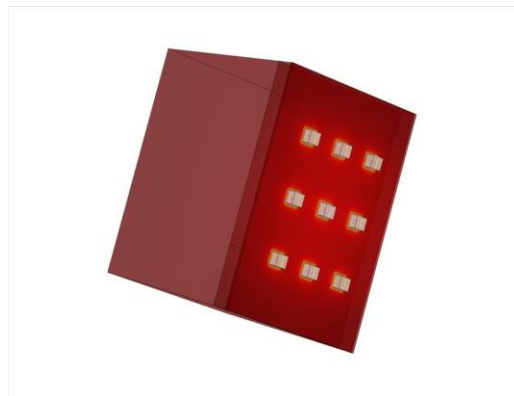


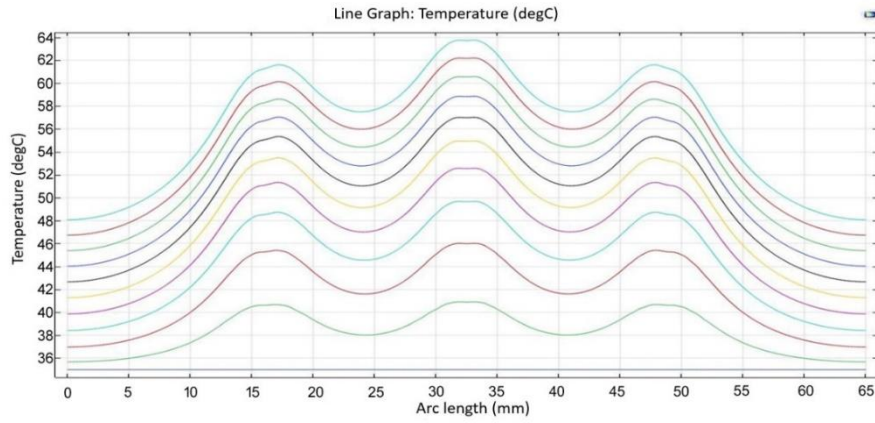
Figure 4.26 Simulation of nine heaters in one region of the board.

As previously mentioned, the size of the frame (honeycomb) is 430 mm x 210 mm. To fabricate the heater system, electrical wiring will need to be placed around the frames, and so some space should be left empty around the frame. Consequently, the actual size of the frame was decided to be 390 mm x 190 mm, and the size of one modelled heated region will be 95 mm x 65 mm. Figure 4.25 provides a visualization of the simulation, featuring nine heaters positioned within a single designated spot on the board.

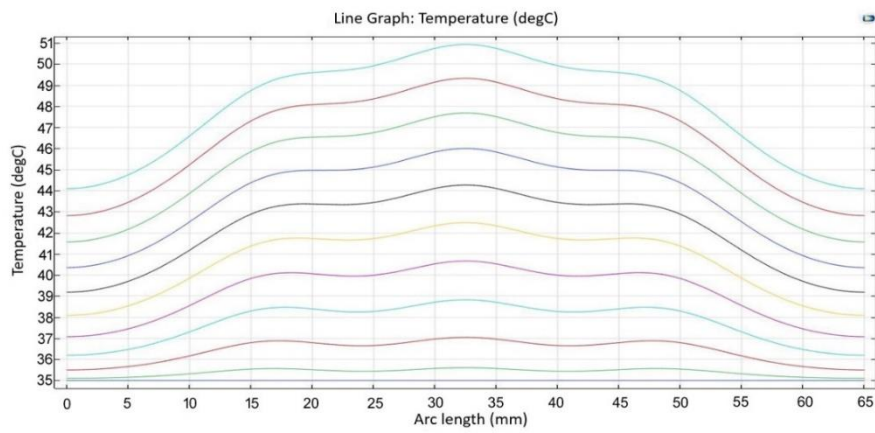
4.2.6.1 Simulation of nine heaters for a region of the board with a copper tape with thickness of 0.03 mm

4.2.6.1.1 Temperature distribution between side heaters

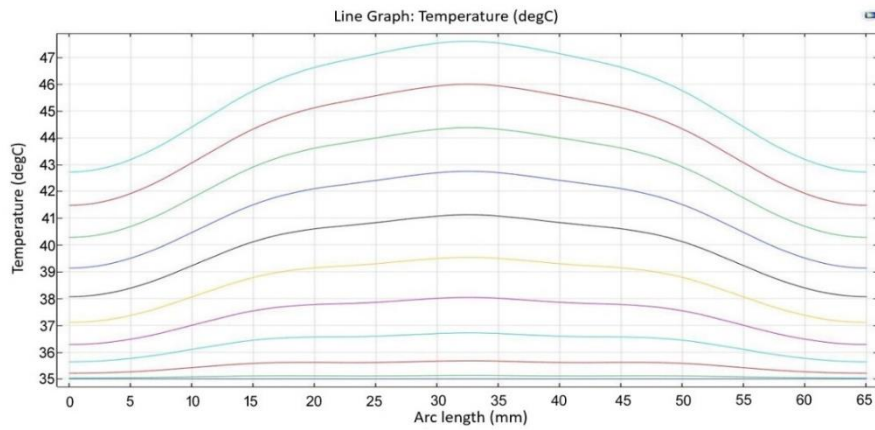
Figure 4.26 presents the temperature distribution between the side heaters on top of the copper tape with thickness of 0.03 mm. This study was taken with the presence of both a 5 mm of water block and a 10 mm of water block when the heating time was increased from zero to 600 seconds in 60 seconds increments.



(a)



(b)

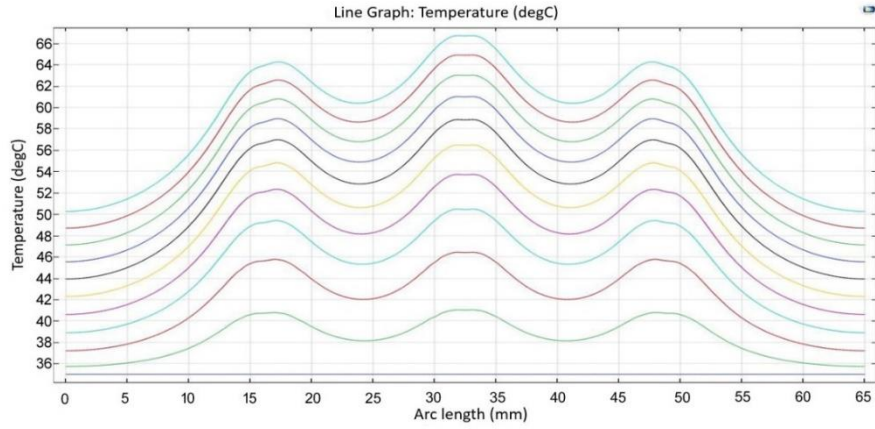


(c)

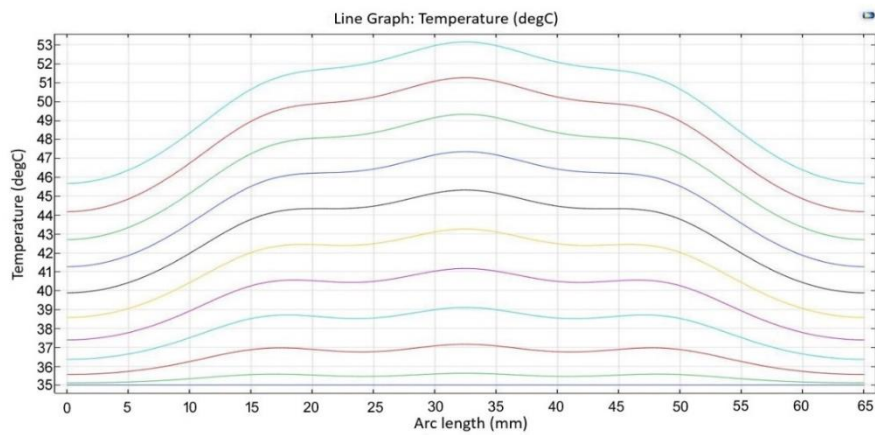
Figure 4.27 Simulation study for 0.03 mm copper tape side of the board. (a) Temperature distribution on top of the copper tape. (b) Temperature distribution at 5 mm in water block. (c) Temperature distribution on top of the 10 mm water block.

4.2.6.1.2 Temperature distribution between heaters in middle of the board

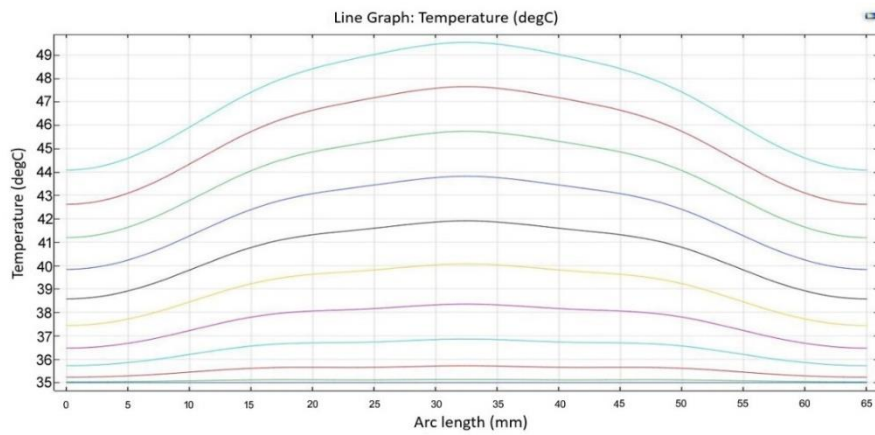
The temperature modelled between the heaters in the center of the board, over the copper tape with thickness of 0.03 mm, in the presence of both a 5 mm of water block and a 10 mm of water block. Figure 4.27 shows the temperature changes over a heating time span ranging zero to 600 seconds in 60 seconds increments.



(a)



(b)



(c)

Figure 4.28 Simulation study for 0.03 mm copper tape middle of the board. (a) Temperature distribution on top of the copper tape. (b) Temperature distribution at 5 mm in water block. (c) Temperature distribution on top of the 10 mm water block.

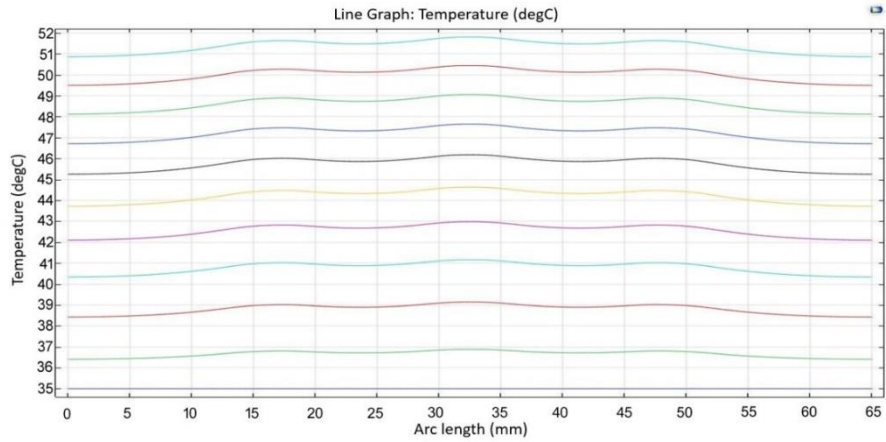
Table 4.8 Heat distribution with 0.03 mm copper tap when the heaters are inside and middle of the board.

	Heat distribution side of the board (°C)			Heat distribution middle of the board (°C)		
	Heater 1	Heater 2	Heater 3	Heater 1	Heater 2	Heater 3
Top of the copper tape	62	64	62	64	67	64
5 mm of water	49.5	50.5	49.5	51.5	53.2	51.5
10 mm of water	46.5	47.8	46.5	48.2	49.5	48.2

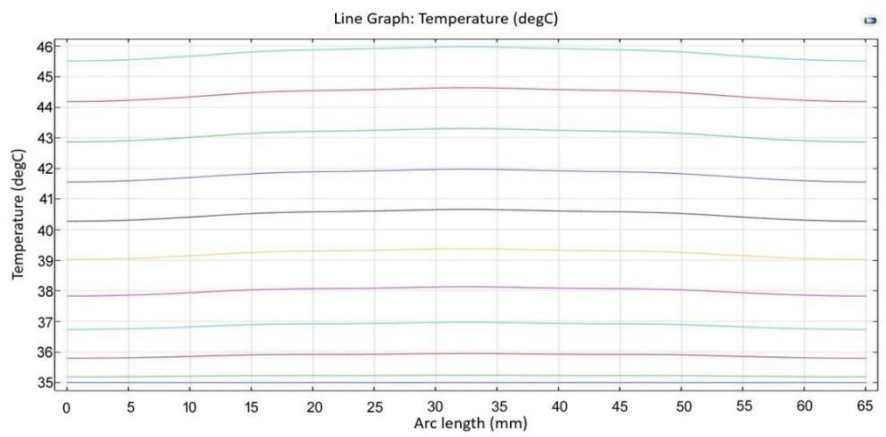
4.2.6.2 Simulation of nine heaters for a region of the board with a copper tape with thickness of 0.7 mm

4.2.6.2.1 Temperature distribution between side heaters

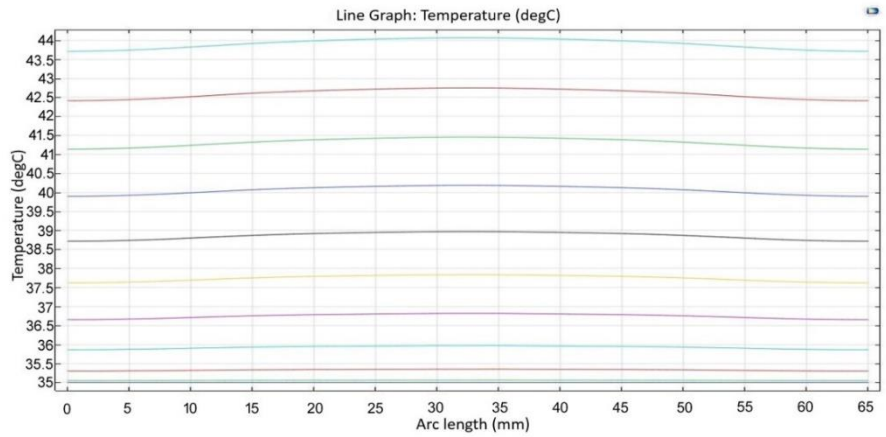
Figure 4.28 shows the temperature distribution between side heaters on top of the copper tape with thickness of 0.7 mm, in the presence of both a 5 mm of water block and 10 mm of water block when the heating time was increased from zero to 600 seconds in 60 seconds increments.



(a)



(b)

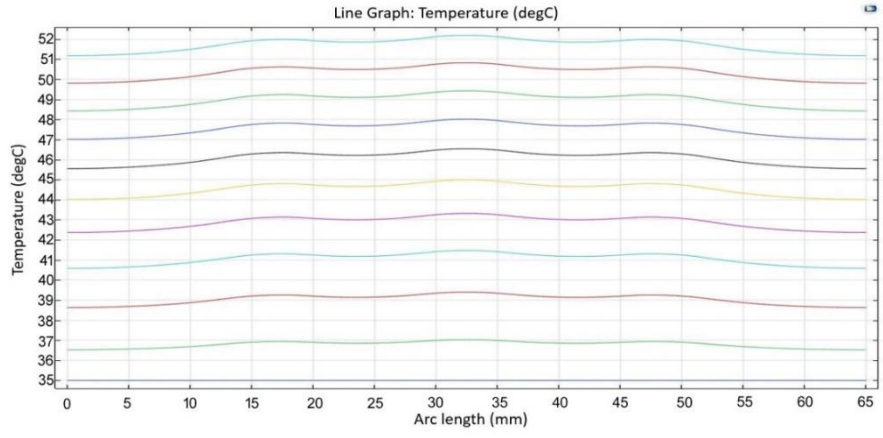


(c)

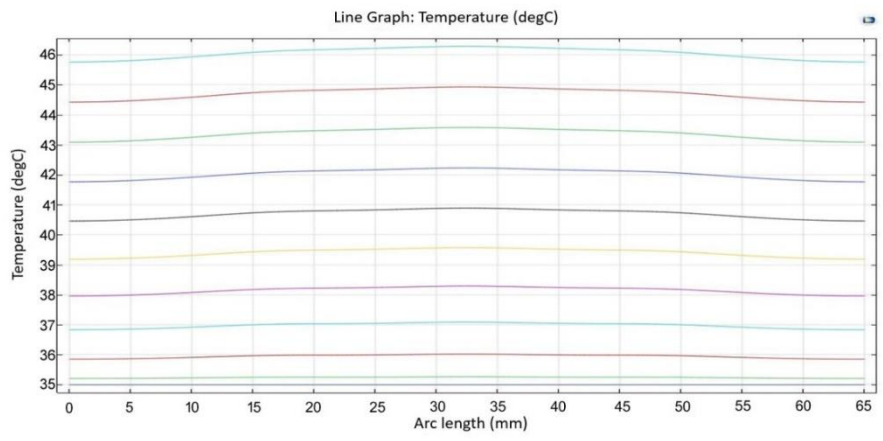
Figure 4.29 Simulation study for 0.7 mm copper tape. (a) Temperature distribution on top of the copper tape. (b) Temperature distribution at 5 mm in water block. (c) Temperature distribution on top of the 10 mm water block.

4.2.6.2.2 Temperature distribution between Heaters in Middle of the Board

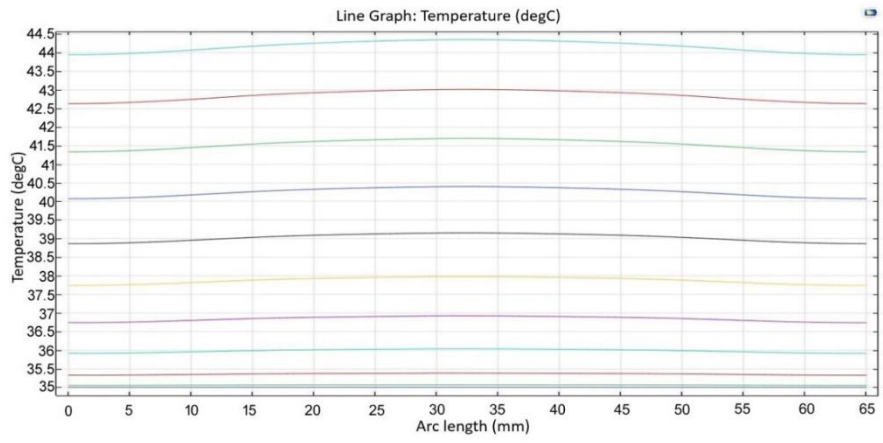
Figure 4.29 shows the temperature distribution between the heaters in the middle of the board on top of the copper tape with thickness of 0.7 mm, in the presence of both a 5 mm water block and 10 mm of water block. The data was modelled for a heating time between zero and 600 seconds with 60-second intervals.



(a)



(b)



(c)

Figure 4.30 Simulation study for 0.7 mm copper tape. (a) Temperature distribution on top of the copper tape. (b) Temperature distribution on top of 5 mm water block. (c) Temperature distribution on top of the 10 mm water block.

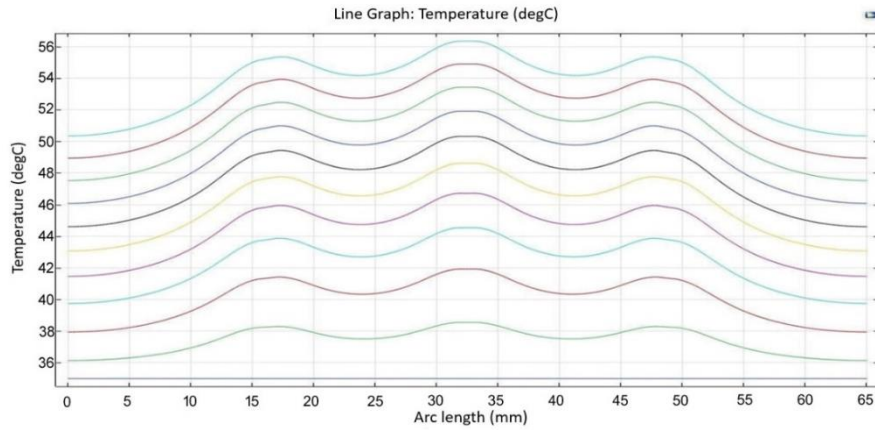
Table 4.9 Heat distribution with 0.7 mm copper tap when the heaters are inside and middle of the board.

	Heat distribution side of the board (°C)			Heat distribution middle of the board (°C)		
	Heater 1	Heater 2	Heater 3	Heater 1	Heater 2	Heater 3
Top of the copper tape	51.2	51.5	51.2	51.8	52	51.8
5 mm of water	45.7	46	45.7	46.1	46.3	46.1
10 mm of water	43.8	44	43.8	44	44.2	44

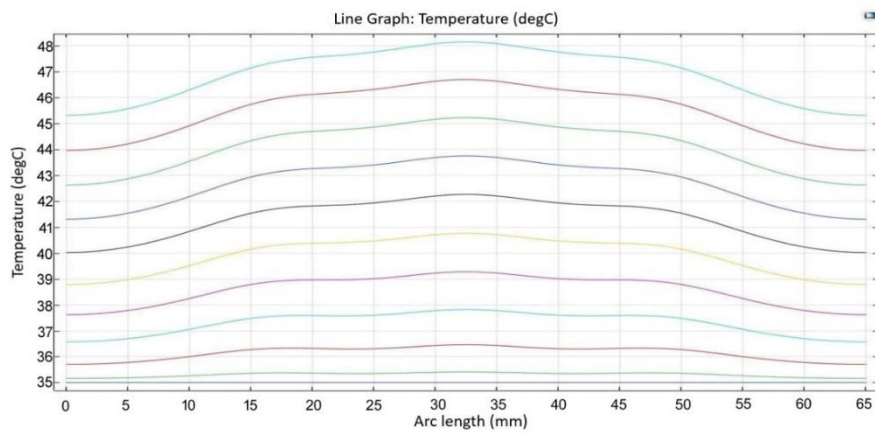
4.2.6.3 Simulation of nine heaters for a region of the board with a copper tape with thickness of 0.1 mm

4.2.6.3.1 Temperature distribution between side heaters

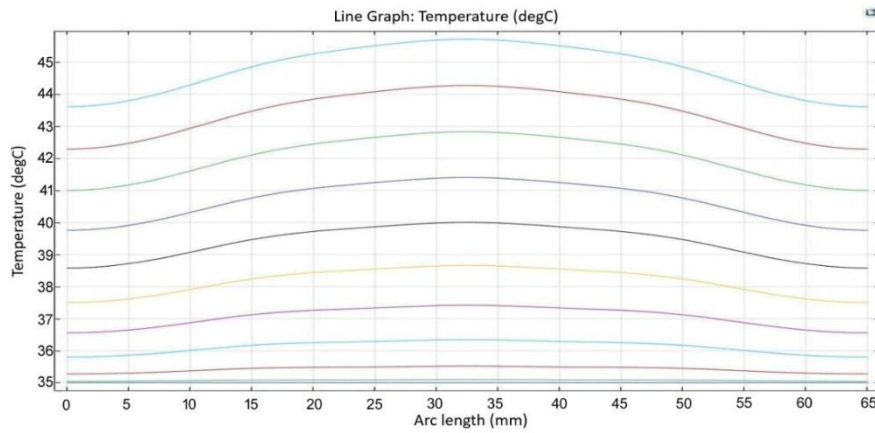
Figure 4.30 depicts the temperature distribution between the side heaters at top of the copper tape with thickness of 0.1 mm, while utilizing a 5 mm of water block and 10 mm of water block. The heating time was increased from zero to 600 seconds with readings recorded at 60-seconds intervals.



(a)



(b)

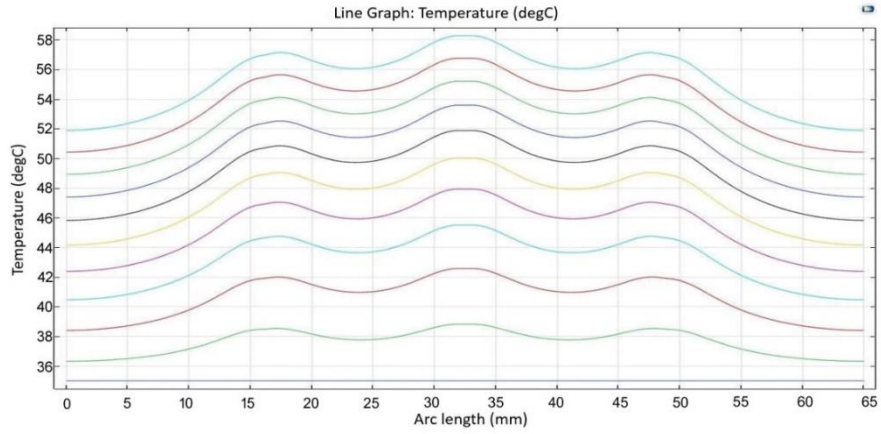


(c)

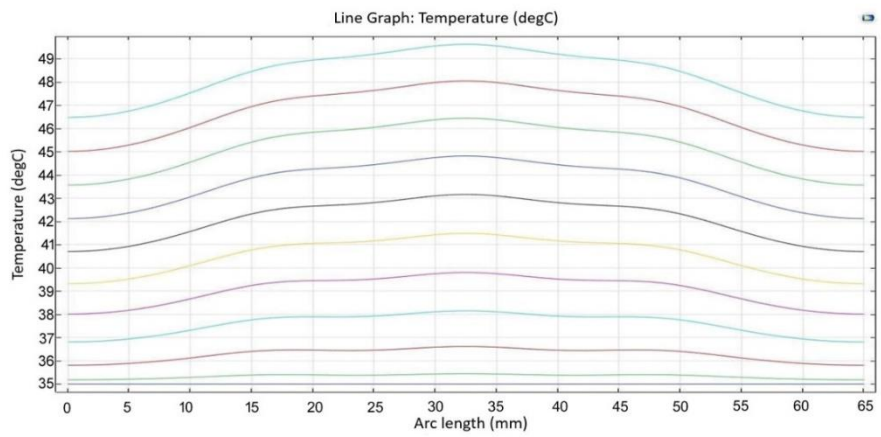
Figure 4.31 Simulation study for 0.1 mm copper tape. (a) Temperature distribution on top of the copper tape (b) Temperature distribution at 5 mm in water block. (c) Temperature distribution on top of the 10 mm water block.

4.2.6.3.2 Temperature distribution between Heaters in Middle of the Board

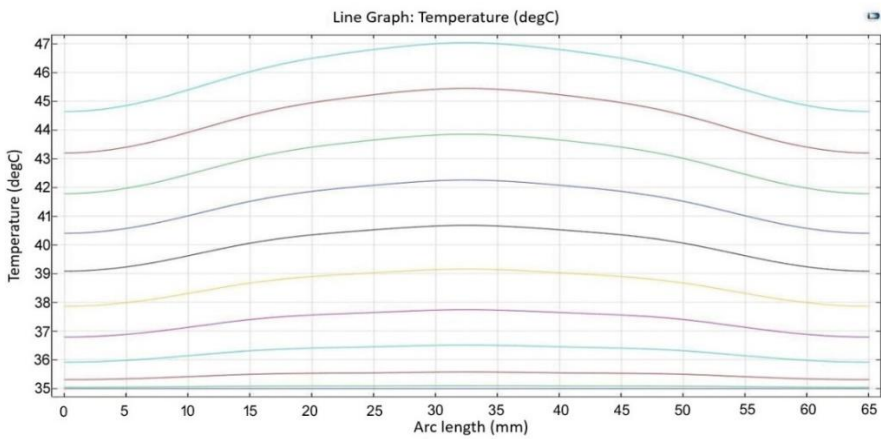
Figure 4.31 shows the temperature distribution between the heaters in the middle of the board on top of the copper tape with thickness of 0.1 mm by utilizing a 5 mm of water block and a 10 mm of water block when the heating time was increased from zero to 600 seconds in 60 seconds increments.



(a)



(b)



(c)

Figure 4.32 Simulation study for 0.1 mm copper tape. (a) Temperature distribution on top of the copper tape. (b) Temperature distribution on top of 5 mm water block. (c) Temperature distribution on top of the 10 mm water block.

Table 4.10 Heat distribution with 0.1 mm copper tap when the heaters are inside and middle of the board.

	Heat distribution side of the board (°C)			Heat distribution middle of the board (°C)		
	Heater 1	Heater 2	Heater 3	Heater 1	Heater 2	Heater 3
Top of the copper tape	55	57	55	57	58.2	57
5 mm of water	47.5	48.2	47.5	49	49.5	49
10 mm of water	45.2	45.8	45.2	46.5	47	46.5

4.2.7 Comparison of Simulations Results

From these simulations a difference can be observed in the simulated temperature at the top of the 5 mm water level and the 10 mm water level. This discrepancy can be attributed to variations in the specific heat capacity and thermal conductivity of the materials involved. As previously discussed, specific heat capacity and thermal conductivity are important in these observations. Based on the simulations, it can be observed that the temperature on top of the copper tape with a thickness of 0.03 mm is higher than that on the copper tape with a thickness of 0.7 mm and 0.1 mm. In fact, more energy was required to raise the temperature on top of the 0.7 mm and 0.1 mm thick copper tape due to its mass and specific heat capacity, while heat was more evenly distributed on top of the copper tape with thickness of 0.7 mm and 0.1 mm.

Despite the fact that the use of copper tape with thickness of 0.03 mm results in higher temperature on top of the heaters compared to copper tape with thickness of 0.7 mm and 1 mm, the temperature is more evenly distributed between the heaters when copper tape with thicknesses of 0.7 mm and 0.1 mm are used. As mentioned before Varroa mites go to feed from larva, they will not be on top of the water level, and they should be around larva's nest and below 5 mm of

water level. Therefore, the presented temperature control system that is discussed in this thesis can heat all areas of the board properly to eliminate the mites.

4.2.8 Further Models and Simulations for Determining Board Requirements

According to the thermal conductivity and the specific heat capacity of the materials that are used in the simulations, a PCB board with thickness of 1.6 mm can be employed, and 39-ohm resistors can be utilized as heaters on one side of board. As previously mentioned, the board has been divided to 12 regions, with each region requiring nine heaters to heat top of the water level to 47 °C. Therefore, a honeycomb needs 108 resistors (heaters) to heat all spots to 47 °C. An external 5-volt power can provide 0.750 W of energy, which is sufficient to increase the temperature to 47 °C. A cylindrical tube enveloped by a thin copper tape with a diameter of 1 mm can be used to transfer the heat to top the copper tape on the other side of the board. Some temperature sensors can be employed to control temperature throughout the board. The sensor DS1822 can be a good temperature sensor to measure temperature throughout the board. The DS1822 is produced by Maxim Integrated, an American company specializing in the design and manufacture of analog and mixed-signal integrated circuits. The DS1822 offers several advantages. It can measure temperatures ranging from -55 °C to 125 °C and operates using a power supply between 3 and 5.5 volts, making it compatible with the Arduino UNO used in the simulation. Another notable feature is its 1-wire addressable temperature system. In addition, if thicker copper tape is utilized, it is not necessary to use many DS1822 sensors because the heat distribution tends to be more uniform across the board. The remote heating system needs a switch to turn the heaters on or off when needed, and a PMOS transistor like BSS84AKV would be good to turn on and off heaters when necessary.

4.3 Chapter Summary

The chapter explores system fabricated on a PCB dedicated to monitoring hive temperature and controlling temperature. It is designed to enable combatting Varroa mites within beehives. Through detailed simulations, it was determined that employing thin copper tape is effective in distributing heat due to its favorable thermal conductivity and thermal mass. However, thicker copper tapes require more time and energy to achieve the desired temperature of 47 °C, while they exhibit a more even distribution of heat at the top of the water level.

The optimal thickness identified for achieving uniform temperature distribution at the top of the water level is 0.03 mm for the copper tape. A notable aspect of the initial design involves controlling each heater with a separate transistor and digital output from the Arduino. While effective, this approach may pose challenges, especially when dealing with multiple boards in a hive, each requiring a substantial number of heaters (108 heaters per board).

Simulations showed that by employing nine heaters in each region of the board, temperature can be raised to approximately 47°C evenly over the board in order to eliminate Varroa mites. Additionally, to optimize heat transfer through the board, a heat conductor with dimensions of 1x1x1.6 mm can be employed, complemented by a copper tape measuring 0.03 mm in thickness to ensure uniform heat distribution over the board surface.

Chapter 5: Conclusions and Future Work

Section 5.1 provides a summary of previous chapters, including the results and conclusions from the simulations and lab tests discussed in those chapters. Section 5.2 outlines potential future work and research to further develop and expand the results discussed in the previous sections.

5.1 Conclusions

The goal of this thesis was to aid beekeeping by designing a suitable electronic frame for usage in brood box of a beehive to:

- 1- Measuring the honey level remotely within the hive supers and brood nest by using capacitor sensors.
- 2- Monitoring temperature within the brood nest and killing Varro mites by increasing temperature in each area of the hive.

The first component designed in this thesis was a capacitance board that serves to monitor the cell contents within both the honey supers and brood box. This simulation was performed to determine an interdigitated capacitance sensor (IDC) for monitoring cell content and to pinpoint a dependable electrode geometry for this purpose. According to the simulations, it was found that a noticeable capacitance changes in the picofarad range occurred when the level of liquid is varied from 0-10 mm. Additionally, it was discovered that, more significant changes occurred when a lower level of the liquid was added on top of empty cells, while smaller changes were noted when the liquid level was at the highest. The other factor that can affect capacitance is relative permittivity, and since water has a higher relative permittivity than honey, it can cause a greater change in capacitance change than the same amount of honey. According to the different type of

simulations that tested in this thesis, an IDC sensor was shown to be a viable design to measure the level of liquid on top of the frame (and in the honeycomb cells). Various electrode finger geometries were tested to identify which IDC sensor design would be more suitable for measuring the capacitance change to the varying honey levels from 0-10 mm thickness. Based on the simulations, all designs were able to determine capacitance changes at lower levels of liquid. However, not all designs could clearly recognize changes in capacitance above approximately a seven millimeter level of liquid. It was found that the fourth capacitance design was more accurate than the other designs.

Prototypes of these capacitor sensors were made to validate the result of simulations. Copper tape with 3 mm width was employed to make the IDC electrodes to collect data and compare them to the simulations. A thin layer of silicone wax was applied on top of the electrodes to simulate beeswax, and a 5 V power source was utilized in the simulations. The PCB board was divided into 12 regions. Based on the experiments, the fourth IDC design which had 15 mm space between electrodes provided better results for each level of liquid from 1 mm to 10 mm.

The second component designed in this thesis was a heater system to control the temperature over the frames inside the brood nest of a hive. This was designed to enable heating of the frame to kill detected infections by Varroa mites by selectively increasing the temperature in specific areas to eliminate them. This part of thesis focused on simulations of heat flow over frames in the brood nest which had a heater system on them, and copper metal for heat distribution. Firstly, simulations were made with different size of heat conductor to determine which size of heat conductors can transform heat from the heaters, through the PCB, to the opposite surface. It was determined that a 1x1x1.6 mm heat conductor was the most efficient in terms of transferring heat quickly compared to the other side. Copper tape with different thicknesses were simulated to

determine which could transfer heat faster over the PCB surface. According to the results, 0.03 mm copper tape is capable of distributing heat faster than a thicker copper tape to the top of the liquid level. Based on the simulations, each region of the heated frame needs nine heaters to enable even distribution of heat on the board surface.

The temperature control system can also be employed in the honey super boxes, which would be useful to keep temperature around 35 °C, so that bees can continue being active without needing to expend effort to heat the hive on colder days. Therefore, beekeepers do not need to be as worried about temperature changes because this system will control and adjust the temperature automatically.

5.2 Future Work

Simulations and lab tests have now been concluded. For the IDC sensor frames that measure honey level, tests should be undertaken within a beehive environment to obtain real world results. For the heated frames, each comb needs to have 108 heaters and each colony has between 8 and 10 frames. Due to the considerable number of wires that will be required to connect the heaters, this aspect needs to be thought through carefully. Additionally, a system needs to be provided to detect the presence of Varro mites, and their precise location, to enable the heated frames to kill the mites without unnecessarily damaging other areas of the frame and hive. This system could potentially involve the use of specific sensors, cameras, or other technologies.

References:

- [1] M. Bixby, S. H. Hoover, R. McCallum , A. Ibrahim , L. Ovinge , S. Olmstead, S. F. Pernal, A. Zayed, L. J. Foster and M. M. Guarna, “Honey Bee Queen Production: Canadian Costing Case Study and Profitability Analysis,” *Journal of Economic Entomology*, vol. 113, no. 4, pp. 1618-1627, August 2020.
- [2] Canadian Honey Council, “Industry Overview,” [Online]. Available: https://honeycouncil.ca/archive/honey_industry_overview.php. [Accessed: Nov. 11, 2021].
- [3] D. D. Dasig and J. M. Mendez, “An IoT and Wireless Sensor Network-Based Technology for a Low-Cost Precision Apiculture,” *Big Data Internet of Things and Analytics for Agriculture*, vol. 2, pp. 67-92, January 2020.
- [4] B. Ruzzo, “Monitoring Honeybees with SmartHives Tech-Urban Beekeeping Lab,” January 2017. [Online]. Available: <https://urbanbeelab.org/remote-bee-monitoring/> [Accessed Sept. 12, 2021].
- [5] W. G. Meikle and N. Holst, “Application of continuous monitoring of honeybee colonies”, *Apidologie*, vol. 46, pp.10-22, Jun 2014.
- [6] A. Qurthobi, R. F. Iskandar, A. Krisnatal, and Weldzikarvina, “Design of capacitive sensor for water level measurement,” 8th International Conference on Physics and its Applications (ICOPIA), Denpasar, Indonesia, August 2016.
- [7] V. Bande, D. Pitcia and C. Loan, “Multi - Capacitor sensor algorithm for water level measurement,” 35th International Spring Seminar on Electronics Technology (ISSE), Bad Aussee, Austria, 2012.

- [8] S. Phimpisan and W. Sa-ngiamvibool, "Determination of water added in raw milk using interdigital capacitor sensor," *Przeglad Elektrotechniczny*, vol. 91, pp. 265-267, Warsaw, Poland, 2015.
- [9] B. A. Lawton and R. Pethig, "Determining the fat content of milk and cream using AC conductivity measurements," *Measurement Science and Technology*, IOPScience, vol. 4, no. 1, pp. 38-41, IOP Publishing, United Kingdom, 1993.
- [10] C. Felice, R. E. Madrid, J. M. Olivera, V. I. Rotger, and M. E. Valentinuzzi, "Impedance microbiology: quantification of bacterial content in milk by means of capacitance growth curves," *Journal of Microbiological Methods*, vol. 35, no. 1, pp. 37-42, February 1999.
- [11] H. Abou-Shaara and A. Al-Ghamli, "Tolerance of two honeybee races to various temperature and relative humidity gradients," *The 28 meeting of the Saudi Biological Society*, Jun./Jul. 2016.
- [12] N. E. Gary, "Activities and Behavior of Honeybees," *The Hive and the Honey Bee*, revised ed. Dadant & Sons, Eds. Hamilton, IL, pp. 185-264, 1975.
- [13] P. D. Cooper, W. M. Schaffer, and S. L. Buchmann, "Temperature Regulation of Honeybees (*Apis mellifera*) Foraging in the Sonoran Desert," *Journal of Experimental Biology*, vol. 7, no. 2, pp. 123-145, Arizona, U.S.A., June 1984.
- [14] Arnia remote hive monitoring, "Temperature and Thermoregulation in the Beehive," [Online]. Available: <https://www.arnia.co.uk/temperature-and-thermoregulation-in-the-beehive>, [Accessed: Nov. 11, 2021].
- [15] E. Southwick and G. Gerhard Heldmaier, "Temperature Control in Honeybee Colonies," *American Institute of Biological Sciences*, vol.37, no.6, pp. 395-399, June 1987.

- [16] Z. Huang, "Mite zapper - A new and effective method for Varroa mite control," American Bee Journal, Hamilton, Illinois, October 2001.
- [17] M. Milbrath, "Keeping your bees safe from the Varroa mite," Michigan state university extension, Michigan, United States, April 2016.
- [18] M. Arawwawala and S. Hewageegana, "Health Benefits and Traditional Uses of Honey: A Review," Journal of Apitherapy, vol. 2, no. 1, pp. 9, January 2017.
- [19] National Agricultural Statistics Service, USDA, "Honey Bee Colonies," August 2021.
- [20] "Statistical Overview of the Canadian Honey and Bee Industry," 2019. [Online]. Available: http://multimedia.agr.gc.ca/pack/pdf/honey_miel_2019-eng.pdf, [Accessed: June 2021].
- [21] Government of Canada / Gouvernement du Canada, "Statistical Overview of the Canadian Honey and Bee Industry," July 2020. [Online]. Available: <https://www.agr.gc.ca/eng/horticulture/horticulture-sector-reports/statistical-overview-of-the-canadian-honey-and-bee-industry-2019/?id=1594646761058>. [Accessed: Oct. 22, 2021].
- [22] C. E. Aslan, C. T. Liang, B. Galindo, K. Hill, and W. Topete, "The Role of Honeybees as Pollinators in Natural Areas," Natural Areas Journal, Bend, Oregon, United States, October 2016.
- [23] D. P. Abrol, "Pollination Biology," 1st ed, Elsevier, Academic Press, 2012.
- [24] B. K. Klatt, A. Holzschuh, C. Westphal, Y. Clough, I. Smit, E. Pawelzik and T. Tschamntke, "Bee pollination improves crop quality, shelf life and commercial value," Biological sciences / The Royal Society, vol. 281, November 2013.

- [25] J. Zawislak, “Bees as Pollinators: Arkansas Pollinators,” [Online]. Available: <https://www.uaex.edu/farm-ranch/special-programs/beekeeping/pollinators.aspx>. [Accessed: Oct. 28, 2020].
- [26] “5 Ways Bees are Important to the Environment,” [Online]. Available: <http://www.pthomeandgarden.com/5-ways-bees-are-important-to-the-environment/>. [Accessed: Oct. 28, 2021].
- [27] S. User, “Honey Trivia,” [Online]. Available: <https://www.honeyassociation.com/about-honey/honey-trivia>. [Accessed: Oct. 29, 2020].
- [28] Government of Canada / Gouvernement du Canada, “Statistical Overview of the Canadian Honey and Bee Industry and the Economic Contribution of Honey Bee Pollination 2016,” January 2018. [Online]. Available: <https://www.agr.gc.ca/eng/horticulture/horticulture-sector-reports/statistical-overview-of-the-canadian-honey-and-bee-industry-and-the-economic-contribution-of-honey-bee-pollination-2016/?id=1510864970935>. [Accessed: Nov. 02, 2021].
- [29] “Seasonal Cycles of Activities in Colonies,” [Online]. Available: <https://agdev.anr.udel.edu/maarec/honey-bee-biology/seasonal-cycles-of-activities-in-colonies/>. [Accessed: Nov. 02, 2021].
- [30] M. L. Smith, J. D. Davidson, B. Wild, D. M. Dormagen, T. Landgraf, and I. D. Couzin, “Behavioral variation across the days and lives of honeybees,” *Journal Abbreviation*, vol. 25, no. 9, pp.10842, July 2022.
- [31] “Bee Facts,” [Online]. Available: http://honeycouncil.ca/archive/bee_facts.php. [Accessed: Nov. 02, 2020].

- [32] “The Amazing Honey Bee,” 2019. [Online]. Available:
[http://www.bartelhoneyfarms.ca/index/Bee_FAQs_\(and_Facts\).html](http://www.bartelhoneyfarms.ca/index/Bee_FAQs_(and_Facts).html). [Accessed: Nov. 02, 2021].
- [33] W. Wright, “How Many Eggs CAN a Queen Lay?,” November 2008. [Online]. Available:
<https://www.beesource.com/threads/how-many-eggs-can-a-queen-lay.365708/>. [Accessed: Nov. 02, 2021].
- [34] Canada Science and Technology Museum, “Life in a Hive,” [Online]. Available:
<https://bees.techno-science.ca/english/bees/life-in-a-hive/stages.php>. [Accessed: Nov. 02, 2021].
- [35] B. Bee-Health, “Bee Brood (Basic Bee Biology for Beekeepers),” August 2019. [Online]. Available: <https://bee-health.extension.org/bee-brood-basic-bee-biology-for-beekeepers/>. [Accessed: Nov. 02, 2021].
- [36] J. Sartell, “The Life Cycle of a Baby Bee Keeping Backyard Bees,” October 2017. [Online]. Available: <https://www.keepingbackyardbees.com/the-life-cycle-of-a-baby-bee/>. [Accessed: Nov. 02, 2020].
- [37] Terminix, “The Lifecycle of a Honeybee,” [Online]. Available:
<https://www.terminix.com/blog/science-nature/life-cycle-of-honey-bee/>. [Accessed: Nov. 02, 2020].
- [38] “Beehive,” October 2020. [Online]. Available: <https://en.wikipedia.org/wiki/Beehive>. [Accessed: Nov. 03, 2020].
- [39] “Hive Information - Basic Types of Modern or Movable Hives in Common Use,” April 2018. [Online]. Available: <https://www.mdbka.com/hive-information/>. [Accessed: Nov. 03, 2020].

[40] A. A. Oyerinde and T. E. Achong, “Comprehensive Value Chain Development of Natural Resources for Economic Diversification: The Apiculture Approach,” *Advances in Entomology*, vol. 9, no.2, pp. 21-42, Ithaca, NY, March 2021.

[41] M. Bee, “Types of Modern Hives,” August 2019. [Online]. Available: https://honeycostarica.com/blog/bee-hives/types-of-modern-hives/?utm_source=rss. [Accessed: Nov. 16, 2021].

[42] “The Different Types of Commercial Beehives for Sale,” July 2020. [Online]. Available: <http://completebeehives.com/commercial-beehives-for-sale/>. [Accessed: Nov. 03, 2021].

[43] “How to Build a Langstroth Beehive,” March 2020. [Online]. Available: <https://beekeepclub.com/how-to-build-a-langstroth-beehive/>. [Accessed: Nov. 03, 2021].

[44] H. Blackiston, “The Parts of a Beehive,” [Online]. Available: <https://www.dummies.com/home-garden/hobby-farming/beekeeping/the-parts-of-a-beehive/>. [Accessed: Nov. 09, 2021].

[45] “Parts of a Beehive - Beginner Beekeeper's Guide - Beekeeping,” May 2020. [Online]. Available: <https://www.beverlybees.com/parts-beehive-beginner-beekeeper/>. [Accessed: Nov. 03, 2020].

[46] R. Conrad, “All boxes are not created equal. Pick the one best for you,” *Bee Culture*, November 2014.

[47] J. Stamp, “The Secret to the Modern Beehive is a One-Centimeter Air Gap,” *Smithsonian Magazine*, September 06, 2013.

- [48] J. Skinner, “What is 'Bee Space' and why is this important to beekeeping?” August 2019. [Online]. Available: <https://bee-health.extension.org/what-is-bee-space-and-why-is-this-important-to-beekeeping/>. [Accessed: Jan. 05, 2022].
- [49] E. Maund, “Eight is the magic number, sort of,” October 2014. [Online]. Available: <https://missapismellifera.com/2014/10/04/eight-is-the-magic-number-sort-of/>. [Accessed: Dec. 25, 2020].
- [50] C. C. Dadant, “Beekeeping Equipment,” *The Hive and the Honey Bee*, revised ed, Dadant & Sons, Eds. Hamilton, IL, pp. 303–328, 1975
- [51] “Foundation or Foundationless Beekeeping?” [Online]. Available: <https://www.perfectbee.com/your-beehive/beehives-and-accessories/foundation-or-foundationless>. [Accessed: Feb. 09, 2021].
- [52] “Top 9 Best Beehive Foundation for Sale (2020),” January 2020. [Online]. Available: <https://beekeepclub.com/best-beehive-foundation-for-sale/>. [Accessed: Nov. 09, 2020].
- [53] E. Egstad, “The Great Divide: Foundation vs. Foundationless Beekeeping,” June 2017. [Online]. Available: <http://www.beeandbloom.com/blog/foundation-vs-foundationless>. [Accessed: Nov. 09, 2020].
- [54] J. L. Gould and C. G. Gould, “The Honeybee,” *Scientific American Library*, New York, NY, 1988.
- [55] M. A. Y. Oddie, P. Neumann and B. Dahle, “Cell size and Varroa destructor mite infestations in susceptible and naturally-surviving honeybee (*Apis mellifera*) colonies,” *Apidologie*, vol. 50, October 2018.

- [56] T. S. K. Johansson and M. P. Johansson, “Substitutes for beeswax in a comb and comb foundation,” *Bee World*, vol. 52, no. 4, pp. 146–156, 1971.
- [57] “Beekeeping Basics – Foundation vs Foundationless Beekeeping,” March 2020. [Online]. Available: <https://beekeepclub.com/foundation-vs-foundationless-beekeeping/>. [Accessed: Feb. 11, 2021].
- [58] E. Crane, “Bees and Beekeeping – Science, Practice and World Resources,” Ithaca, NY: Comstock Publishing Associates, May 2011.
- [59] J. A. Berry, W. B. Owens, and K. S. Delaplane, “Small-cell comb foundation does not impede Varroa mite population growth in honey bee colonies,” *Apidologie*, vol. 41, no. 1, pp. 40-44, Athens, GA, January 2010.
- [60] S. Gil-Lebrero, F. Quiles-Latorre, M. Ortiz-López, V. Sánchez-Ruiz, V. Gámiz-López, and J. Luna-Rodríguez, “Honey Bee Colonies Remote Monitoring System,” *Special Issue State-of-the-Art Sensors Technology*, vol. 17, no. 12, p. 55, Spain, December 2016.
- [61] “Arnia Remote Hive Monitoring System,” July 2020. [Online]. Available: <https://www.podgroup.com/resources/case-studies/arnia-remote-hive-monitoring-system/>. [Accessed: Nov. 14, 2020].
- [62] “Solutionbee,” [Online]. Available: <https://solutionbee.com>. [Accessed: Nov. 2021].
- [63] “Smarthives - bee controlled,” [Online]. Available: <https://okoskaptar.hu/>. [Accessed: Nov. 15, 2020].

[64] O. Anwar, A. Keating, R. Cardell-Oliver, A. Datta and G. Putrino, “Apis-Prime: A deep learning model to optimize beehive monitoring,” vol.144, pp.57-100, Crawley, Australia, July 2022.

[65] “Fighting Honey-Bee Colony Mortality through IoT,” [Online]. Available: <https://io-bee.eu/>. [Accessed: Feb. 14, 2021].

[66] “Hivemind Precision Apiculture,” 2020. [Online]. Available: <https://hivemind.co.nz>. [Accessed: Feb. 21, 2021].

[67] D. Hadley, “The Amazing Honey-Making Process of Bees,” May 2018.

[68] R. T. Moriarty, “Backyard Beekeeping in the Beehive State: Salt Lake City’s Beekeeping Regulations, Nuisance Concerns, and the Legal Status of Honey Bees,” Utah Law Review, vol. 2018, no. 1, 2018.

[69] N. Godfrey, “Anthropogenic and climatic factors affecting honey production: The case of selected villages in Manyoni District, Tanzania,” Journal of Agricultural Biotechnology and Sustainable Development, vol. 10, no. 3, pp. 45-57, 2018.

[70] K. Urquhart, “9 Ways to Reduce the Stress on Your Bees,” November 2020.

[71] “About Honey,” [Online]. Available: <http://www.honeybeecentre.com/learn-about-honey>. [Accessed: Mar. 07, 2021].

[72] Government of Canada, “Canadian Grade Compendium Volume 6,” June 2018. [Online]. Available: <https://www.inspection.gc.ca/about-cfia/acts-and-regulations/list-of-acts-and->

[regulations/documents-incorporated-by-reference/canadian-grade-compendium-volume-6/eng/1523388139064/1523388171017](https://www.canada.ca/en/govext/doc/1523388139064/1523388171017). [Accessed: Mar. 27, 2021].

[73] E. C. Martin, "Some aspects of hygroscopic properties and fermentation of honey," *Bee World*, vol. 39, no. 7, pp. 165–178, United Kingdom, February 2020.

[74] E. Notes, "Dielectric Constant & Relative Permittivity," [Online]. Available: https://www.electronics-notes.com/articles/basic_concepts/capacitance/dielectric-constant-relative-permittivity.php. Accessed: Mar. 11, 2021].

[75] "Relative Permittivity - the Dielectric Constant," [Online]. Available: https://www.engineeringtoolbox.com/relative-permittivity-d_1660.html. [Accessed: Mar. 27, 2021].

[76] H. He, W. Zou, S. Jones, D. Robinson, R. Horton, M. Dyck, V. Filipović, K. Noborio, K. Bristow, Y. Gong, W. Sheng, Q. Wu, H. Feng and Y. Liu, "Chapter Four - Critical review of the models used to determine soil water content using TDR-measured apparent permittivity," Academic Press, vol.182, pp.169-219, 2023.

[77] Z. An, J. Ningde, Z. Lusheng, and G. Zhongke, "Liquid holdup measurement in horizontal oil–water two-phase flow by using concave capacitance sensor," *Measurement*, vol. 46, no. 10, pp. 3887-3898, December 2013.

[78] A. Fendri, A. Y. Kallel, H. Nouri, H. Ghariani, and O. Kanoun, "Measurement System for Lossy Capacitive Sensors: Application to Edible Oils Quality Assessment," *Sensors*, vol. 19, 2019.

- [79] G. De La M. Nichols & D.S.M. Phillips, "A capacitor milk meter for data logging," *New Zealand Journal of Agricultural Research*, vol. 13, no. 1, pp. 198-203, August 1970.
- [80] S. Phimpisan and W. Sa-ngiamvibool, "Determination of water added in raw milk using interdigital capacitor sensor," *Przegląd Elektrotechniczny*, vol. 91, no. 9, pp. 265, Warsaw, Poland, 2015.
- [81] M. V. Zambrano, B. Dutta, D. G. Mercer, H. L. MacLean, and M. Touchie, "Assessment of moisture content measurement methods of dried food products in small-scale operations in developing countries: A review," *Trends in Food Science & Technology*, vol. 88, June 2019.
- [82] C. J. Felice, R. E. Madrid, J. M. Olivera, V. I. Rotger, and M. E. Valentinuzzi, "Impedance microbiology: quantification of bacterial content in milk by means of capacitance growth curves," *Journal of Microbiological Methods*, vol. 35, no. 1, pp. 37-42, 1999.
- [83] N. Angkawisittpan and T. Manasri, "Determination of Sugar Content in Sugar Solutions using Interdigital Capacitor Sensor," *Materials Science (Medžiagotyra)*, vol. 12, no. 1, pp. 8-11, January 2012.
- [84] D. Wang, "Basics of Capacitive Sensing and Applications," Texas Instruments Incorporated, Tech, pp. 1-8, Dallas, Texas, June 2021
- [85] H. Endres and S. Drost, "Optimization of the geometry of gas-sensitive interdigital capacitors," *Sensors and Actuators B: Chemical*, vol. 4, no. 1-2, pp. 95-98, 1991.

[86] J. Kim and D. Lee, “Analysis of dielectric sensors for the cure monitoring of resin matrix composite materials,” *Sensors and Actuators A: Physical*, vol. 70, no. 2-3, pp. 138-144, October 1998.

[87] Freescale Semiconductors, (September 2010). “MPR121 Proximity Capacitive Touch Sensor Controller,” [Online]. Available:

<https://www.sparkfun.com/datasheets/Components/MPR121.pdf> [Accessed: January 2022].

[88] Adafruit. (n.d.). MPR121 12-Key Capacitive Touch Sensor Breakout Tutorial (Datasheet).

Available: <https://cdn-shop.adafruit.com/datasheets/MPR121.pdf>

Appendix A

```
//Sajad Mirzaei(2020)-IDC Sensor

#include <Wire.h>

#include "Adafruit_MPR121.h"

#include <SD.h>

#include "RTClib.h"

#include "DataLogger.h"

#define NUM_CAP_SENS 12 //the number of capacitors attached to the sensor

//define DELAY_MS 600000 //delay in ms between capacitance readings

#define DELAY_MS 1800000 //delay in ms between capacitance readings, 30 minutes

//define DELAY_MS 3000 //delay 3 seconds

#define VDD 3 //the sensor is a 3V sensor, but the board has a 5V->3V

#define NUM_BOARDS 3 //number of capacitance boards attached

#define NUM_READS 10

// You can have up to 4 on one i2c bus but one is enough for testing!

// Adafruit_MPR121 cap1 = Adafruit_MPR121();

// Adafruit_MPR121 cap2 = Adafruit_MPR121();

// Adafruit_MPR121 cap3 = Adafruit_MPR121();

const uint8_t CAP_ADDR[NUM_BOARDS] = {0x5A, 0x5C, 0x5D}; //0x5A: ADDR->GND, 0x5C: ADDR-
>SDA, 0x5D: ADDR->SCL

Adafruit_MPR121 caps[NUM_BOARDS]= {Adafruit_MPR121(),Adafruit_MPR121(),Adafruit_MPR121()};

DataLogger dl;

//char * capLog = "halfhr.txt"; //capacitance log file name

//File file; // log file

char * capLogs[NUM_BOARDS]={"board0.txt", "board1.txt", "board2.txt"}; //file names

File files[NUM_BOARDS]; //file variables

uint8_t CDC[NUM_BOARDS]; // currently these are the same for all electrodes but that can be adjusted if needed
```

```

float CDT[NUM_BOARDS]; // needs to be a double incase it is .5us

void setup() {

  while (!Serial);    // needed to keep leonardo/micro from starting too fast!

  Serial.begin(115200);

  Serial.println(F("Adafruit MPR121 Capacitive Touch sensor test"));

//Start each of the capacitor chips

  for (int i=0; i<NUM_BOARDS; i++)

    {

      if (!caps[i].begin(CAP_ADDR[i]))

        {

          Serial.print(F("Capacitance board "));

          Serial.print(i);

          Serial.println(F(" not found, check wiring?"));

          // while (1);

        }

      else

        {

          Serial.print(F("Added: "));

          Serial.println(i);

        }

    }

  Serial.println(F("All 3 boards found!"));

//check each capacitance chip's current and time constant

  for (int i=0; i<NUM_BOARDS; i++)

    {

      CDC[i] = getGlobalCurrent(caps[i]);

      uint8_t time = getGlobalTime(caps[i]);

      if (time==1)

```

```

    CDT[i] = 0.5;

else

    CDT[i] = 1<<(time-2);

Serial.print(F("Board "));

Serial.print(i);

Serial.print(F(": CDC: "));

Serial.print(CDC[i]);

Serial.print(F(" CDT: "));

Serial.println(CDT[i]);

}

//Start the SD card

if(!dl.startSD())

{

    Serial.println(F("SD not Started"));

    while(1);

}

//start each of the logFiles

for (int i=0; i<NUM_BOARDS; i++) {

    files[i] = dl.startLogFile(capLogs[i]);

    files[i].close();

}

}

void loop()

{

    //loop through each board

    for (int b=0; b<NUM_BOARDS; b++)

    {

```

```

//read each board NUM_READS time to eliminate noise in the data
for (int r=0; r<NUM_READS; r++)
{
    files[b] = dl.logInfo("\n\0", capLogs[b]);
    dl.logInfo(dl.getFullTimeStamp(), files[b]); //opens the correct file and logs a timestamp
    //loop through each electrode
    for (int i=0; i<NUM_CAP_SENS; i++)
    {
        uint16_t data = caps[b].filteredData(i);
        double reading = calcCap(data, i,caps[b],b);

        char s [40] = "\0";
        char buf [20] = "\0";
        sprintf(buf, "%u", data);
        strcat(s,buf);
        strcat(s, "\0");
        dtostrf(reading,3,1,buf);
        //sprintf(buf, "%.1f", reading);
        strcat(s,buf);
        strcat(s,"pF\0");
        dl.logInfo(s, files[b]);
    }
    files[b].close();
}
}

delay(DELAY_MS);
}

// double calcCapChange (uint8_t electrode)

```

```

// {
// double base = calcCap(cap.baselineData(electrode), electrode);
// double raw = calcCap(cap.filteredData(electrode), electrode);
// double result = raw-base;
// return result;
// }

double calcCap (uint16_t voltageReading, uint8_t electrode, Adafruit_MPR121 cap,uint8_t board)
{
double capacitance;
uint8_t localCDC = cap.readRegister8(MPR121_CHARGECURR_0+electrode) & 0x3F; // charge current
float localCDT; //charge time
uint8_t time = 0;
if (electrode%2==0) //even electrodes
{
time = cap.readRegister8(MPR121_CHARGETIME_1+electrode/2) & 0x07;
}
else //odd electrodes
{
time = cap.readRegister8(MPR121_CHARGETIME_1+electrode/2) & 0x70;
time = time>>4;
}
if (time==1)
{
localCDT = 0.5;
}
else
{
localCDT = 1<<(time-2);
}
}

```

```

    }
    if (localCDT < 0.4)
    {
        localCDT = CDT[board];
    }
    if (localCDC == 0)
    {
        localCDC = CDC[board];
    }
    capacitance = (localCDC*localCDT)/(voltageReading*VDD/1024.0);
    return capacitance;
}

```

```

/*****setGlobalCurrent

```

This function sets the global current value used for measuring the capacitances.

Param: The value of the current, this must be a value between 1uA and 63uA

```

*/

```

```

/*

```

```

void setGlobalCurrent(uint8_t current)

```

```

{

```

```

    if (current>0 && current<64)

```

```

    {

```

```

        Serial.print("Before: ");

```

```

        Serial.println(cap.readRegister8(MPR121_CONFIG1));

```

```

        uint8_t reg = cap.readRegister8(MPR121_CONFIG1);

```

```

        uint8_t val = reg | current; //*****WRONG, logic won't set the current properly

```

```

        cap.writeRegister(0x5C, 0x20);

```

```

        uint8_t val2 = getGlobalCurrent();

```

```

        Serial.print("After: ");

```

```

Serial.println(cap.readRegister8(0x5C));

while(1);

}

else

Serial.println("Error: Cannot set global current, value not between 1 and 63");

return;

}

*/

uint8_t getGlobalCurrent(Adafruit_MPR121 cap)
{
uint8_t result = cap.readRegister8(MPR121_CONFIG1) & 0x3F;

return result;

}

/*

void setGlobalTime(uint8_t time)
{
if (time>0 && time<8)
{
Serial.print("Before: ");

Serial.println(cap.readRegister8(MPR121_CONFIG2));

uint8_t reg = cap.readRegister8(MPR121_CONFIG2);

uint8_t val = reg | (time<<5); // *****WRONG logic won't set time properly

cap.writeRegister(MPR121_CONFIG2, val);

Serial.print("Wrote: ");

Serial.println(val);

uint8_t val2 = getGlobalCurrent();

Serial.print("After: ");

```

```
Serial.println(cap.readRegister8(MPR121_CONFIG2));  
while(1);  
}  
else  
Serial.println("Error: Cannot set global time, value not between 1 and 7");  
return;  
}  
*/  
uint8_t getGlobalTime(Adafruit_MPR121 cap)  
{  
uint8_t result = (cap.readRegister8(MPR121_CONFIG2) & 0xE0) >> 5;  
return result; }  
}
```